Universidade do Minho
Escola de Medicina

Deolinda Isabel Fernandes da Silva

Mesenchymal Stem Cell Secretome Loaded StarPEG-GAG Hydrogels as a New Route to Induce Spinal Cord Injury Regeneration

abril de 2023

Mesenchymal Stem Cell Secretome Loaded StarPEG-GAG Hy drogels as a New Route to Induce Spinal Cord Injury Regenerationulo

Deolinda Isabel Fernandes da Silva

UMinho | 2023

Universidade do Minho

Escola de Medicina

Deolinda Isabel Fernandes da Silva

Mesenchymal Stem Cell Secretome Loaded StarPEG-GAG Hydrogels as a New Route to Induce Spinal Cord Injury Regeneration

Tese de Doutoramento
Doutoramento em Ciências da Saúde

Trabalho efetuado sobre a orientação de
Doutor António José Braga Osório Gomes Salgado
e do
Doutor Rui Pedro Romero Amandi de Sousa

Abril de 2023

Agradecimentos

Life is made up of moments, memories, accomplishments, failures, and people who force you to learn and grow. Um agradecimento, em primeiro lugar, para a orientação científica. Obrigada, "Tó" pela paciência, pelos conselhos e aprendizagens transmitidas ao longo destes anos. Ao Rui Sousa por aceitar esta orientação e por a Stemmatters ser uma parte fundamental neste projeto. To thank Carsten for his warm welcome at the Max Bergmann Institute and for his contributions to my work. Lucas and Passant, thank you for guiding me and being partners in this journey. Às equipas que me acolheram nesta aventura, à "Tó team" que guardo com carinho especial, somos uma equipa como há poucas, e fica a amizade para além do trabalho, à equipa do laboratório do Carsten e à da Stemmatters que me receberam sempre com carinho.

Um agradecimento muito especial à minha família. Aos meus pais, pela união que construíram, pelos valores que me transmitiram e pelos esforços que fizeram para me trazer até aqui. Pai, sei que estás orgulhoso desta conquista! Aos meus irmãos (ãs), cunhados (as) e sobrinhos (as). Somos muitos, mas somos incríveis. São a minha "casa". Os que sempre persistem mesmo quando o mundo parece desmoronar, a eles devo a pessoa que sou. Às pessoas que chegaram e ficam para a vida. A Inês, a Sandra, a Tiffany, a Raquel, a Aline, o João Afonso nunca vou esquecer o gesto que tiveste para comigo, ao Rui. À Catarina e à Cláudia que me acompanham desde a infância. Por fim, agradeço a todas as pessoas, sem exceção, que cruzaram o meu caminho nestes últimos anos mas que não consigo enunciar aqui. De todas levo algum ensinamento, todas me ajudaram a crescer e hoje sou mais feliz porque a cada dia construo uma pessoa melhor em princípios, valores e realização.

The work presented in this thesis was performed in the Life and Health Sciences Research Institute (ICVS), at School of Medicine, Minho University, Stemmatters, Biotecnologia e Medicina Regenerativa SA., Barco, Guimarães and at Max Bergmann Center of Biomaterials, Dresden, Germany. This work was supported by Prémios Santa Casa Neurociências–Prize Melo e Castro for Spinal Cord Injury Research (MC-04/17; MC-18-2021) and the Portuguese Foundation for Science and Technology (Ph.D. Fellowship to D.S (PD/BDE/135567/2018 and COVID/BDE/152051/2022); funded by FEDER, through the Foundation for Science and Technology (FCT), under the scope of the projects UIDB/50026/2020; UIDP/50026/2020; POCI-01-0145-FEDER-029206; POCI-01-0145-FEDER-031392; PTDC/ MED-NEU/31417/2017; NORTE-01-0145-FEDER-029968; POCI-01-0145-FEDER-029751; POCI-01-0145-FEDER-032619. This work has been funded by ICVS Scientific Microscopy Platform, a member of the national infrastructure PPBI - Portuguese Platform of Bioimaging (PPBI-POCI-01-0145-FEDER-022122. This work has also been developed under the scope of the project NORTE-01-0145- FEDER-000013 and NORTE-01-0145-FEDER-000023, supported by the Northern Portugal Regional Operational Programme (NORTE 2020), under the Portugal 2020 Partnership Agreement, through the European Regional Development Fund (FEDER). Work supported by the Portuguese Foundation for Science and Technology (FCT): projects UID/FIS/04650/2020, PTDC/EMD-EMD/28159/2017, and PTDC/BTM-MAT/28237/2017.

STATEMENT OF INTEGRITY

I hereby declare having conducted this academic work with integrity. I confirm that I have not used plagiarism or any form of undue use of information or falsification of results along the process leading to its elaboration.

I further declare that I have fully acknowledged the Code of Ethical Conduct of the University of Minho.

Secretoma de Células Estaminais Mesenquimatosas Encapsulado em Hidrogel StarPEG-GAG como uma Nova Terapia para a Regeneração de Lesões Vertebro-medulares.

Resumo

As lesões medulares têm sido descritas como "uma doença não tratável" desde os tempos do antigo Egipto. Esta é uma condição que afeta milhões de pessoas em todo o mundo, comprometendo tanto as funções motoras como sensoriais do corpo humano, impactando negativamente a qualidade de vida dos pacientes a nível físico, psicológico e económico. Várias terapias foram testadas em ensaios clínicos demonstrando capacidade de melhoria das funções motoras e sensoriais, no entanto não foram eficazes a chegar à clínica por promoverem diversas reações adversas. Nesta tese, o nosso objetivo foi desenvolver um sistema de libertação controlada baseado num hidrogel para libertar o secretoma de células estaminais derivadas do tecido adiposo (ASC) promovendo processos regenerativos, como crescimento axonal, redução da inflamação, aumento da sobrevivência celular e remodelação vascular, levando à recuperação motora. No entanto, embora a via sistémica (por exemplo, i.v. (intravenosa)) possa causar efeitos colaterais em diferentes órgãos, a administração local tem baixa eficiência devido à rápida difusão por fluidos corporais. O sistema de libertação baseia-se num hidrogel formado por poli(etilenoglicol) (starPEG) e o glicosaminoglicano (GAG) heparina (Hep) com cargas aniónicas que promovem uma elevada afinidade para fatores de crescimento, citocinas, e quimiocinas devido a interações eletrostáticas. Demonstramos que o hidrogel é adequado para libertação continua de factores pró-regenerativos, tais como interleucina (IL)-4, IL-6, fator neurotrófico derivado do cérebro (BDNF), fator neurotrófico de células glial (GDNF), e fator de crescimento beta-nervoso (β-NGF) durante dez dias. A rápida libertação após dois dias, está relacionada com a libertação de fatores neuroinflamatórios e angiogénicos, enquanto a libertação contínua e prolongada até dez dias é maioritariamente impulsionada por fatores de crescimento neuroreguladores. O secretoma libertado promoveu a diferenciação de células progenitoras neurais humanas (hNPCs) e o crescimento de neurites em fatias organotípicas da medula espinal. Finalmente, no modelo de transceção T8 em rato, a libertação de secretoma levou a melhorias motoras significativas comparado com animais lesionados ou tratados com secretoma localmente. As melhorias motoras são promovidas essencialmente pela redução da percentagem de microglia ameboide e níveis sistémicos elevados de citocinas anti-inflamatórias, tais como a IL-10. A libertação de secretoma de ASC do hidrogel starPEG-Hep pode oferecer opções sem precedentes para a terapia regenerativa de lesões medulares

Palavras-chave: lesões medulares, hidrogel, secretoma, sistemas de libertação, starPEG, heparina

Mesenchymal Stem Cell Secretome Loaded StarPEG-GAG Hydrogels as a New Route to Induce Spinal Cord Injury Regeneration

Abstract

SCI has been described as "an ailment not to be treated" since ancient Egyptian times. Every year, millions of people worldwide are affected by this condition, which affects both motor and sensory functions of the human body with a negative impact on the quality of life of patients who are afflicted not only physically but also psychologically and economically. Several therapies have reached clinical trials and shown to be effective in promoting motor and sensorial improvements in patients. However, severe side effects or problems with route of administration have left those therapies on the way to clinic. We aimed to develop a release system based on a biohybrid hydrogel to deliver the secretome of adipose tissue-derived stem cells (ASCs) locally and in a time-dependent manner, which has been shown to promote several regenerative mechanisms, including inducing axonal growth, reducing inflammation, promoting cell survival, and vascular remodeling, ultimately leading to functional recovery. However, while systemic delivery (e.g., *i.v.* (intravenous)) may cause off-target effects in different organs, the local administration has low efficiency due to fast clearance by body fluids. We started by developing the release system, which is based on a hydrogel formed of star-shaped poly (ethylene glycol) (starPEG) and the glycosaminoglycan (GAG) heparin (Hep) with anionic charges resulting in high affinity for a broad range of growth factors, cytokines, and chemokines due to electrostatic interactions. Due to this particularity, we have shown that the hydrogel is suitable to continuously release pro-regenerative signaling mediators such as interleukin (IL)-4, IL-6, brain-derived neurotrophic factor (BDNF), glial-cell neurotrophic factor (GDNF), and beta-nerve growth factor (β-NGF) over ten days. A burst release was observed after two days, mainly related to the release of neuroinflammatory and angiogenic factors, while the continuous and prolonged release until ten days is driven mainly by neuroregulatory growth factors. The released secretome was shown to significantly induce differentiation of human neural progenitor cells (hNPCs) and neurite outgrowth in organotypic spinal cord slices. Finally, in the *in vivo* complete transection SCI rat model, the secretome-loaded hydrogel significantly improved motor function in comparison to lesioned or secretome locally treated animals. Motor improvements were mainly supported by reducing the percentage of ameboid microglia and systemically elevated levels of anti-inflammatory cytokines, such as IL-10. Delivery of ASC-derived secretome from starPEG-Hep hydrogels may therefore offer unprecedented options for regenerative therapy of SCI.

Keywords: spinal cord injury, hydrogels, secretome, delivery systems, starPEG, heparin

Table of contents

List of Abbreviations

A

AI – Artificial intelligence

AIS - Impairment Scale

ALS - amyotrophic lateral sclerosis

ASIA - American Spinal Injury Association

ATI 355 - human anti-human Nogo-A antibody

B

BA-210 – Cethrin

BBB - Basso, Beattie, Bresnahan

BDNF - brain-derived neurotrophic factor

BMSCs - Bone Marrow Stem Cells

BSCB – Blood Spinal cord Barrier

C

CAQK - cystine-alanine-glutamine-lysine

ChABC - chondroitin ABC

CHREB – Conjoit Health Research Ethics Board

CNS – Central Nervous System

CPGs – central pattern generators

CSF – Cerebrospinal Fluid

CSF-1 - colony-stimulating factor

CSPG - chondroitin sulphate proteoglycans

CST – Cortical spinal tract

D

DAPI - 4-6-diamidino-2-phenylindoledhydrochloride

DCX - doublecortin

DRG - dorsal root ganglia

DS – Delivery system

DS - dextran sulfate

dscECM - decellularized spinal cord extracellular matrix

DTX – docetaxel

E

EDC – 1-Ethyl-3-(3-dimethylaminopropyl)carbodiimide

EVs - extracellular vesicles

F

FBS - Fetal Bovine Serum

FDA - Food and Drug Administration

FGF – fibroblast growth factor

FITC - fluorescein isothiocyanate

FRAP - fluorescent recovery after bleaching

FTIR - Fourier transforms infrared

G

G-CSF - Granulocyte Colony-stimulating Factor

GAGs – glycosaminoglycans

Gal-T - ß1-4-galoctosyltransferase

GBD – Global Burden Diseases

GDNF - glial-derived neurotrophic factor

GFAP – glial fibrillary acidic protein

GIH - gastrointestinal hemorrhage

GM – monosialoganglioside

GM-CSF – granulocyte-macrophage colony stimulating factor

GMP - Good Manufacturing Practices

GRGDS - fibronectin

GT - gelation temperature

H

HA - hyaluronic acid

HB-EGF – heparin-binding epidermal growth factor

HBSS - Hanks' Balanced Salt Solution

HEMA - 2-hydroxyethil methacrylate

Hep – Heparin

HGF - Hepatocyte growth factor

HP - Heparin poloxamer

hPDLSCs - human periodontal ligament stem cells

HSV - herpes simplex virus

HT- serotonin fibers

HUCMC - human umbilical cord matrix cells

HUCPVCs - umbilical cord perivascular cells

I

IFN - interferon

IKVAV – laminin

IL - interleukin

INSPIRE - Neuro-Spinal Scaffold

IP – intraperitoneal

IR – Infrared irradiation

L

LSCM - Laser Scanning Confocal Microscopy

M

MA - methacrylic acid

MA – metacrylate

MAP2 - microtubule associated protein-2

MASC - Minocycline in Acute Spinal Cord Injury

MBP – myelin basic protein

MC – methylcellulose

MCF – Michigan Cancer Foundation

MCP-1 – monocyte chemoattractant protein

MEM - Minimum Essential Medium

MH – Minocycline

MMPs – matrix metalloproteinase

MPSS – Methylprednisolone

MSCs - Mesenchymal Stem Cells

MST – Motor swimming test

MW – molecular weight

N

NADPH - Nicotinamide adenine dinucleotide phosphate

NASCIS - National Acute Spinal Cord injury Study

Nb – Neurobasal

NbA – Neurobasal A

NBCS - newborn calf serum

NCT - National Clinical Trial

NF – Neurofilament

NGF - Nerve growth factor

NHS - N-hydroxysuccinimide

NISCI - NISC – Nogo Inhibition in Spinal Cord Injury

NMDA - N-methyl-D-aspartate

NPCs – Neural Progenitor Cells

NPs – nanoparticles

NSCs – Neural stem cells

NT – neurotrophin

O

OCT - optimal cutting temperature compound

OL – oligodendrocytes

OPC- oligodendrocyte precursors cells

P

PA - peptide amphiphilic

PAN – polyacrylonitrile

PBS - phosphate buffered saline

PBS-T - phosphate buffered saline Triton

PEDF - Pigment epithelium-derived factor

PEG - Polyethylene glycol

PFA - paraformaldehyde

PHEMA - poly (2-hydroxyethyl methacrylate

PhMNs - phrenic motor neuros

PLA - Polylactic Acid

PLGA – poly(lactic-co-glycolic acid)

PLLA - poly(-L-lactic acid)

PLO - poly-L-ornithine

PPF - poly (propylene fumarate)

PPO – polyoxypropylene

PTEE - poly(tetrafluoro-ethylene)

PTEN – Phosphatase and tensin homolog

PVC – polyvinylchloride

R

RISCIS - Riluzole in Acute Spinal Cord Injury Study

ROS – reactive oxygen species

RT – room temperature

S

SC – Spinal Cord

SCI – Spinal Cord injury

SDF - Stromal-derived factor

SEM - Scanning electron microscopy

SEM – standard error of the mean

SH3 - Src homology 3 domain

SMI – Anti-Blood Brain Barrier antibody

StarPEG - star-shaped PEG

T

TGF - Transforming growth factor

TIMP - Tissue inhibitor matrix metalloproteinase

TNF - tumor necrosis factor

TSG-6 - tumor necrosis factor-inducible protein

List of Figures

CHAPTER I

CHAPTER II

List of tables

Supplementary Table III. S6 Pairwise comparisons between groups using Tukey's correction for SMI-71 quantification.

Thesis aims and Layout

The primary goal of this thesis was to create a drug delivery system that could load the secretome of human adipose tissue derived stem cells and promote their extended release in order to induce spinal cord injury regeneration.

As a result, this thesis is divided into four chapters:

The anatomy of the spinal cord and SCI pathophysiology are covered in **Chapter I**. An overview of current clinical practice and pipeline therapeutic strategies, including drugs used and cell-based therapy approaches, is provided. Furthermore, an overview of current biomaterials approaches used in the field was made, with a focus on the key characteristics to consider when developing efficient drug delivery systems.

The development of the hydrogel release system is presented in **Chapter II**. StarPEG-Hep hydrogels were chosen for the purpose because of their high affinity for growth factors and cytokines, which are the most abundant molecules in the secretome. These hydrogels are mechanically suitable for implantation. *In vitro* studies also show that they have the ability to release a secretome over a 10-day period that can induce neuronal differentiation in hNPCs and neurite outgrowth in spinal cord slices.

In **Chapter III**, the therapeutic potential of the starPEG-Hep+secretome is assessed in a thoracic transection rat model. Locomotor functional recovery and histological analysis of spinal cord tissue were carried out. Hydrogel loading secretome treatment has been shown to improve motor recovery and reduce inflammation following injury.

Chapter IV is a general discussion that incorporates all of the previous chapters' findings. It also goes over the limitations and clinical relevance of these treatments in the clinic. Future work and perspectives were discussed, with the primary goal of improving the findings of this work as a potential combination of different strategies aimed at improving the patients' condition.

CHAPTER I

Introduction

This chapter is based on the published work in an international peer reviewed journal:

Hydrogels as delivery systems for spinal cord injury regeneration

Deolinda Silva, Rui A. Sousa, António J. Salgado

Article published in Materials Today Bio, January 2021

DOI: 10.1016/j.mtbio.2021.100093

Link: https://doi.org/10.1016/j.mtbio.2021.100093

1. Nervous system and spinal cord organization

Central Nervous System (CNS) is the structure that controls all functions in the human body. It is responsible for controlling all voluntary and involuntary movements caused by internal or external stimuli. The CNS is divided into two parts: the Brain and the Spinal Cord (SC). The general anatomy of the SC is divided into five categories of segments: cervical (eight segments), thoracic (twelve segments), lumbar (five segments), sacral (five segments) and coccygeal (one segment). This organization can differ between species. The fact that each segment is composed of a pair of roots, dorsal corresponding to sensorial fibers and ventral associated to motor fibers, is shared by all. The dural sleeve and neural foramina allow these roots to enter the SC [1]. Cervical and lumbar regions have higher concentration of motor neuros, which are responsible for finely tuned movements, which explains the enlargement in these regions [1]. Furthermore, SC is made up of the central canal, which is filled with cerebrospinal fluid (CSF) and surrounded by glial cells. The grey matter (nuclei) encloses this structure, and the ascending and descending tracts, white matter, enfold both structures, as shown in Figure I. 1A [2]. All structures are protected by the Blood Spinal Cord Barrier (BSCB), which is made up dura, arachnoid and pia, responsible to maintain SC homeostasis by mediating molecular exchange between the blood and SC [3].

SC has been described as a relay between brain and the peripheral organs, acting as a conduit for neural information to be transmitted from brain to all peripheral nervous system and vice-versa. The SC is a center for some reflexes and has the ability to maintain homeostasis. For example, it oversees coordinating sympathetic and parasympathetic reflexes (Figure I. 1B) [4]. The sympathetic division's cells bodies are located at T1-L2/L3, while for parasympathetic division cell bodies are located at S2-S4 region [5]. Both divisions have the ability to act antagonistically, independently or synergistically. While the sympathetic nervous system is in charge of responses in times of danger, such as controlling arterial pressure, the parasympathetic system controls functions during rest, such as digestion and energy conservation. Both systems, which perform opposing functions, innervate the heart, bronchi, stomach and bladder. Blood vessels, and brown adipose tissue, found in newborn humans and animals, are only innervated by sympathetic nervous system or ciliary muscle, and the nasopharyngeal glands are only controlled by parasympathetic system [6].

Furthermore, neuroscientist have demonstrated in recent years that the SC is a key structure in controlling peripheral functions due to the presence of central pattern generators (CPGs). These are neuronal networks that can be instructed to move. CPGs controlling ejaculation, defection and micturition, for

example, are found in the lumbar and sacral segments of animal models. CPGs involved in locomotion have also been identified in animals and humans [4,7].

Based on these facts, any injury to the SC could jeopardize the body's normal function. The impact of a mechanical insult in SC will be described in the following sections, as well as the consequences and potential therapies to restore functions.

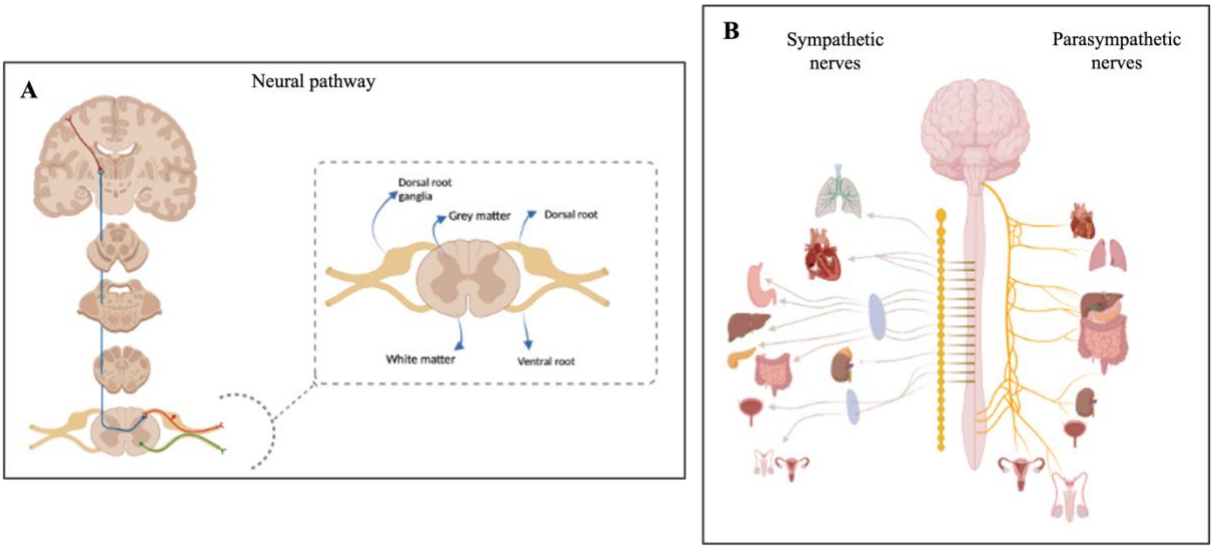

Figure I. 1 Organization of Spinal Cord. A – neural pathway to transmit neuronal information, and organization of spinal cord section. B – Sympathetic and parasympathetic enervation of different organs.

2. Spinal Cord Injury historical perspective

Spinal cord injury (SCI) was firstly described by Edwin Smith in an ancient Egyptian papyrus [8]. At that time, it was possible to study injuries in the central nervous system (CNS) due to the high number of accidents caused by construction of Egyptian pyramids. In this document they describe SCI as a loss of function and sensitivity below the level of injury. Moreover, they described it as "an ailment not to be treated" [9]. Later on, Hippocrates associated other complications to this condition, like constipation, dysuria, skin problems and edema, which could lead to patient's death [9].

The first big improvement in SCI patient care came as consequence of the drastically high numbers of deaths caused by SCI during World War I, due to low level of palliative cares provided to patients. As a consequence, a significant effort was made to establish multidisciplinary care centers and recruiting specialist to treat and follow civilians and military in the World War II [3, 4]. As a result, an improvement in life expectancy of SCI patients in the last decades was achieved, disclosing levels slightly lower than

the average rate for non-SCI individuals. However, there are some facts than can influence life expectancy, namely severity of injury, age, gender and also the fact that low income countries have higher mortality rates due to the lack of economic resources available for medical care [12,13].

2.1. Epidemiology

In a study performed by the Global Burden of Diseases (GBD) in 2016 the incidence of new SCI cases was 0.93 millions with a prevalence of 27 millions, being higher in high income countries (0.29 millions) as USA or Canada, compared with low income (0.08 millions) like Zimbabwe, and Mozambique [14]. Curiously, the incidence of SCI is also different among genders in these regions. In high income men are slightly more affected than women, specially between 20-40 years old, while in low income there is a high incidence of men affected, mainly because most of women stay at home to take care of family [13,14]. This is also related with the direct causes of SCI, which mostly are falls, traffic accidents, sport activities. In some regions of North Africa and Middle East terrorism and violence are the main cause of traumatic injuries [14,15]. Regarding non-traumatic injuries, the principal causes are associated with cord infarction, transverse myelitis, spinal abscess, or spinal canal stenosis [16]. SCI can also affect different functions of the body, depending on the region it occurs. Among all, around 50% of injuries occur at cervical level with an impact in respiratory functions, movement of arms and all functions below the neck. Overall, these are the most severe and also the worst regarding survival and life expectancy. Injuries at thoracic, lumbar or sacral regions are less frequent with a better prognosis of survival. Normally, these kind of injuries compromise the control of abdominal muscles, loss of bladder and bowel control as well as sexual function, hips and legs movement [17]. Both can be complete, with a total loss of function below the injury, or incomplete, where only one part of the spinal cord is affected, in which some function bellow the injury level can happen [18].

The visible image of a patient with a SCI is a wheelchair-dependent person, however, there are far more than motor and physiological consequences. For instance, SCI patients are prone to have depression, anxiety, sleep disturbances and autonomic dysreflexia [19], which frequently lead to an increase in suicide among SCI people [20].

2.2. Pathophysiology and barriers for regeneration

Pathophysiology of SCI comprises three phases, the primary injury caused by a mechanical insult of the bone, followed by the secondary injury and then the onset of the chronic phase (Figure I. 2). Primary injury starts when Spinal Cord (SC) is compressed, contused, lacerated or transected. Immediately upon injury occurs the disruption of ascending and descending pathways, beginning secondary phase, which leads to permanent neuronal damage. Additionally, with the disruption of the blood spinal cord barrier (BSCB) there is the massive infiltration of inflammatory cells [21], that lead to a release of pro-inflammatory cytokines like TNF-α, IL-1β and IL-1α [22] to the extracellular milieu. Further, the damage of spinal neurons, axons and astrocytes leads to a massive release of glutamate that will bind to NMDA receptors promoting their overactivation allowing higher flow of calcium that triggers cell death and consequently death of healthy neurons [23]. Additionally, T cells may play a role in activation of NADPH oxidase, a protein complex that is involved in the production of reactive oxygen species (ROS), enhancing the inflammatory response and impacting in the clearance of myelin debris [24]. On top of this, the death of oligodendrocyte precursors cells (OPC), responsible for myelination of axons, will not allow the myelination of sprouting axons [25]. Thenceforth a chronic phase is established, with demyelination of white matter and dissolution of grey matter, formation of cystic cavity due to enhancement of astrogliosis and surrounded by reactive astrocytes, microglia/macrophages and components of the ECM, particularly chondroitin sulphate proteoglycans (CSPG) [26].

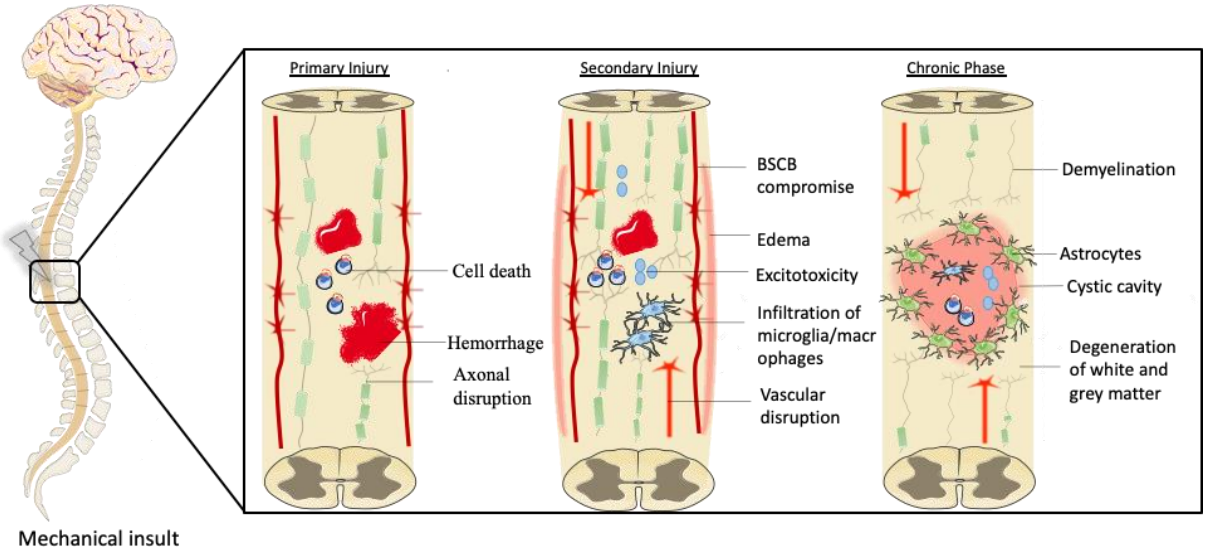

Figure I. 2 Underlying events that comprise the pathophysiology of SCI. The mechanical insult triggers a cascade of events mainly occurring at secondary phase with a massive damage of neuronal tissue.

Later on, a chronic state is established, and the extremely inhibitory environment hinders tissue regeneration.

2.3. Current Clinical approaches

2.3.1. Surgical decompression

When an injured patient first arrives to the hospital there are a number of protocols that can be followed in order to minimize tissue degeneration and ameliorate the patient's condition. Such protocol starts right on the injury place, where proper immobilization is performed. This step alone has shown to reduce neurological deficits in 25% of the patients [27]. Once in the hospital, and after performing imaging to understand the level of injury, a surgical decompression is performed to mitigate secondary injury by ameliorating the mechanical pressure caused by hemorrhage and edema [28]. The timing to perform surgery in SCI patients remains controversial. While some studies defend that early surgery could improve neuronal outcomes as well as improve the score on the ASIA (American Spinal Injury Association) Impairment Scale (AIS) [29] others indicate that late surgery will allow better diagnose and detection of possible other fractures and will not promote more damage to the spine [30]. Therefore, it is also important to establish a reasonable time for early and late surgery. However, it is important to notice that this could be dependent of the time that patients take to arrive to hospital, and also the kind of injury that could lead to different outcomes. A study performed by Kim *et al.*, show that 48h is the most likely time for stabilization of the patient to go into early surgery. They also compare the early and late surgery improvements after 6 months. They show that SCI patients, regardless the region that was affected, tend to benefit with surgery within the first 48h after injury, either if it is a complete or incomplete lesion. [31].

2.3.2. Rehabilitation

Rehabilitation of SCI is a challenging process. Nowadays rehabilitation centers are specialized in non-invasive approaches, focusing in motor training using ladder walking, treadmill, swimming, bicycling, electrostimulation or even robot-assisted training. In fact, training after injury can activate or modulate some pathways that lead to motor recovery, namely through neuro-plasticity triggered phenomena [32]. In 2008, Beaumont *et al.* conducted a study where they compare the recovery of lesioned rats with or without training. The training was performed between day 7 and 28 post-injury daily in their cages. They found out an increase in level of endogenous BDNF in trained animals and also a preservation of tibial

motoneurons, which are important to preserve the integrity of spinal cord [33]. Moreover, body weight-supported locomotor training in individuals with chronic incomplete SCI could improve body function/structure with better sitting and standing capability after 120 sessions with a small gain of bladder, bowel and sexual function. Importantly, the acquired function persisted for up to 12 months, which supports the effectiveness of locomotor training for patients [34]. In recent years robot-assisted treadmill training has been introduced in rehabilitation programs mainly because it can increase the training intensity and specificity, simplify the measurement of motor improvements and automatization [35]. Incomplete SCI patients following robot-assisted training programs for 6 weeks showed an improvement in motor function, cardiovascular rate, mainly systo-diastolic function, reduced inflammation [36] and improve respiratory function by muscle activation [37]. Furthermore, the introduction of epidural stimulation relies on the possibility of combining it with locomotor training to restore some of the function below the level of injury. For instance, patients with cervical or thoracic complete SCI were subjected to intensive training for 9 weeks, without positive outcomes. After that, electrodes were implanted epidurally and training sessions were performed with stimulation. The patients were able to walk over ground or accomplish independent stepping with weight support, using an assisted device [38]. The mechanism behind recovery after training is attributed to the natural plasticity of the CNS after injury, however other authors suggest a reorganization of spinal circuits with memory from interrupted neuronal signals [39]. Additionally, innervation of serotoninergic and dopaminergic fibers were increased, oligodendrogenesis was promoted [40], as also endogenous neuronal differentiation and reconnection of some neuronal tracts [41].

Overall, rehabilitation programs have shown to be essential in motor performance recovery, despite patients are not able to walk without assistance.

2.4. Clinical trials

Animal studies have shown promising results to translate therapies from bench to clinic. The strategies are focused in reducing or inhibiting secondary injury events by neuroprotection, promoting the protection of injured tissue as well as stop the inflammation to spread, or neuroregenerative approaches of endogenous tissue (Figure I.3).

2.4.1. Neuroprotection

2.4.1.1. Methylprednisolone

Methylprednisolone (MPSS) was the first drug to show promising results in promoting recovery after injury. MPSS is a glucocorticoid which act on cytoplasmic receptors upregulating anti-inflammatory factors and modulating the action of proinflammatory cytokines [28]. Beside the promising results in first clinical trial (the National Acute Spinal Cord injury Study, NASCIS I) the dose administration of MPSS was still controversial so in NASCIS II was tested an higher dose (30mg per kilogram) by bolus injection followed by a dose of 5.4mg per kilogram per hour in the following 23h. They also compared the impact of administration within 8h post-injury or later. It was observed an improvement in motor function, pinprick and touch 6 week and 6 months after injury, respectively. It was also reported that the drug was more effective if administered within the first 8h [42]. However, concerns were raised about side effects, as the administration of high doses of MPSS caused gastrointestinal hemorrhage (GIH), respiratory, urinary and wound infections, sepsis, deep vein thrombosis/pulmonary embolism and can lead to death [43]. Moreover, severity of side effects do not offset motor gains, which is a disadvantage for patients [44]. Due to this situation, the recent guidelines from the Congress of Neurological Surgeons/American Association of Neurological Surgeons go against the MPSS administration in SCI patients [45].

2.4.1.2. Riluzole

Riluzole is a benzothiazole anticonvulsant approved by the U.S. Food and Drug Administration (FDA) and is used to treat amyotrophic lateral sclerosis (ALS) [46]. In SCI it can modulate excitatory neurotransmitters by blocking the excess release of glutamate and sodium [47,48]. Preclinical trials deeply support the positive effects in neuronal preservation and functional recovery [49]. In Phase I clinical trials, riluzole was administered orally or by nasogastric tube every 12h. With this treatment there was improvement in motor performance after 90 days. Moreover, there were no related side effects associated, only an increase in bilirubin levels, that return to normal after some time [50]. This drug is now recruiting to proceed to Phase II/III (Riluzole in Acute Spinal Cord Injury Study (RISCIS)—NCT01597518).

2.4.1.3. Minocycline

Minocycline (MH) is a synthetic tetracycline, used for the treatment of acne [51]. The efficacy in SCI is related with inhibition of microglial activation and proliferation, reduce excitotoxicity, reduce neuronal and oligodendroglial apoptosis and neutralization of oxygen radicals [52]. In Phase II MH was intravenously administered in two different doses, 200mg two-times daily and 800mg in a rate of 100mg every 12h until reach 400mg and then maintained till day 7. Despite no differences were observed between placebo and minocycline treated groups, there was a recovery of motor and sensory functions that plateau after 3 months, as assessed by ASIA scores. Regarding side effects, it was reported an increase in liver enzymes, stabilizing with the ending of drug administration [53]. Minocycline is now on Phase III (Minocycline in Acute Spinal Cord Injury (MASC)—NCT01828203)

2.4.1.4. Granulocyte Colony-stimulating Factor (G-CSF)

G-CSF factor is a hematopoiesis-stimulating cytokine that is involved in survival, proliferation and differentiation of cells, and also the maturation of Bone Marrow Stem Cells (BMSCs) into neutrophils [54]. In SCI, studies in animal models revealed that it administration enhanced autophagy and reduced apoptosis of neurons [55]. In Phase III study, a random cohort of SCI patients were treated with 300 μg G-CSF administered subcutaneously daily up to 7 days. Patients were able to recover motor functions in ASIA scores and also improve touch, pinprick, walking, bladder and bowel control. Side effects like neuropathic pain, headache, nausea and vomiting, fever, transient itching and skin rash and upper quadrant pain were reported [56].

2.4.1.5. Hepatocyte growth factor (HGF)

There is an increased interest in using growth factors in preclinical therapies for SCI, because they can modulate cellular functions such as intracellular communication, cell adhesion differentiation and migration [57]. HGF was administered intrathecally in a replication-incompetent herpes simplex virus-1 (HSV-1) vector (rhHGF) in a contusion thoracic rat model. The results show that HGF could reduce the levels of cleavage of caspase-3 in neurons and oligodendrocytes, promoting their survival and induce the regrowth of 5-HT positive fibers [58]. Considering these promising results, a Phase I/II clinical trial was conducted in Japan between June 2014 and May 2018 (Phase I/II Study of PK-100IT in Acute Spinal Cord Injury - NCT02193334) where patients were treated with a dose of 0.6mg of rhHGF intrathecally

72h after injury 5 times a week at lumbar level. The motor recovery and adverse effects, namely production of autoantibodies against rhHGF are still under analysis [59].

2.4.2. Neuroregeneration

2.4.2.1. Cethrin

BA-210, the commercial name for Cethrin, is an inactivator of Rho pathway that when activated can inhibit axonal regrowth, and also reduce inflammation levels [60]. In a SCI preclinical model, BA-210 reduced lesion extension, and improved functional recovery [61]. In a Phase I/IIa, Cethrin was administered using a fibrin sealant placed on top of the dura mater of the spinal cord, both for thoracic and cervical lesion. Most of the patients enrolled in this study were ASIA grade A and after treatment recovered for ASIA grade C or D. Related side effects like urinary infections, were rarely reported [62].

2.4.2.2. Anti Nogo-A

The administration of antibodies gained interest when Schwab and colleagues developed a therapy to deplete the effect of Nogo-A, a protein membrane that arrest the neurite growth. Antibodies strongly neutralize the Nogo-A activity [63]. Furthermore, subdural administration in injured rats showed an increase in cortical spinal tract (CST) sprouting of axons, as well as functional recovery [64]. With these promising results, later on, in collaboration with Novartis (www.novartis.com) a human anti-human Nogo-A antibody (ATI 355) was produced and started the Phase I clinical trial [65]. The antibody was delivered intrathecally by continuous infusion by external pump or by bolus injection in patients with acute traumatic paraplegia and tetraplegia. This first in-human study pointed the safety and absence of immunogenic response of ATI355, minor adverse effects were reported and also some gain of neurological function either motor or sensorial [66].

Additionally, another two more clinical trials are currently running to tackle Nogo-A activity. NISC – Nogo Inhibition in Spinal Cord Injury (NISCI - NC NCT03935321) in Phase I/II aims to test the efficacy of NG-101 antibody by bolus injection in cervical acute SCI patients. AXER – 204 in Participants With Chronic Spinal Cord Injury (RESET – NCT03989440) will test the effect of AXER-204, a human fusion protein that rescue the activity of myelin-associated inhibitors of axonal growth [67], administered in a single dose in Phase I and repeated doses in Phase II in chronic cervical SCI patients.

2.4.2.3. Stem Cells

Autologous transplantation of stem cells strives in the change of the microenvironment created after lesion, assisting remyelination processes, or cell differentiation into new neurons to reconnect loss of neuronal transmission [68]. Mesenchymal Stem Cells (MSCs) are multipotent Stem Cells that can be isolated from different tissues, such as adipose tissue (Adipose Tissue Derived Stem Cells - ASCs) or Bone Marrow (Bone Marrow Stem Cells - BMSCs), from bone marrow. These cells have the capability to reduce inflammation, and differentiate in adipocytes, chondrocytes and osteoblasts [69]. Adipose Stem Cells for Traumatic Spinal Cord Injury (CELLTOP – NCT03308565) Phase I trial treated cervical SCI patients with auto transplantation of ASCs by intrathecal delivery. ASIA motor score was improved as also the sensory functions after 18 months follow up. More important is the fact that patients noticed an improve of their life quality [70].

Safety Study of Local Administration of Autologous Bone Marrow Stromal Cells in Chronic Paraplegia (CME-LEM1 – NCT01909154) tested the effect of administering BMSCs in acute and chronic phase of dorsal thoracic SCI patients. In general, was observed an improvement in neurophysiological functions, namely bladder function [71].

Herein are shown some examples of Stem Cells in forefront of clinical trials, other trials with different cells are currently ongoing (clinicaltrials.gov). However, some concerns remain controversial in this field, like the source of cells which is best for autologous transplantation and some ethical issues in using cell therapy.

2.4.2.4. Neuro-Spinal Scaffold (INSPIRE)

In the beginning of 2000, Teng and colleagues developed a scaffold with an inner and outer surface composed of a blend of 50:50 PLGA and a block of PLGA-polylysine. Moreover, murine NSCs were seeded in the scaffold and implanted in a thoracic hemisection injury rat model. Functional outcomes revealed improvement of motor function with frequent-to-consistent plantar stepping and coordination, reduction of glial scar with both the implant alone or seeded with cells [72]. Later on, the implantation of this scaffold in a hemisection African green monkey model showed proof of safety, as well as some degree of recovery and neural plasticity [73]. In 2016 the first in human implantation of a bioresorbable polymer was reported. After a motocross accident, a patient was diagnosed with T11-12 dislocation fracture, and after spinal decompression the Neuro-Spinal Scaffold was implanted. The patient was followed for 6

months after which improvements in sensorimotor functions and reduction of neuropathic pain was achieved. Additionally, this study showed the safety and feasibility of scaffold implantation in SCI patients [74]. This study is now in process to recruit patients for clinical trials (INSPIRE 2 - NCT03762655)

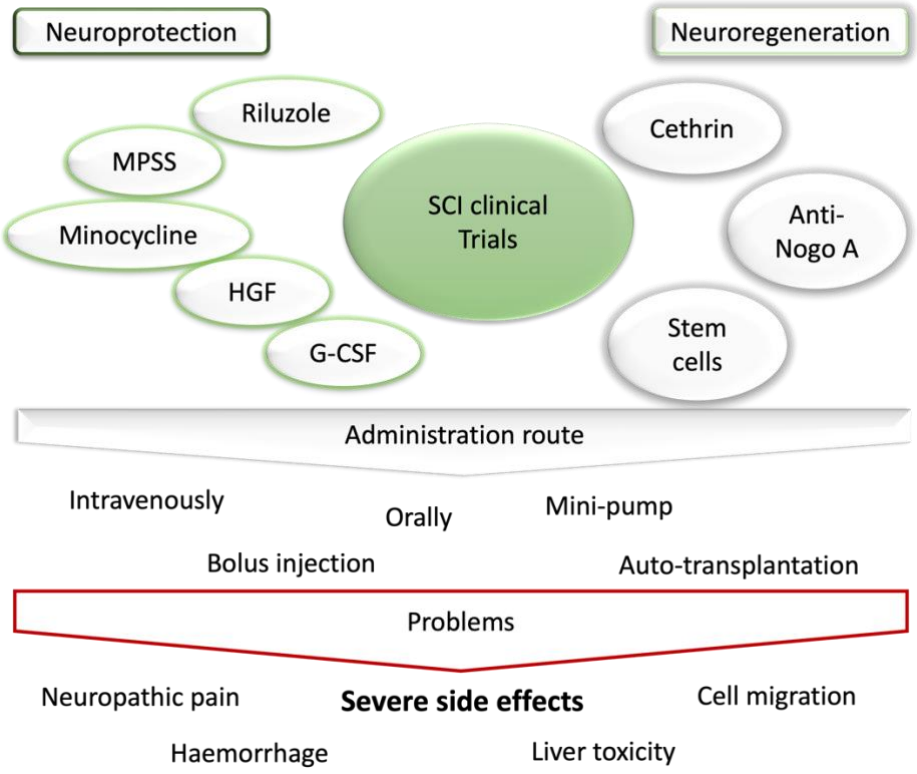

Figure I. 3 Clinical trials in SCI, related administration routs and side effects.

3. Hydrogels as delivery systems in Spinal Cord Injury

Over the last decades there was an increased number of clinical trials conducted in SCI. However, a considerable number failed to promote an effective recovery. Despite some promising results in promoting gain function, most therapies presented upwards, such MPSS or MH, are not already in clinics due to the high risk to trigger of severe side effects (Figure I. 3). For researchers it is quite a challenge to reduce these effects because they are mainly due to the administration route that requires the use of high doses to have a local effect, which became toxic for other organs, particularly liver [75]. On the other side, local administration is also not an option due to fast clearance by fluids. In some cases, the administration is done by mini pumps intrathecally, which is still an invasive method with some risk of infection [76,77].

In an attempt to overcome these problems, biomaterials have flourished as a promising tool in SCI therapeutic strategies. Particularly hydrogels, which are high water content crosslinking structures, with a particularity of being similar to nervous tissue. They are known of being biocompatible, have the capacity to fill the cystic cavity and support axonal growth or cell differentiation. Specifically they can be implanted or injected at lesion site without promoting a further immune response [78]. These characteristics made hydrogels very attractive to be used as DS of drugs, growth factors, to be injected locally in a minimally invasive way for site oriented effect avoiding the use of high doses of therapeutic agents and consequent adverse side effects [79]. Moreover, several preclinical trials have shown the accomplishment of using hydrogels as DS (Table I. 1).

Although, cell transplantation is considered as a very promising approach, there is the concern of cell migration for other regions of CNS, forming ectopic colonies or triggering abnormal tissue formation [80,81]. Once more, hydrogels can be used as matrixes to retain cells locally. Furthermore, hydrogels can be functionalized with peptides, such as fibronectin (GRGDS) or a laminin motifs (IKVAV), that support cell adhesion and growth and have shown to improve recovery after lesion [78,82].

As previously referred, hydrogels appear as excellent and versatile platforms to be used in SCI therapies. More than being used as depots for drugs, growth factors or increasing the potential effect of transplanted cells they protect molecules from being degraded by enzymes or an adverse immune response as they can support axonal growth, and promote tissue regeneration while they are degraded [83]. Another advantage is that their formulation characteristics can be modulated in order to improve their performance *in vivo*, reducing further inflammatory responses as well as control drug delivery. An ideal DS will promote a burst release in the first days, and a slow release for the maximum time possible. This implies that a therapeutic agent has an immediate relief upon injection, normally in the first 2-3 days, but with a prolonged effect with a continuous release, which will allow a continuous therapeutic effect without needing to perform several administrations in time [84].

Below some important characteristic of hydrogels will be highlighted in order to improve the hydrogel designing and consequently the deliver efficacy.

3.1. Hydrogels formulation methods and characterization techniques

Hydrogels can be obtained from natural, synthetic sources, or formed by both natural and synthetic polymers forming a hybrid hydrogel [85]. While natural sources have the advantage of higher biocompatibility and biodegradability, synthetic biomaterials have high water absorption, long life and higher variety in chemistry which confers them strength and resistance [78,82]. Formulation of hydrogels

is of extreme importance when considering their use in context of SCI, they require outstanding improvements in order to enhance therapeutic effect and avoid additional surgical interventions. As an alternative injection of *in situ* forming hydrogels is a more reliable strategy. Upon injection the fast transition from liquid to gel allows a better adaptation to the tissue at injury site, eliminating free spaces and forming a template for tissue regeneration. Another advantage of this method is the easy formulation of hydrogels with cells, growth factors or drugs in liquid state formerly injection [86]. In this sense, several methods can be used to synthetize them, herein a brief introduction of the main processes used will be presented (Figure I. 4).

Hydrogels can be physically or chemicaly crosslinked, depending if it is a non-covalent bond promoted by ionic interations, hydrogen bounds or hydrophobic interations, or if the covalent bond is formed by irradiation or a chemical crosslinker, respectively. Comparing both methods physical hydrogels have a reversible sol-gel transition and are formed by non-covalent cross-links, while chemical formulations have the disadvantage of using a chemical crosslinker, which can be toxic and interfere in the integrity of loading molecules [87]. However they do offer the advantage of an easy control over mechanical properties and form irreversible ligations [88,89]. As an example of chemical crosslinking EDC/NHS reaction is conducted to activate carboxyl groups of heparin for posterior formation of an amide bond between them and the amine groups of Poloxamer. These hydrogels were formulated to deliver GDNF orthotopically in a compression injury rat model [90].

A wide range of chemical coupling reactions are used to sinthetise hydrogels namely click reactions such as Michael type addition, thiol-maleimide reaction and Diels-Alder chemistry. The term “click chemistry” is used to characterize quick and versatile reactions, with high yield and highly selective resulting low toxic bioproducts with well-defined spatiotemporally controlled chemical network structures [91,92]. Mentioned chemical reactions allow the formation of hydrogels in water solution at physiological pH and formation of *in situ* hydrogels, which in context of SCI will help the hydrogels to better accommodate to the lesion site. Briefly, a maleimide-KAFAK was covalently bonded to methylcellulose by thiol-maleimide click chemistry for the delivery of BDNF improving neural behavior in a SCI rat model [93].

Among several other methods to formulate hydrogels, photopolymerization is used with intention to induce *in situ* polymerization controlled by photo-induced gelation by ultraviolet or visible light [86]. In this process the photo-initiator react to form a covalent bond via reacting groups. The main concern with this approach is cell viability that can be compromised by the radiation applied, mainly those with high proliferation rate. In this sense it has to be done a compromise to have a fast light exposure that will promote fast polymerization [94]. Piantino *et al.* developed a PLA-PEG-PLA triblock copolymer that are

assembled by photopolymerization of methacrylated groups of the macromers for delivery of NT-3. Upon injection hydrogel was exposed to light for 60s, an adequate time to induce polymerization and prevent dispersion of the hydrogel from the injection site [95].

Another interesting strategy is the use of self-assembly peptides. This strategy allows the formation of micro-building blocks rationally and coherently into a tissue-like assembly, more likely synthetic aminoacids based molecules that have a fast sol-gel transition at neutral pH. Moreover, self-assembly is a natural phenomenon used to construct complex structures from simple building blocks. For instance microgels can be induced by magnetic, acoustic, mechanical, capillary forces, surface tension or polarity [94,96].

Considering hydrogel characterization, it is crucial to study their structure and functionality. For that purpose, several microscopical techniques are the gold standard to explore hydrogel structure. Scanning electron microscopy (SEM) is by far the most popular technique used to perform morphological characterization of hydrogels. In this context SEM allows the identification of pore formation and size, crosslinking status of a hydrogel and evaluate the effect of loading molecules in general structure of matrices [97]. Although SEM is widely used it has a limitation capacity of generation two-dimensional projections. To overcome this limitation Laser Scanning Confocal Microscopy (LSCM) has been introduced in the field. Additionally, LSCM can be combined with fluorescent dyes, like fluorescent recovery after bleaching (FRAP) to study the diffusivity from hydrogels, which will contribute to predict the release profile in DS [97,98]. Spectroscopic methods include Fourier transforms infrared (FTIR) spectroscopy is an analytical method used to study the bonding structure of atoms based on the interaction between infrared (IR) irradiation with matter [99]. It can be used to characterize reactions between specific chemical groups such as chitosan and β-glycerophosphate [100].

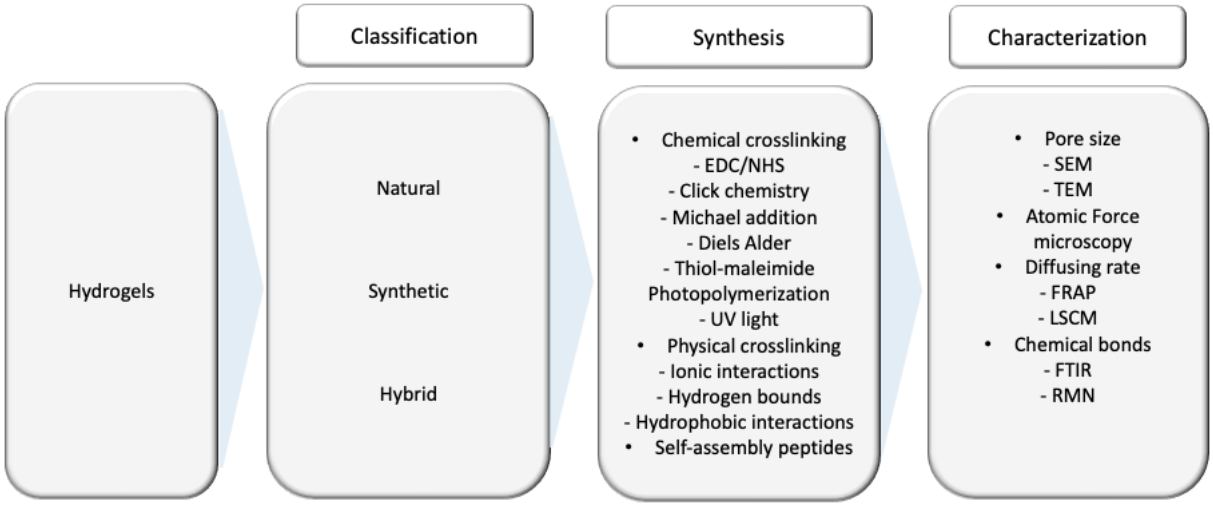

Figure I. 4 Hydrogel classification, formulation methods and characterization techniques applied in the context of DS.

3.2. Rheology

Mechanical properties of hydrogels are of the utmost importance when they are considered for implantation. Rheology is a process where the hydrogel is subject to small deformation, normally small amplitude oscillatory shear measurements, in a rheometer where is measured the deformation energy stored during the shear process (G') also mentioned as elastic modulus or stiffness, and the energy dissipated during the process (G") also referred as viscosity. Hydrogels are more elastic if G'> G'' or are more viscous if G" > G'[101]. In 2010 Lampe and co-workers investigated the effect of different macroscopic properties of polyethylene glycol (PEG) hydrogels in the growth and differentiation of neural progenitor cells (NPCs), in which by increasing the amount of polymer in solution, hydrogels ranging from of 1kPa to 20kPa elastic modulus were obtained. In 3D models the increased stiffness hindered the metabolic activity of cells leading to a higher apoptotic rate. Noteworthy, with increased polymer concentration the access to nutrient could be hampered by the reduced mesh size, which could explain cell apoptosis [102]. In line with this finding, hyaluronic acid (HA) hydrogels were modified with increased methacrylate (MA) groups ratio in order to increase the hydrogel stiffness. Elastic modulus varied between 3kPa to 5kPa with increased MA substitution. Notably, neuronal differentiation was better supported by soft hydrogels, in which more mature neurons and increased axonal length were detected. Surprisingly no effect of mechanical properties was noticed in the morphology of astrocytes isolated from SC [103].
Later on, Schultz *et al.* developed a DS using a very soft agarose hydrogel with approximately 1.5kPa. In this work, they aimed the release of thyroid hormone 3,3',5-triiodothy-ronine (T3) in order to tackle the enhancement of oligodendrocytes (OL) at injury site favoring the myelination of sprouting axons [104].

The release of T3 in a unilateral cervical contusion injury rat model increased the number of newly formed mature OLs and consequent axonal myelination rostral to lesion site [105].

In a different approach, hydrogels can be used in a strategy to decrease the mechanical properties of scaffolds. The combination of collagen in a scaffold of poly (propylene fumarate) (PPF), allow the formation of a porous structure filled with collagen for the development of a DS. Furthermore, collagen ameliorated the release of neurotrophin-3 (NT3), previously combined with collagen binding domain (CBD) which binds to biomaterials and can retain high content of neurotrophic factors, for 7 days. In a complete SC transection at thoracic level the scaffold surpasses organized axonal growth throughout the porous structure. The incorporation of collagen improved the production of mature neurons and NT3 enhanced survival of endogenous NPCs [106].

Beyond elastic modulus, viscosity of hydrogels must also be considered. It is related with the capacity of hydrogels to be injected through a needle and can diffuse prior to gelation [107]. Heparin poloxamer (HP) was used to deliver bFGF at a thoracic SCI hemisection. The hydrogel viscosity ranged between 8 Pa·s to 10 Pa·s as the temperature change from 32 °C to 37 °C [108]. Imidazole-poly(organophophazenes) polymer hydrogel (I-5), was implanted in a thoracic contusion injury rat model. This hydrogel has the capacity to rapidly form a gel-like material with a viscosity of 50 Pa·s and in just 150s achieving a viscosity of 600 Pa·s at body temperature. *In vivo*, its implantation almost eliminated cystic cavity and promote neuron repair and motor recovery [109].

Accordingly, hydrogels to be used in SCI therapies should mimic the mechanical properties of host tissue to allow the regenerative processes to take place. In agreement with literature the stiffness of SC could range between 3kPa and 300kPa [110,111] which means that hydrogels have to be stiff enough to assemble itself and soft enough to create an appropriate environment for cells to growth, adhere and differentiate. Moreover, it was shown that soft hydrogels (< 1kPa) with low viscosity are suitable for SCI implantation to favor tissue regeneration [112].

3.3. Mesh size

Hydrogels are polymer networks that form a gel when exposed to a polymerizing agent promoting the crosslinking between polymer chains. The free space between two points is named as mesh or pore of a hydrogel. Depending on the distance between the entangled points, hydrogels could be classified as macro-porous, micro-porous or non-porous [113]. Mesh size can be modulated by polymer and crosslinker concentration or external stimulus as pH or temperature. The porosity of hydrogels is crucial

for delivery of therapeutic agents in injury because in most cases this process occurs by diffusion or by interactions between polymer and loading agent. If the pores are smaller than the size of therapeutic agent, it will be entrapped into the hydrogel and will not be released. On the other hand, if the hydrogel pores and molecule size are similar the result will be a slow release. Contrarily if pores are higher than the agent, small molecules will move freely in the network and release will occur by diffusion, release is not directly correlated with mesh size [114]. Recent developments have been made to determine mesh size. Among them FRAP bleaching is used to study the diffusivity of fluorescent molecules from hydrogels. This technique has the advantage of being performed in a common confocal laser scanning microscope with a fluorescent probe capable of photobleaching [98]. Fluorescence correlation spectroscopy (FCS) is a complement to FRAP, once it correlates diffusivity coefficients from resident times of fluorescent particles moving through a small, static illuminated volume, being ideal for microscale heterogeneities in the hydrogel structure. This method has the advantage of using less powerful laser than FRAP as well as low fluorophore concentrations [115].

Currently, the most effective technique to determine mesh size (ξ), is correlating with swelling data, a theory of Canal and Pepas, equation 1 [116,117]

$$\xi = \varphi^{-\frac{1}{3}} \left(\left(1 - \frac{2}{\mathrm{f}} \right) l^{-2} C_{\infty} \frac{\lambda M_c}{M_r} \right)^{\frac{1}{2}} \qquad \text{(Equation 1)}$$

where, φ is polymer volume fraction, l polymeric carbon-carbon bond length, C_∞ is the polymer-specific characteristic ratio for a chain of ∞ repeating units, λ polymer backbone bond factor, M_c number of average molecular weight between crosslinks in a polymer network and M_r molecular weight of the polymer repeating unit.

Porosity in network structure is also imperative for diffusion of nutrients within the lesion site or even to allow the migration of cells or axons to growth through the implanted hydrogel. Chen *et al.* developed a macro-porous hydrogel based on 2-hydroxyethil methacrylate (HEMA) with MOETACL to deliver bFGF at injury site. This network was favored by communicating pores with an average size of 80μm. In a complete thoracic transection, the implantation of this DS allowed the recovery or motor performance evidenced by the increase ingrowth of axons and blood vessel in the hydrogel only 5 days after injury [118].

In the field of DS the possibility to modulate pore size is of extreme importance, considering also the injectability of the matrix. In this sense the formulation of matrices as DS using an oil-in-water emulsion at different ratios and surfactant concentrations allows the control over porous structure. Briefly

conjugation of both methods allows *in situ* pore formation by incorporation of oil droplets within crosslinkable precursor solution and polymerization induced by UV light, upon immersion in water the diffusion of oil droplets results in pore formation. Pore size was of the oil droplet size, but with increasing concentration of surfactant pore size diminish [119].

In a more simple and easy way, pore size can be tunable by controlling crosslinking degree, namely increased crosslinking degree or hydrogel precursor content decrease mesh size in a matrix hydrogel [120].

3.4. Swelling

Swelling behavior of the hydrogels is the process in which water molecules will enter in the structure of the polymer promoting the expansion of mesh size which will allow more water molecules to enter. In this process elasticity offset the extreme expansion of the network, avoiding it destruction. Thus, the equilibrium is reached when there is a balance of these two forces, also known as swelling pressure (P_{sw}), is equal to zero. Generally speaking, swelling takes in account the increase in weight, volume or length of a hydrogel, and can be measured as degree of swelling (D_{sw}), equation 2 [121]

$$D_{sw} = m_{hw}/m_{hd} \quad \text{(Equation 2)}$$

where m_{hw} and m_{hd} is the weight of wet and dry hydrogels, respectively. It could also be measured by the diameter of swollen hydrogels, equation 3 [122]

$$D_{sw} = (d_{hw}/d_{hd})^3 \quad \text{(Equation 3)}$$

where d_{hw} and d_{hd} are, respectively, diameter of hydrogels after and before swelling, which always assume values $D_{sw} \geq 1$ [121].

After SCI there is an increased pressure in surrounding tissues responsible by the edema formation, which causes cell death and tissue loss [107]. Considering this, hydrogels to be used in therapeutic strategies should not hold a high degree of swelling in order to avoid more pressure in the site of implantation [107]. Moreover, it is also important to control the swelling behavior in order to control the

release of molecules. Hydrogel swelling is directly correlated with porous structure, so all strategies to modulate mesh size mentioned ahead influence swelling behavior. Hydrogels with small pores will swell very slowly while macroporous structures swell fast [123].

For instance the increase of crosslinking density of HA-tyramine conjugate by increasing the concentration of H_2O_2 will decrease the swelling ratio and therefore decrease the rate of protein release [124]. Besides, swelling can also be controlled by the thiolation process of chitosan, that when modified with Traut's reagent immediately swell after chitosan and PEG precursors are mixed and form a gel, slightly shrinking. Such approaches can reduce the likeliness of hydrogels to swell in the injury site, avoiding adverse reactions such as inflammation [125].

Likewise, hydrogel swelling can be modulated by incorporation of thermoresponsive segments in a hydrogel matrix. They have the particularity of being sensitive to thermal stimuli. Basically, these segments are water soluble and at low temperatures they are hydrated due to interactions between water molecules and hydrophilic domains extending polymer chains. On the other hand, high temperatures promote their dehydration and polymer chains aggregate due to hydrophobic interactions. Briefly at low temperature hydrogels swell while at high temperatures the swelling is slow, so hydrogel swelling can be controlled by combining hydrophilic and hydrophobic components [126]. Such polymers are poly(ethylene glycol)/ poly(propylene glycol), poly (glycidyl ethers) cellulose derivates, poly (N-substituted acrylamide) [127–129]. The main advantage of this strategy for injectable hydrogels is that hydrogels will polymerize upon injection normally at body temperature.

3.5. Degradation

Introduction of biomaterials in regenerative strategies for CNS imply that progressively after implantation they will degrade as axons regenerate. This is extremely important to avoid inflammation or nerve compression. Accordingly, despite some promising results with synthetic nondegradable materials, such as silicone, polyacrylonitrile/polyvinylchloride (PAN/PVC), poly(tetrafluoro-ethylene) (PTEE), and poly (2-hydroxyethyl methacrylate) (PHEMA), their use is not frequent due to their non-biodegradability. On the other hand, most of degradable materials used are provided by natural sources or synthetic materials, such as PLGA, PLA, PGA or PEG also used in medical devices [130].

Network degradation plays an important role in controlling molecular release, this is, controlling hydrogel degradation alter release of therapeutic agent. Piantino *et al.* controlled the release of NT3 by modulating the number of degradable units and macromer concentration in an acrylated PLA-b-PEG-b-PLA polymer.

This hydrogel is formed by the addition of degradable lactic units of hydroxyl groups. NT3 had a burst release in the first 24h, being slowly released thereafter for periods up to 2 weeks. This sustained release in a thoracic SCI transection promoted recovery of motor function as plasticity of raphespinal tracts [95]. Hydrogel degradation can also be modulated by crosslinking with specific sequences that will be recognized for endogenous or implanted enzymes. For instance, a HA hydrogel crosslinked with MMP-sensitive peptide was tested in a thoracic compression injury rat model for BDNF delivery. When implanted *in vivo*, the endogenous cells secrete MMPs that degrade the sensitive peptides and consequently promote the release of BDNF, which induce motor neuron regeneration and motor function recovery [131]. Delivery of BDNF was also performed using a peptide amphiphilic (PA) hydrogel. In this work, a hydrogel was functionalized with IKVAV. The particularity of this hydrogel is that when implanted *in vivo*, it will assemble in nanofibers and BDNF release is controlled by electrostatic interactions. However, ultimately the release is controlled by hydrogel degradation once nanofibers will get shorter and mesh size will increase. This explains the release profile with a burst release in the first 3 days, followed by a slow release until 21 days post-implantation. In a thoracic compression injury rat model, such approach preserved axonal degeneration and diminish astrogliosis [132].

3.6. Gelation temperature

The gelation timing of a hydrogel to be used in DS is crucial to determine the therapeutic effect of loading agent. The gelation temperature (GT) is determined when elastic modulus is the halfway for gel formation [133]. Hydrogels can also be responsive to stimulus, in this case can gelate in response to temperature. The ideal behavior is that hydrogels are liquid at room temperature, and gel at body temperature, *in situ* gelation. This will ensure that hydrogel could be injected in the lesion site using a needle and, once there, a fast gelation process will allow prolonged therapeutic effect avoiding wash away by CSF [134]. One example of thermoresponsive hydrogels is poloxamers, that are composed of a triblock with a central hydrophobic block of polyoxypropylene (PPO) flanked by two hydrophilic blocks of polyoxyethylene (PEO) [135]. Liu and co-workers investigated the impact of polymer concentration on GT. They formulated hydrogels with different ratios of PPO:PEO, Pol-1(PEO_{101}-PPO_{60}-PEO_{101}) and Pol-2 (PEO_{88}-PPO_{27}-PEO_{80}), which form a gel at 15°C and 50°C, respectively. Interactions between hydrophilic PEO and hydrophobic units will determine the GT and nature of hydrogel. None of the created hydrogels were suited for implantation, so they combine both and investigated the GT by varying their concentrations and found out that forming a hydrogel with 5% (w/w) Pol-2 and 17,8% (w/w) Pol-1 the GT was around 39°C. GT was determined by

varying G' and G'' as function of temperature and heating rate of 1°C min^{-1}. Furthermore, it was used to deliver monosialoganglioside (GM1) in a T10 dorsal hemisection rat model. The loading of this molecule decreased the GT for 36°C due to the presence of two long fatty acids, which reduce the ratio of hydrophilic and hydrophobic units in the hydrogel. GM1 was released for 1 month and inhibited the formation of glial scar enhancing neuron regeneration [136]. Poloxamer are also functionalized with heparin to delivery bFGF. These hydrogels have the ability to undergo from liquid to gel transition in about 100s as the temperature increases to 34°C. More importantly, loading bFGF does not change the gelation properties of hydrogel. In a T9 hemisection model induced axonal regeneration, apoptosis decrease and recovery of motor function [108]

3.7. Surface Charge

The physical and mechanical properties of the hydrogel surface also influence cell adhesion or axonal growth. The coating of surfaces with positive materials enhance cell adhesion and growth [137]. Hejc ̌l et al. investigate the impact of HEMA hydrogels with different charges in thoracic hemisection injury rat model. They designed HEMA hydrogels with negative charge (hydrogel crosslinking with methacrylic acid in sodium salt (MA)), positive charge (crosslinking with $MOETA^{+}$) and a neutral polymer with positive and negative charges combined by crosslinking with both agents used before. The growing connective tissue was favored by the positive charges with the pores of the hydrogel being filled by it with evident longer neurites growing throughout the polymer with positive functional groups, which isn't found in polymers without charge. On the other hand, astrocyte ingrowth was only detected in the periphery of negatively charge implant and also in uncharged polymer [138]. In order to overcome the negative effect of negatively charge alginate hydrogels in cell adhesion or axonal growth, hydrogels can be coated with positively charged poly-amino acids and laminin. *In vitro*, neurite growth was more pronounced in hydrogels coated with poly-L-ornithine (PLO) /laminin and absent in uncoated hydrogels. In a cervical hemisection rat model more neurites growth through the hydrogel in rostral zones and also more infiltration of host cells [139].

4. Strategies for delivery control

4.1. Affinity-based systems

The efficacy of a therapeutic strategy relies on the targeted events and the time window in which it will have the best regenerative influence. Having this in mind, besides controlling hydrogel network,

establishing interactions between drug and polymer network could be crucial for sustained or on-demand release. This led to the development of affinity-based systems, in which drugs are attached to the hydrogel by covalent conjugation or through secondary bounds such as electrostatic interactions, taking advantage of protein's natural affinity for specific ligands [114]. HA methylcellulose (MC) hydrogels were modified with a Src homology 3 domain (SH3) that were bound in the MC hydroxyl groups in order to improve release of chondroitin ABC (ChABC) which has thermal instability [140]. SH3 peptide binds reversibly to SH3 protein and once expressed slow the protein release. Moreover, by combining with ChABC the release rate is controlled by the ratio between SH3 peptide and SH3 protein for an *in vitro* release for 7 days [141]. In a compression injury rat model ChABC treated animals have a decrease in CSPG levels and wide distribution of NPCs in the SC [142]. Following the affinity-based systems, the incorporation of heparin in poloxamer hydrogels increases the affinity for proteins, growth factors, cytokines by binding to hydrogels through -COOH or -OH and proteins with -SH groups in order to extend the release. Moreover, these hydrogels are thermosensitive with a controlled sol-gel transition temperature with porous structure, which favors the delivery. HP hydrogels were used to deliver aFGF in a compression injury rat model. The release of aFGF was improved with heparin, being released about 55% after 28 days, while in hydrogel without heparin the release was about 25% of loaded aFGF. This promoted protection of BSCB, improved remyelination, reduced neuronal death contributing for motor recovery [143]. Besides enhancing drug delivery HP hydrogels do not have the capacity to store or stabilize growth factors once they are released, compromising it role in regeneration. To overcome this, hydrogels are combined with decellularized spinal cord extracellular matrix (dscECM) that is crucial for cell adhesion, growth factors support, cell growing and survival [144]. Xu *et al.* incorporated dscECM loading bFGF in HP hydrogels. In this system, bFGF was released by affinity from dscECM and then by diffusion through porous structure of HP, which resulted in 25% of loaded bFGF still remained in hydrogel after 7 days. The implantation in an hemisection injury rat model promoted a reduction in cell apoptosis, neuronal regeneration contributing to motor function recovery [145].

4.2. Incorporation of nanoparticles

Furthermore, to protect a therapeutic agent from degradative enzymes or to enhance delivery, hydrogels are combined with nanoparticles (NPs). This hybrid system aimed to recapitulate the specificity of bolus injection with sustained release offered by mini pump or catheter but avoiding further tissue damage. Nanoparticles are used as carry and delivery agents while hydrogel ensures they are localized in the injury

site to promote regeneration [83]. PLGA NPs are widely used in SCI due to its good biodegradability, and it incorporation in HAMC hydrogels allow the formulation to deliver NT-3 a modulator of maintenance, proliferation and differentiation of neurons [146], in a thoracic compression model. NT-3 was released for 28 days *in vivo*, and the release is mediated by electrostatic or hydrophobic interactions between NT-3 and PLGA NPs. This resulted in an increased axonal density surrounding the injury site with a slightly improved motor function [147]. A similar effect was observed when using the same system to co-deliver NT-3 and anti-NogoA, for 28 days and 10 days, respectively. Moreover, the author suggest that co-delivery of NT-3 can enhance Anti-NogoA effect resulting in both tissue and motor improvement [148]. Chitosan is a natural positively charged polymer often used in the formulation of particles in SCI therapeutic strategies due to its biocompatibility, biodegradability and low toxicity, antitumor activity and low immunogenicity [149,150]. A regenerative effect was observed when chitosan particles loaded with NT-3 were embedded in collagen hydrogel, and used in the treatment of thoracic hemisection monkey model, where increased axonal growth and revascularization were observed at injury site [151]. Furthermore, chitosan can be used to form particles or self-assemble with other materials like dextran-sulfate to deliver BDNF. In this context was observe a preservation of diaphragmatic function as well as enhancing serotonergic enervation of phrenic motor neuros (PhMNs) [152].

Chitosan has the advantage of being a soft material, has a higher water content and viscoelasticity, which recapitulate the mechanical properties of SC tissue. Moreover, structurally is similar to glycosaminoglycans, one of the most abundant polysaccharides of ECM [153,154]. All these characteristics made chitosan very attractive to use in SCI.

Other organic polymers, such as liposomes, have been also combined with hydrogel for co-delivery of docetaxel (DTX), a microtubule-binding agent important for growth cone development [155], BDNF and aFGF. Wang and colleagues developed a scar-homing liposome to load BDNF in the inner aqueous phase and DTX in lipid membrane modified with a tetrapeptide (cystine-alanine-glutamine-lysine) (CAQK) that binds to CSPGs. The liposomes were embedded in HP hydrogels loading aFGF. Importantly, sol-gel transition occurs at 24°C, still suitable for injection and polymerization *in situ*, and a porous sponge-like structure with interconnected pores allow the diffusion of liposomes to release the loaded molecules at injury site, being DTX, BDNF and aFGF sustainably released for 10 and 21 days, respectively. *In vivo*, in a thoracic contusion SCI model, the combinatorial therapy contributed for mild SC lesions, increase of molecules responsible for axonal remyelination, such as MBP, induced microtubule stabilization essential for growth cone maintenance favoring axonal growth, leading to locomotion improvements [156].

4.3. Ion-mediated interactions

As mentioned above, MH is a promising candidate to treat SCI, however it administration is still a challenge, for one hand systemic administration gives rise to multiple side effects, on the other side loading into hydrogels is still difficult once MH is water soluble, which means it will be released very fast and is also fast degradable in solution at body temperature [157]. The formulation of dextran sulfate (DS)-MH complexes self-assembled by metal ion binding-mediated interaction allow sustained release of MH [158] that were loaded in agarose hydrogels to ensure local delivery. Moreover, Mg^{2+} allow the formation of insoluble complexes between DS and MH, being it release mediated by strong metal ion-mediated interactions between DS and MH. This complex combination allows the modulation of MH release by reducing the ratio of DS/MH and MG^{2+} concentration or by adding chitosan that compete with MH to bind to DS and Mg^{2+}. In this way, MH has a high dose being released at acute phase to tackle the primary inflammatory events, and a low dose sustainably released to hindering chronic inflammation and oligodendrocytes death. Its administration in a unilateral cervical injury model was more effective than intraperitoneal (IP) injection in reducing cystic cavity, was able to reduce inflammatory response and contribute to motor recovery [159]. Likewise, MH delivery preserved diaphragm innervation of PhMNs axons, protecting respiratory circuit from degeneration and hampered further inflammation by inhibiting M1 polarization [160].

5. PEG hydrogels as delivery systems

Polyethylene glycol (PEG), is a linear polymer and synthetic material. The living anionic ring-opening polymerization of ethylene oxide produces it. The molecular weight can vary between 0.4 to 100kDa [161]. PEG hydrogels are appealing for regenerative medicine applications due to their aqueous nature and porosity, which allows for easy uptake and diffusion of cells and molecules [162]. Implantation of PEG hydrogels can promote motor recovery [163] reduce inflammation and inhibits nerve fiber degeneration [164] and can modulate signaling pathways diminishing cell apoptosis or caspase-3 activity [165].

More interestingly, PEG hydrogels can be used as drug or cell carriers, and due to their high versatility, can be easily modified and their properties modulated in order to improve biological properties *in vivo*. However, PEG by itself may have a low loading capacity. To overcome this disadvantage, PEG can be combined with nanoparticles not only to reduce nanoparticle clearance, but also to increase loading capacity and target therapy, thereby improving cell viability [166]. Likewise, PEG can be coupled with

other materials, such as poly(-L-lactic acid) (PLLA), to form biodegradable hydrogels with tunable pore size, which can support nerve growth when combined with biomimetic scaffolds [167,168].

Zheng *et al.* also developed a thermosensitive hydrogel made of PEG and PLGA. At 35°C, this formulation forms a hydrogel, allowing for the injection of liquid hydrogel at injury site, which then gels *in-situ*. Furthermore, loading baricitinib promotes functional recovery and reduces neural death. The main disadvantage of this system is its rapid release, reaching 80% total release after 3 days [169]. The development of a release system as the primary goal of extending the therapeutic effect for an extended period of time without the need for additional intervention. To address this, PEG was combined with glycosaminoglycans (GAGs), which promote protection and the sustained released of several growth factors, cytokines and chemokines [170]. The attractiveness of these systems to formulate release systems resides in Heparin characteristics. Heparin is a 15kDa molecular weight polysaccharide component of the ECM. It is a linear structure composed of repeated units of 1—4 linked pyranosyluronic acid and 2-amino-2-deoxyglucopyranose (glucosamine) residues. They also contain sulfate groups at the N-, 2-O, and 6-O- positions [170]. This distribution confers to heparin the most negative charge density of known molecules. Both negative charge and spatial distribution of sulfate units give rise to strong electrostatic interactions between heparin and a wide range of positively charge biological mediators, such as growth factors, cytokines, chemokines. In this manner, incorporating heparin in hydrogels make possible to modulate the release, localization and activity of loading agents in tissues [171–173]. Moreover, a click reaction between end-functionalized star-shaped PEG (starPEG) and Heparin's maleimide groups can form hybrid materials, 3D-network structures with tunable physical properties and biomolecular functionalization. For example, varying the cross-linking degree alters physical characteristic such as storage modulus, mesh size, and swelling while maintaining biomolecular composition [174]. When functionalized with a variety of peptides, these materials can also act as cell-instructive matrices, promoting cell growth, their adhesion and differentiation [175,176]. In this sense, these hydrogels can drive dermal fibroblast differentiation *in vitro* by delivering TGFß for seven days [177], as well as the sustainable release of IL-4 for 14 days, inducing the polarization of macrophages into a more pro-regenerative state M2 [178].

6. Role of MSCs secretome in promoting regeneration in CNS

There has been a surge in interest in studying the role of cell-based therapies in the context of regenerative medicine in recent years. Mesenchymal Stem Cells (MSCs) are currently the most promising for this

purpose [179,180]. MSCs are found throughout the human body, including bone marrow, the umbilical cord, the brain or even in adipose tissue. Furthermore, the isolation process is simple, and MSCs can be easily identified by surface markers such as positive expression of CD105, CD73 and CD90 and negative expression of CD34, CD45, HLA-DR, CD-14, CD19 [181] [182].

Adipose tissue-derived stem cells (ASCs) are a type of MSCs derived from the adipose tissue, a highly available and abundant source. Several studies pointed their influence in providing protection, survival and differentiation of neural cells and support neuroregeneration with their beneficial immunomodulatory profile [183–185], as well as their relevance in promoting recovery after SCI [186]. The comparison of the effect of BMSCs and ASCs populations was conducted by Zhou et al. in a bilateral dorsal SCI laminectomy. Two cell dosages were administered, one caudal and one rostral to the lesion. When compared to BMSC transplantation, the authors found that ASCs significantly increased angiogenesis, axonal regeneration, reduced inflammatory cell infiltration, and promoted functional recovery [187]. Other authors demonstrated their ability to improve functional recovery, reduce inflammation, and preserve neural tissue in a contusion SCI model [188].Moreover, our group also showed that the transplantation of a combination of ASCs and olfactory ensheathing cells (OECs) within a gellan gum hydrogel improved motor function by reducing inflammatory cells in the lumbar [187] and thoracic hemisection SCI rat model [188]. This approach was capable of increasing diaphragmatic activity and partially restoring sensory function in cervical level 2 (C2) hemisection SCI in rats [189]. More interestingly, the role of ASCs *per se* was demonstrated when no difference in motor recovery was demonstrated between groups treated with cells alone or with cells plus growth factors such as granulocyte colony-stimulating factor (GCSF)[192]. In a recent pilot study in SCI dogs, allogenic ASC transplantation was effective in reducing urinary incontinence and improving neurological outcomes such as restoring normal proprioception [190]. The role of cell transplantation in modulating regenerative processes has gained a lot of interest from researchers, however this also poses some concerns for SCI application like the higher number of cells needed for transplantation, the low survival and the possibility of migration from injury site. In line with this, the attention has been refocused on their secreted bioactive molecules (secretome), due to their neuroprotective, neuroregenerative, and immunomodulatory capabilities [68,183].

Remarkably, enormous efforts have been made to decipher all of the components of the secretome and its mechanism of action. The secretome is divided into two parts: a protein fraction, which includes several soluble growth factors, pro- and anti-inflammatory cytokines, extracellular matrix proteins and a vesicular fraction, which includes mostly exosomes and microvesicles [191,192]. Pires *et al.* compared the secretome of BMSCs, adipose tissue (ASCs) and umbilical cord perivascular cells (HUCPVCs),

demonstrating that their secretory profile differ [193]. Only 134 of the 451 proteins found were shared by all cell types. Some proteins involved in CNS processes were found to be expressed only in certain cell types. Indeed, ß1-4-galoctosyltransferase (ß4Gal-T) was only found in ASCS, whereas Stromal-derived factor-1α (SDF-1α) and Gelsolin were found in BMSCs, and Cyr61 and colony-stimulating factor (CSF-1) were found in HUCPVs. Moreover, anti-oxidative and anti-apoptotic molecules CYPA and CYPB were found to be upregulated in BMSCs. These results suggest that BMSCs may have higher anti-oxidative profile. In addition, molecules involved in axonal growth, such as SEM7A and GDN, were found to be upregulated in BMSCs and ASCs, indicating that these cells may play an important role in promoting neurite outgrowth. When compared to the secretome of BMSCs, the secretome of ASCs was able to induce significantly higher neurite outgrowth of dorsal root ganglia (DRGs) cultures [194]. Thus, ASCs-derived secretome has been shown to protect pheochromocytoma (PC12) cells from glutamate excitotoxicity and apoptosis by reducing the levels of cleaved-caspase-3 [184]. Regarding inflammation, the ASCs secretome is able to reduce the release of pro-inflammatory tumor necrosis factor-α (TNF-α) after exposure to an inflammatory stimulus, as well as to induce actively macrophages (M2) polarization and the secretion of anti-inflammatory cytokines IL-10 and transforming growth factor (TGFβ1) [195]. Furthermore, the ASCs secretome was shown to be capable of promoting neuronal survival and differentiation [196,197], axonal outgrowth in dorsal root ganglia (DRG) explants [188,194] and also tissue vascularization [198]. Moreover, after exposure to spinal cord injury conditioned medium, the secretome of ASCs can increase MAP2 positive neurons, while decreasing GFAP cells, acting primarily as a protective factor in cortical neurons [199]. Exosomes or extracellular vesicles (EVs), in addition to proteins, make up the secretome. These structures can be important in cell-to-cell communication as well as transporting other proteins, mRNA, miRNA and organelles [200,201]. *In vitro*, EVs can protect neurons from glutamate excitotoxicity. Moreover, in a contusion SCI rat model they induce autophagy to reduce neural cell apoptosis, inflammation and contribute to improved motor performance [202].

Because it can address a wide range of pathways involved in trauma or disease, the secretome has emerged as a promising approach in SCI. The positive effects on neuroregeneration after SCI was demonstrated for the first time by our group. The multiple systemic injections of ASCs secretome after a contusion SCI in a mice model promoted functional recovery [203]. The beneficial effects have only been observed by systemic administration in this study, whereas the action of local injection was greatly diminished due to its quick clearance of the secretome from the target site. Furthermore, the authors emphasized the importance of administering the secretome as a whole, including both vesicular and protein fractions, after single administration did not significantly promote motor recovery.

Overall, these studies demonstrated the feasibility of using ASCs secretome in SCI regenerative therapies. These cells have the ability to release bioactive molecules that are involved in neuroprotective, neuroregenerative and immunomodulatory pathways, which help to restore lost functions. Moreover, using ASCs secretome overcomes concerns associated with cell transplantation, such as host rejection or incorrect differentiation.

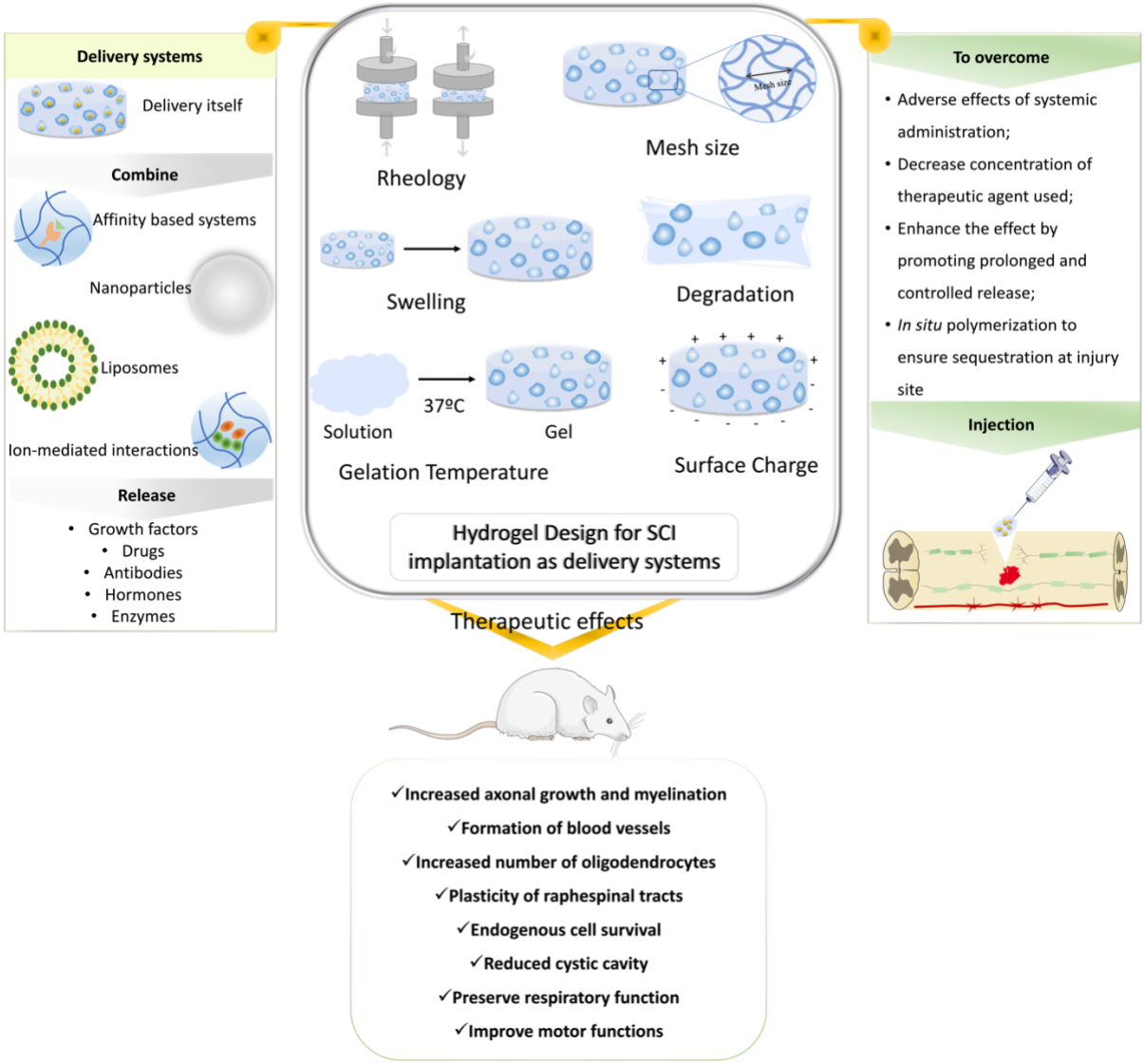

Figure I. 5 Hydrogels have been applied in SCI as delivery systems to improve the therapeutic effect of loading agents. Characteristics as rheology, mesh size, swelling, degradation rate, gelation temperature or surface charge, illustrated in the center of figure, can be modulated in order to improve their performance when injected at injury site. Additionally, hydrogels can be combined with other molecules to deliver agents at and extended time. Among all, growth factors, drugs, antibodies, hormones or

enzymes are the most frequent therapeutic agents loaded in hydrogels in SCI. In preclinical models of SCI these systems have shown promising impact in promoting tissue regeneration.

7. Conclusions and future perspective

Spinal cord injury affects both motor and sensorial functions of millions of people worldwide being a serious social, economic and emotional problem. Despite the growing research in the field with multidisciplinary approaches raising to promote regeneration there is still a lack of an effective therapy in the clinic that could improve life quality of patients. Biomaterials can represent a good alternative to apply as DS, overcoming side effects reported in several clinical trials. As discussed, it is possible to modulate their designing characteristics to improve its performance at injury site and support regenerative events promoted by delivered molecular therapies. In preclinical trials, the use of these systems has allowed preservation of respiratory functions reduction of inflammation, enhanced axonal regeneration, reducing cellular apoptosis leading to recovery of motor function (Figure I. 5). While all reported strategies are relevant when considering the design of effective DS some can be considered most favorable to further explore, mainly due to easy chemistry used or simplest modulation of important characteristics. For instance, it is clear that the modulation of characteristics such as stiffness, mesh size, swelling and gelation temperature have in common alterations of crosslinking degree achieved by altering hydrogel precursor content. In this context poloxamer hydrogels appear to easily modulate these characteristics. Moreover, they have the advantage of being thermoresponsive hydrogels undergoing sol-gel transition at body temperature. Additionally, the possibility of incorporating molecules for affinity-based release, like heparin, is advantageous once is based on natural affinity for proteins or growth factors, prolonging the release profile and taking also advantage of heparin being a glycosaminoglycan present in ECM.

Notwithstanding the promising results achieved in preclinical trials there is still a big question related to biomaterials, that why so few of them have reached clinical trials. The long path from bench to clinics comprehends the regulatory approval, which often tends to be quite challenging for strategies dealing with scaffolds [204]. Moreover, production of biomaterials for human implantation has to ensure Good Manufacturing Practices (GMP), as well as low batch to batch variability of natural or synthetic materials, a fact that is also challenging when scaling up lab run processes to an industrial scale [84]. Upon overcoming all mentioned problems, another concern is the injection method, which needs to be fast and

low invasive, do not promote further damage as well as protecting all therapeutic agents within the formulation.

As mentioned, most of the strategies to test hydrogels are conducted in transection models, because of the gap created by the lesion that will allow the hydrogel to fill the cavity without fostering pressure to surrounding tissue. However, most human SCI are contusions/compressions, so another facing problem for clinical translation is the injection of biomaterials in these conditions.

Upon several developments in SCI therapies, there is a strong know-how about its pathophysiology, which is crucial when developing effective therapies. Taking this into consideration, the development of a therapy will benefit from a multidisciplinary strategy of integrated knowledge of several areas, namely biology, physics, medicine, engineering and bioengineering and material science to try to tackle all degenerative events. Hydrogels can help with the adhesion of cells, their differentiation in neurons or uphold axonal growth, while at the same time have the ability to release growth factors or drugs that will reduce inflammation, induce axonal growth or decrease tissue damage. Likewise, materials with electrical properties could be embedded in hydrogels as well as the combination with stimulation will favor tissue regeneration and improve patient's rehabilitation. Nonetheless, stem cell-based therapy has been shown in numerous studies to be a promising option to tackle SCI condition. Their therapeutic potential has been attributed primarily to secreted bioactive molecules that modulate neuroprotective, neuroregenerative, and immunomodulatory processes, as well as promoting motor recovery following SCI. As a result, a new era in cell-based therapy has begun with a better understanding of the key mechanisms modulated by these factors, as well as the development of an efficient and feasible method to inject secretome. This option may overcome the issues raised by cell transplantation. As a result, hydrogels could be a promising vehicle for delivering the secretome to the site of injury. Altogether, overcoming these problems will contribute to improve patient's life quality.

Acknowledgements

This work was supported by Prémios Santa Casa Neurociências–Prize Melo e Castro for Spinal Cord Injury Research (MC-04/17; MC-18-2021) and the Portuguese Foundation for Science and Technology (Ph.D. Fellowship to D.S (PD/BDE/135567/2018 and COVID/BDE/152051/2022). This work was funded by national funds and FEDER, through the Foundation for Science and Technology (FCT), under the scope of the projects UIDB/50026/2020; UIDP/50026/2020; POCI-01-0145-FEDER-029206; POCI-01-0145-FEDER-031392; PTDC/ MED-NEU/31417/2017; NORTE-01-0145-FEDER-029968; POCI-01-0145-FEDER-029751; POCI-01-0145-FEDER-032619. This work has been funded by ICVS Scientific

Microscopy Platform, a member of the national infrastructure PPBI - Portuguese Platform of Bioimaging (PPBI-POCI-01-0145-FEDER-022122. This work has also been developed under the scope of the project NORTE-01-0145- FEDER-000013 and NORTE-01-0145-FEDER-000023, supported by the Northern Portugal Regional Operational Programme (NORTE 2020), under the Portugal 2020 Partnership Agreement, through the European Regional Development Fund (FEDER). Work supported by the Portuguese Foundation for Science and Technology (FCT): projects UID/FIS/04650/2020, PTDC/EMD-EMD/28159/2017, and PTDC/BTM-MAT/28237/2017.

Table I. 2 Current hydrogels delivery systems applied in SCI model and it potential to induce regeneration

Hydrogel type		Functionalization	Therapeutic agent	Characteristics	Injury model	Delivery approach	Therapeutic effects	Reference
Natural	HAMC	KAFKA	BDNF	• Low swelling • Release for 4 days	Rat T10 clip compression	Local administration after injury	• Locomotor recovery • Inhibition of proinflammatory cytokines expression • Upregulation of anti-inflammatory cytokines	[93]
	Alginate	PLGA NPs	MH and PTX in NPs	• Irregular microporous structure • Low viscosity allowing syringe injection • MH and PTX released for 63 days	Rat T8 lateral hemisection	Local administration after injury	• Axonal regrowth • Neuroprotection mediated by reducing proinflammatory cytokines • Locomotor recovery	[205]

	Gelatin	CBD	HGF	• Photo-crosslinkable hydrogel • Furfurylamine enhanced retention of CBD-HGF into hydrogel • Release for 7 days	Mice compression injury	Intrathecal injection after injury	• Reduction of scar formation • Reduced inflammatory response • Motor recovery	[206]
	Agarose	DS-CH	BDNF	• Released over 17 days	Rat unilateral C4/C5 contusion	Local administration after injury	• Preservation of respiratory function • Enhanced diaphragm innervation • Increase 5-HT positive fibers	[207]
	Chitosan	Collagen	Serp-1		Rat T10 compression	Local administration after injury	• Improved motor function • Reduced SC damage • Reduced CD3-positive cell at injury site	[208]

		β-glycer-ophosphate/hydroxyethylcellulose	lentiviral mediated NGF-overexpressing ADSCs		Rat T8-T9 moderate contusion	Local injection one week post-injury	• Higher survival and proliferation cells at injury site • Improved motor function • Reduced cavity formation	[100]
Synthetic	Laponite	Heparin	FGF4	• Elastic modulus of 0.1 kPa • 3D porous structure • Easily injected using syringe • FGF4 released for 35 days	Rat T9 clip compression	Orthotopic injection	• Reduced cystic cavity • Axonal regeneration and remyelination • Suppression of astrocyte migration and polarization • Reduction of M1 phenotype macrophages	[209]
	Fmoc	RGD	S-220 (Epac2 agonist that could enhance axonal growth)	• Stiffness ~100 Pa • Release for 28 days	Rat T10 contusion	Local injection 3 weeks after injury	• Improve in control limb movements • Enhanced neurite growth • Suppression of astrocyte activation	[210]

	Poloxamer	Heparin	GDNF	• Gelation temperature at 37°C • Porous structure • 80% GDNF released after 24h	Rat T9 compression	Orthotopic injection after injury	• Neuroprotection of injured SC • Enhanced axonal repair • Inhibited expression of caspase-3	[90]
			NGF	• Porous sponge like structure • Interconnected inner porous	Rat T9 contusion	Orthotopic injection after injury	• Motor recovery • Decreased astrocytes at injury site • Increased number of CD31 positive cells • Reduced apoptosis	[211]

References

[1] A. Tracey, C. Minneap, M. February, S.C. Disorders, Spinal_Cord_Functional_Anatomy___Erratum.3, 21 (2015) 13–35.

[2] O. Bican, A. Minagar, A.A. Pruitt, The Spinal Cord. A Review of Functional Neuroanatomy, Neurol. Clin. 31 (2013) 1–18. https://doi.org/10.1016/j.ncl.2012.09.009.

[3] L.Y. Jin, J. Li, K.F. Wang, W.W. Xia, Z.Q. Zhu, C.R. Wang, X.F. Li, H.Y. Liu, Blood-Spinal Cord Barrier in Spinal Cord Injury: A Review, J. Neurotrauma. 38 (2021) 1203–1224. https://doi.org/10.1089/neu.2020.7413.

[4] I. Steuer, P.A. Guertin, Central pattern generators in the brainstem and spinal cord: An overview of basic principles, similarities and differences, Rev. Neurosci. 30 (2018) 107–164. https://doi.org/10.1515/revneuro-2017-0102.

[5] A. Farley, E. Mclafferty, C. Johnstone, C. Hendry, Nervous system: part 3 Farley, Nurs. Stand. 28 (2013) 46–50.

[6] E.A. Wehrwein, H.S. Orer, S.M. Barman, Overview of the Anatomy, Physiology, and Pharmacology of the Autonomic Nervous System, Compr. Physiol. 6 (2016) 1239–1278. https://doi.org/10.1002/cphy.c150037.

[7] K. Minassian, U.S. Hofstoetter, F. Dzeladini, P.A. Guertin, A. Ijspeert, The Human Central Pattern Generator for Locomotion: Does It Exist and Contribute to Walking?, Neuroscientist. 23 (2017) 649–663. https://doi.org/10.1177/1073858417699790.

[8] R. Porter, The Cambridge Illustrated History of Medicine, Ann. Intern. Med. 128 (1996) 415. https://doi.org/10.7326/0003-4819-128-5-199803010-00020.

[9] L. Anderberg, H. Aldskogius, A. Holtz, Spinal cord injury - Scientific challenges for the unknown future, Ups. J. Med. Sci. 112 (2007) 259–288. https://doi.org/10.3109/2000-1967-200.

[10] J.F. Ditunno, Linking spinal cord injury rehabilitation between the World Wars: The R. Tait McKenzie legacy, J. Spinal Cord Med. 40 (2017) 641–648. https://doi.org/10.1080/10790268.2017.1370522.

[11] D.J. Lanska, The influence of the two world wars on the development of rehabilitation for spinal cord injuries in the United States and Great Britain, Front. Neurol. Neurosci. 38 (2016) 56–67. https://doi.org/10.1159/000442569.

[12] G. Savic, M.J. Devivo, H.L. Frankel, M.A. Jamous, B.M. Soni, S. Charlifue, Long-term survival after traumatic spinal cord injury: A 70-year British study, Spinal Cord. 55 (2017) 651–658. https://doi.org/10.1038/sc.2017.23.

[13] T. Øderud, Surviving spinal cord injury in low income countries, African J. Disabil. 3 (2014) 1–9. https://doi.org/10.4102/ajod.v3i2.80.

[14] S.L. James, A. Theadom, et.al, Global, regional, and national burden of traumatic brain injury and spinal cord injury, 1990–2016: a systematic analysis for the Global Burden of Disease Study 2016, Lancet Neurol. 18 (2019) 56–87. https://doi.org/10.1016/S1474-4422(18)30415-0.

[15] N. Level, Facts and Figures at a Glance, J. Spinal Cord Med. 30 (2018) 304–305. https://doi.org/10.1080/10790268.2007.11753944.

[16] P.W. New, R. Marshall, International Spinal Cord Injury Data Sets for non-traumatic spinal cord injury, Spinal Cord. 52 (2014) 123–132. https://doi.org/10.1038/sc.2012.160.

[17] L.H.S. Sekhon, M.G. Fehlings, Epidemiology, demographics, and pathophysiology of acute spinal cord injury, Spine (Phila. Pa. 1976). 26 (2001) 2–12. https://doi.org/10.1097/00007632-200112151-00002.

[18] M.J. Eckert, M.J. Martin, Trauma: Spinal Cord Injury, Surg. Clin. North Am. 97 (2017) 1031–1045. https://doi.org/10.1016/j.suc.2017.06.008.

[19] N.T. North, The psychological effects of spinal cord injury: a review, J. Spinal Cord Med. (1999) 671–679.

[20] P. Kennedy, L. Garmon-Jones, Self-harm and suicide before and after spinal cord injury: A systematic review, Spinal Cord. 55 (2017) 2–7. https://doi.org/10.1038/sc.2016.135.
[21] J.T. Maikos, D.I. Shreiber, Immediate damage to the blood-spinal cord barrier due to mechanical trauma, J. Neurotrauma. 24 (2007) 492–507. https://doi.org/10.1089/neu.2006.0149.
[22] J.W. Rowland, G.W.J. Hawryluk, B. Kwon, M.G. Fehlings, Current status of acute spinal cord injury pathophysiology and emerging therapies: Promise on the horizon, Neurosurg. Focus. 25 (2008) 1–3. https://doi.org/10.3171/FOC.2008.25.11.E2.
[23] A. Alizadeh, S.M. Dyck, S. Karimi-Abdolrezaee, Traumatic Spinal Cord Injury: An Overview of Pathophysiology, Models and Acute Injury Mechanisms, Front. Neurol. 10 (2019) 1–25. https://doi.org/10.3389/fneur.2019.00282.
[24] A. Pajoohesh-Ganji, K.R. Byrnes, Novel Neuroinflammatory Targets in the Chronically Injured Spinal Cord, Neurotherapeutics. 8 (2011) 195–205. https://doi.org/10.1007/s13311-011-0036-2.
[25] A. Alizadeh, S. Karimi-Abdolrezaee, Microenvironmental regulation of oligodendrocyte replacement and remyelination in spinal cord injury, J. Physiol. 594 (2016) 3539–3552. https://doi.org/10.1113/JP270895.
[26] N.A. Silva, N. Sousa, R.L. Reis, A.J. Salgado, From basics to clinical: A comprehensive review on spinal cord injury, Prog. Neurobiol. 114 (2014) 25–57. https://doi.org/10.1016/j.pneurobio.2013.11.002.
[27] J. Toscano, Prevention of neurological deterioration before admission to a spinal cord injury unit, Paraplegia. 26 (1988) 143–150. https://doi.org/10.1038/sc.1988.23.
[28] C.S. Ahuja, M.G. Fehlings, Concise Review : Bridging the Gap : Novel Neuroregenerative and Neuroprotective Strategies in Spinal Cord Injury, (2016) 914–924. https://doi.org/10.5966/sctm.2015-0381.
[29] ASIA, ISCOS, INTERNATIONAL STANDARDS FOR NEUROLOGICAL CLASSIFICATION OF SPINAL CORD INJURY (ISNCSCI), (2019) 4–5.
[30] T. Konomi, A. Yasuda, K. Fujiyoshi, J. Yamane, S. Kaneko, T. Komiyama, M. Takemitsu, Y. Yato, O. Tsuji, M. Matsumoto, M. Nakamura, T. Asazuma, Clinical outcomes of late decompression surgery following cervical spinal cord injury with pre-existing cord compression, Spinal Cord. 56 (2018) 366–371. https://doi.org/10.1038/s41393-017-0019-1.
[31] M. Kim, S.K. Hong, S.R. Jeon, S.W. Roh, S. Lee, Early (≤48 Hours) versus Late (>48 Hours) Surgery in Spinal Cord Injury: Treatment Outcomes and Risk Factors for Spinal Cord Injury, World Neurosurg. 118 (2018) e513–e525. https://doi.org/10.1016/j.wneu.2018.06.225.
[32] H.R. Sandrow-Feinberg, J.D. Houlé, Exercise after spinal cord injury as an agent for neuroprotection, regeneration and rehabilitation, Brain Res. 1619 (2015) 12–21. https://doi.org/10.1016/j.brainres.2015.03.052.
[33] E. Beaumont, S. Kaloustian, G. Rousseau, B. Cormery, Training improves the electrophysiological properties of lumbar neurons and locomotion after thoracic spinal cord injury in rats, Neurosci. Res. 62 (2008) 147–154. https://doi.org/10.1016/j.neures.2008.07.003.
[34] S.A. Morrison, D. Lorenz, C.P. Eskay, G.F. Forrest, D.M. Basso, Longitudinal Recovery and Reduced Costs After 120 Sessions of Locomotor Training for Motor Incomplete Spinal Cord Injury, Arch. Phys. Med. Rehabil. 99 (2018) 555–562. https://doi.org/10.1016/j.apmr.2017.10.003.
[35] N. Yozbatiran, G.E. Francisco, Robot-assisted Therapy for the Upper Limb after Cervical Spinal Cord Injury, Phys. Med. Rehabil. Clin. N. Am. 30 (2019) 367–384. https://doi.org/10.1016/j.pmr.2018.12.008.
[36] M. Turiel, S. Sitia, S. Cicala, V. Magagnin, I. Bo, A. Porta, E. Caiani, C. Ricci, V. Licari, V. De Gennaro Colonna, L. Tomasoni, Robotic treadmill training improves cardiovascular function in spinal cord injury patients, Int. J. Cardiol. 149 (2011) 323–329.

https://doi.org/10.1016/j.ijcard.2010.02.010.
[37] D. Terson de Paleville, W. McKay, S. Aslan, R. Folz, D. Sayenko, A. Ovechkin, Locomotor step training with body weight support improves respiratory motor function in individuals with chronic spinal cord injury, Respir. Physiol. Neurobiol. 189 (2013) 491–497. https://doi.org/10.1016/j.resp.2013.08.018.
[38] C.A. Angeli, M. Boakye, R.A. Morton, J. Vogt, K. Benton, Y. Chen, C.K. Ferreira, S.J. Harkema, Recovery of over-ground walking after chronic motor complete spinal cord injury, N. Engl. J. Med. 379 (2018) 1244–1250. https://doi.org/10.1056/NEJMoa1803588.
[39] M. Martinez, H. Delivet-Mongrain, H. Leblond, S. Rossignol, Incomplete spinal cord injury promotes durable functional changes within the spinal locomotor circuitry, J. Neurophysiol. 108 (2012) 124–134. https://doi.org/10.1152/jn.00073.2012.
[40] W. Zhang, B. Yang, H. Weng, T. Liu, L. Shi, P. Yu, K.F. So, Y. Qu, L. Zhou, Wheel running improves motor function and spinal cord plasticity in mice with genetic absence of the corticospinal tract, Front. Cell. Neurosci. 13 (2019) 1–15. https://doi.org/10.3389/fncel.2019.00106.
[41] P. Yu, W. Zhang, Y. Liu, C. Sheng, K.F. So, L. Zhou, H. Zhu, The effects and potential mechanisms of locomotor training on improvements of functional recovery after spinal cord injury, 1st ed., Elsevier Inc., 2019. https://doi.org/10.1016/bs.irn.2019.08.003.
[42] M.B. Bracken, M.J. Shepard, W.F. Collins, T.R. Holford, W. Young, D.S. Baskin, H.M. Eisenberg, E. Flamm, L. Leo-Summers, J. Maroon, L.F. Marshall, P.L. Perot, J. Piepmeier, V.K.H. Sonntag, F.C. Wagner, J.E. Wilberger, H.R. Winn, A Randomized, Controlled Trial of Methylprednisolone or Naloxone in the Treatment of Acute Spinal-Cord Injury, N. Engl. J. Med. 322 (1990) 1405–1411.
[43] Z. Liu, Y. Yang, L. He, M. Pang, C. Luo, B. Liu, L. Rong, High-dose methylprednisolone for acute traumatic spinal cord injury: A meta-analysis, Neurology. 93 (2019) e841–e850. https://doi.org/10.1212/WNL.0000000000007998.
[44] M.B. Bracken, M.J. Shepard, T.R. Holford, L. Leo-Summers, E.F. Aldrich, M. Fazl, M. Fehlings, D.L. Herr, P.W. Hitchon, L.F. Marshall, R.P. Nockels, V. Pascale, P.L. Perot, J. Piepmeier, V.K.H. Sonntag, F. Wagner, J.E. Wilberger, H.R. Winn, W. Young, Administration of methylprednisolone for 24 or 48 hours or tirilazad mesylate for 48 hours in the treatment of acute spinal cord injury: Results of the Third National Acute Spinal Cord Injury randomized controlled trial, J. Am. Med. Assoc. 277 (1997) 1597–1604. https://doi.org/10.1097/00132586-199808000-00011.
[45] B.C. Walters, M.N. Hadley, R.J. Hurlbert, B. Aarabi, S.S. Dhall, D.E. Gelb, M.R. Harrigan, C.J. Rozelle, T.C. Ryken, N. Theodore, Guidelines for the management of acute cervical spine and spinal cord injuries: 2013 update, Neurosurgery. 60 (2013) 82–91. https://doi.org/10.1227/01.neu.0000430319.32247.7f.
[46] R.G. Miller, J.D. Mitchell, M. Lyon, D.H. Moore, Riluzole for amyotrophic lateral sclerosis (ALS)/motor neuron disease (MND), Cochrane Database Syst. Rev. (2007). https://doi.org/10.1002/14651858.CD001447.pub2.
[47] Y. Wu, K. Satkunendrarajah, Y. Teng, D.S.L. Chow, J. Buttigieg, M.G. Fehlings, Delayed post-injury administration of riluzole is neuroprotective in a preclinical rodent model of cervical spinal cord injury, J. Neurotrauma. 30 (2013) 441–452. https://doi.org/10.1089/neu.2012.2622.
[48] L.A. Tetreault, M.P. Zhu, J.R. Wilson, S.K. Karadimas, M.G. Fehlings, The Impact of Riluzole on Neurobehavioral Outcomes in Preclinical Models of Traumatic and Nontraumatic Spinal Cord Injury: Results From a Systematic Review of the Literature, Glob. Spine J. 10 (2020) 216–229. https://doi.org/10.1177/2192568219835516.
[49] N.L. Vasconcelos, E.D. Gomes, E.P. Oliveira, C.J. Silva, R. Lima, N. Sousa, A.J. Salgado, N.A. Silva, Combining neuroprotective agents: effect of riluzole and magnesium in a rat model of thoracic spinal cord injury, Spine J. 16 (2016) 1015–1024. https://doi.org/10.1016/j.spinee.2016.04.013.

[50] M.G. Fehlings, H. Nakashima, N. Nagoshi, D.S.L. Chow, R.G. Grossman, B. Kopjar, Rationale, design and critical end points for the Riluzole in Acute Spinal Cord Injury Study (RISCIS): A randomized, double-blinded, placebo-controlled parallel multi-center trial, Spinal Cord. 54 (2016) 8–15. https://doi.org/10.1038/sc.2015.95.

[51] S.E. Garner, A. Eady, C. Bennett, J.N. Newton, K. Thomas, C.M. Popescu, Minocycline for acne vulgaris: Efficacy and safety, Cochrane Database Syst. Rev. 2012 (2012). https://doi.org/10.1002/14651858.CD002086.pub2.

[52] V.W. Yong, J. Wells, F. Giuliani, S. Casha, C. Power, L.M. Metz, The promise of minocycline in neurology, Lancet Neurol. 3 (2004) 744–751. https://doi.org/10.1016/S1474-4422(04)00937-8.

[53] S. Casha, D. Zygun, M.D. McGowan, I. Bains, V.W. Yong, R. John Hurlbert, Results of a phase II placebo-controlled randomized trial of minocycline in acute spinal cord injury, Brain. 135 (2012) 1224–1236. https://doi.org/10.1093/brain/aws072.

[54] M.H. Khorasanizadeh, M. Eskian, A.R. Vaccaro, V. Rahimi-Movaghar, Granulocyte Colony-Stimulating Factor (G-CSF) for the Treatment of Spinal Cord Injury, CNS Drugs. 31 (2017) 911–937. https://doi.org/10.1007/s40263-017-0472-6.

[55] Y. Guo, S. Liu, X. Zhang, L. Wang, J. Gao, A. Han, A. Hao, G-CSF promotes autophagy and reduces neural tissue damage after spinal cord injury in mice, Lab. Investig. 95 (2015) 1439–1449. https://doi.org/10.1038/labinvest.2015.120.

[56] N. Derakhshanrad, H. Saberi, M.S. Yekaninejad, M.T. Joghataei, A. Sheikhrezaei, Granulocyte-colony stimulating factor administration for neurological improvement in patients with postrehabilitation chronic incomplete traumatic spinal cord injuries: A double-blind randomized controlled clinical trial, J. Neurosurg. Spine. 29 (2018) 97–107. https://doi.org/10.3171/2017.11.SPINE17769.

[57] A.K.A. Silva, C. Richard, M. Bessodes, D. Scherman, O.W. Merten, Growth factor delivery approaches in hydrogels, Biomacromolecules. 10 (2009) 9–18. https://doi.org/10.1021/bm801103c.

[58] K. Kitamura, A. Iwanami, M. Nakamura, J. Yamane, K. Watanabe, Y. Suzuki, D. Miyazawa, S. Shibata, H. Funakoshi, S. Miyatake, R.S. Coffin, T. Nakamura, Y. Toyama, H. Okano, Hepatocyte Growth Factor Promotes Endogenous Repair and Functional Recovery After Spinal Cord Injury, J. Neurosci. Res. 85 (2007) 2332–2342. https://doi.org/10.1002/jnr.

[59] K. Kitamura, N. Nagoshi, O. Tsuji, M. Matsumoto, H. Okano, M. Nakamura, Application of hepatocyte growth factor for acute spinal cord injury: The road from basic studies to human treatment, Int. J. Mol. Sci. 20 (2019). https://doi.org/10.3390/ijms20051054.

[60] N. Forgione, M.G. Fehlings, Rho-ROCK inhibition in the treatment of spinal cord injury, World Neurosurg. 82 (2014) E535–E539. https://doi.org/10.1016/j.wneu.2013.01.009.

[61] S. Lord-Fontaine, F. Yang, Q. Diep, P. Dergham, S. Munzer, P. Tremblay, L. McKerracher, Local inhibition of Rho signaling by cell-permeable recombinant protein BA-210 prevents secondary damage and promotes functional recovery following acute spinal cord injury, J. Neurotrauma. 25 (2008) 1309–1322. https://doi.org/10.1089/neu.2008.0613.

[62] M.G. Fehlings, N. Theodore, J. Harrop, G. Maurais, C. Kuntz, C.I. Shaffrey, B.K. Kwon, J. Chapman, A. Yee, A. Tighe, L. McKerracher, A phase I/IIa clinical trial of a recombinant Rho protein antagonist in acute spinal cord injury, J. Neurotrauma. 28 (2011) 787–796. https://doi.org/10.1089/neu.2011.1765.

[63] L. Schnell, M.E. Schwab, Axonal regeneration in the rat spinal cord produced by an antibody against myelin-associated neurite growth inhibitors, Nature. 343 (1990) 269–272. https://doi.org/10.1038/343269a0.

[64] T. Liebscher, L. Schnell, D. Schnell, J. Scholl, R. Schneider, M. Gullo, K. Fouad, A. Mir, M. Rausch,

D. Kindler, F.P.T. Hamers, M.E. Schwab, Nogo-A antibody improves regeneration and locomotion of spinal cord-injured rats, Ann. Neurol. 58 (2005) 706–719. https://doi.org/10.1002/ana.20627.

[65] B. Zörner, M.E. Schwab, Anti-Nogo on the go: From animal models to a clinical trial, Ann. N. Y. Acad. Sci. 1198 (2010) 22–34. https://doi.org/10.1111/j.1749-6632.2010.05566.x.

[66] K. Kucher, D. Johns, D. Maier, R. Abel, A. Badke, H. Baron, R. Thietje, S. Casha, R. Meindl, B. Gomez-Mancilla, C. Pfister, R. Rupp, N. Weidner, A. Mir, M.E. Schwab, A. Curt, First-in-man intrathecal application of neurite growth-promoting anti-nogo- a antibodies in acute spinal cord injury, Neurorehabil. Neural Repair. 32 (2018) 578–589. https://doi.org/10.1177/1545968318776371.

[67] X. Wang, T. Zhou, G.D. Maynard, P.S. Terse, W.B. Cafferty, J.D. Kocsis, S.M. Strittmatter, Nogo receptor decoy promotes recovery and corticospinal growth in non-human primate spinal cord injury, Brain. (2020) 1–17. https://doi.org/10.1093/brain/awaa116.

[68] F. Cofano, M. Boido, M. Monticelli, F. Zenga, A. Ducati, A. Vercelli, D. Garbossa, Mesenchymal stem cells for spinal cord injury: Current options limitations, and future of cell therapy, Int. J. Mol. Sci. 20 (2019) 2698. https://doi.org/10.3390/ijms20112698.

[69] C.S. Ahuja, S. Nori, L. Tetreault, J. Wilson, B. Kwon, J. Harrop, D. Choi, M.G. Fehlings, Traumatic spinal cord injury - Repair and regeneration, Clin. Neurosurg. 80 (2017) S22–S90. https://doi.org/10.1093/neuros/nyw080.

[70] M. Bydon, A.B. Dietz, S. Goncalves, F.M. Moinuddin, M.A. Alvi, A. Goyal, Y. Yolcu, C.L. Hunt, K.L. Garlanger, A.S. Del Fabro, R.K. Reeves, A. Terzic, A.J. Windebank, W. Qu, CELLTOP Clinical Trial: First Report From a Phase 1 Trial of Autologous Adipose Tissue–Derived Mesenchymal Stem Cells in the Treatment of Paralysis Due to Traumatic Spinal Cord Injury, Mayo Clin. Proc. 95 (2020) 406–414. https://doi.org/10.1016/j.mayocp.2019.10.008.

[71] J. Vaquero, M. Zurita, M.A. Rico, C. Bonilla, C. Aguayo, J. Montilla, S. Bustamante, J. Carballido, E. Marin, F. Martinez, A. Parajon, C. Fernandez, L. De Reina, An approach to personalized cell therapy in chronic complete paraplegia: The Puerta de Hierro phase I/II clinical trial, Cytotherapy. 18 (2016) 1025–1036. https://doi.org/10.1016/j.jcyt.2016.05.003.

[72] Y.D. Teng, E.B. Lavik, X. Qu, K.I. Park, J. Ourednik, D. Zurakowski, R. Langer, E.Y. Snyder, Functional recovery following traumatic spinal cord injury mediated by a unique polymer scaffold seeded with neural stem cells, Proc. Natl. Acad. Sci. U. S. A. 99 (2002) 3024–3029. https://doi.org/10.1073/pnas.052678899.

[73] C.D. Pritchard, J.R. Slotkin, D. Yu, H. Dai, M.S. Lawrence, R.T. Bronson, F.M. Reynolds, Y.D. Teng, E.J. Woodard, R.S. Langer, Establishing a model spinal cord injury in the African green monkey for the preclinical evaluation of biodegradable polymer scaffolds seeded with human neural stem cells, J. Neurosci. Methods. 188 (2010) 258–269. https://doi.org/10.1016/j.jneumeth.2010.02.019.

[74] N. Theodore, R. Hlubek, J. Danielson, K. Neff, L. Vaickus, T.R. Ulich, A.E. Ropper, First human implantation of a bioresorbable polymer scaffold for acute traumatic spinal cord injury: A clinical pilot study for safety and feasibility, Neurosurgery. 79 (2016) E305–E312. https://doi.org/10.1227/NEU.0000000000001283.

[75] H.J. Lee, J.S. Ryu, P.J. Vig, Current strategies for therapeutic drug delivery after traumatic CNS injury, Ther. Deliv. 10 (2019) 251–263. https://doi.org/10.4155/tde-2019-0006.

[76] K.A. Follett, R.L. Boortz-Marx, J.M. Drake, S. DuPen, S.J. Schneider, M.S. Turner, R.J. Coffey, Prevention and management of intrathecal drug delivery and spinal cord stimulation system infections, Anesthesiology. 100 (2004) 1582–1594. https://doi.org/10.1097/00000542-200406000-00034.

[77] L.L. Jones, M.H. Tuszynski, Chronic intrathecal infusions after spinal cord injury cause scarring

and compression, Microsc. Res. Tech. 54 (2001) 317–324. https://doi.org/10.1002/jemt.1144.
[78] R.C. Assunção-Silva, E.D. Gomes, N. Sousa, N.A. Silva, A.J. Salgado, Hydrogels and Cell Based Therapies in Spinal Cord Injury Regeneration, Stem Cells Int. 2015 (2015). https://doi.org/10.1155/2015/948040.
[79] H.J. Lee, J.S. Ryu, P.J. Vig, Current strategies for therapeutic drug delivery after traumatic CNS injury, Ther. Deliv. 10 (2019) 251–263. https://doi.org/10.4155/tde-2019-0006.
[80] O. Steward, K.G. Sharp, K.M. Yee, M.N. Hatch, J.F. Bonner, Characterization of ectopic colonies that form in widespread areas of the nervous system with neural stem cell transplants into the site of a severe spinal cord injury, J. Neurosci. 34 (2014) 14013–14021. https://doi.org/10.1523/JNEUROSCI.3066-14.2014.
[81] P. Assinck, G.J. Duncan, B.J. Hilton, J.R. Plemel, W. Tetzlaff, Cell transplantation therapy for spinal cord injury, Nat. Neurosci. 20 (2017) 637–647. https://doi.org/10.1038/nn.4541.
[82] A.E. Haggerty, M. Oudega, Biomaterials for spinal cord repair, Neurosci. Bull. 29 (2013) 445–459. https://doi.org/10.1007/s12264-013-1362-7.
[83] A.M. Ziemba, R.J. Gilbert, Biomaterials for local, controlled drug delivery to the injured spinal cord, Front. Pharmacol. 8 (2017) 1–20. https://doi.org/10.3389/fphar.2017.00245.
[84] K. Xue, X. Wang, P.W. Yong, D.J. Young, Y.-L. Wu, Z. Li, X.J. Loh, Hydrogels as Emerging Materials for Translational Biomedicine, Adv. Ther. 2 (2019) 1800088. https://doi.org/10.1002/adtp.201800088.
[85] N.A. Peppas, J.Z. Hilt, A. Khademhosseini, R. Langer, Hydrogels in biology and medicine: From molecular principles to bionanotechnology, Adv. Mater. 18 (2006) 1345–1360. https://doi.org/10.1002/adma.200501612.
[86] M. Bahram, N. Mohseni, M. Moghtader, An Introduction to Hydrogels and Some Recent Applications, Emerg. Concepts Anal. Appl. Hydrogels. (2016). https://doi.org/10.5772/64301.
[87] C. Nishi, N. Nakajima, Y. Ikada, In vitro evaluation of cytotoxicity of diepoxy compounds used for biomaterial modification, J. Biomed. Mater. Res. 29 (1995) 829–834. https://doi.org/10.1002/jbm.820290707.
[88] K. Pal, V.K. Singh, A. Anis, G. Thakur, M.K. Bhattacharya, Hydrogel-Based Controlled Release Formulations: Designing Considerations, Characterization Techniques and Applications, Polym. - Plast. Technol. Eng. 52 (2013) 1391–1422. https://doi.org/10.1080/03602559.2013.823996.
[89] M. Azeera, S. Vaidevi, K. Ruckmani, Characterization Techniques of Hydrogel and Its Applications, (2019) 737–761. https://doi.org/10.1007/978-3-319-77830-3_25.
[90] A.S. Samaddar, P. Chatterjee, A. Roy, Thermosensitive heparin-poloxamer hydrogels enhance the effects of GDNF on neuronal circuit remodelling and neuroprotection after spinal cord injury, Microbiol. Res. 2 (2018) 1–38. https://doi.org/10.1016/j.micres.2018.11.005.
[91] V. V. Rostovtsev, L.G. Green, V. V. Fokin, K.B. Sharpless, A stepwise huisgen cycloaddition process: Copper(I)-catalyzed regioselective "ligation" of azides and terminal alkynes, Angew. Chemie - Int. Ed. 41 (2002) 2596–2599. https://doi.org/10.1002/1521-3773(20020715)41:14<2596::AID-ANIE2596>3.0.CO;2-4.
[92] C.W. Tornøe, C. Christensen, M. Meldal, Peptidotriazoles on solid phase: [1,2,3]-Triazoles by regiospecific copper(I)-catalyzed 1,3-dipolar cycloadditions of terminal alkynes to azides, J. Org. Chem. 67 (2002) 3057–3064. https://doi.org/10.1021/jo011148j.
[93] Z. He, H. Zang, L. Zhu, K. Huang, T. Yi, S. Zhang, S. Cheng, An anti-inflammatory peptide and brain-derived neurotrophic factor-modified hyaluronan-methylcellulose hydrogel promotes nerve regeneration in rats with spinal cord injury, Int. J. Nanomedicine. 14 (2019) 721–732. https://doi.org/10.2147/IJN.S187854.

[94] D. Macaya, M. Spector, Injectable hydrogel materials for spinal cord regeneration: A review, Biomed. Mater. 7 (2012). https://doi.org/10.1088/1748-6041/7/1/012001.
[95] J. Piantino, J.A. Burdick, D. Goldberg, R. Langer, L.I. Benowitz, An injectable, biodegradable hydrogel for trophic factor delivery enhances axonal rewiring and improves performance after spinal cord injury, Exp. Neurol. 201 (2006) 359–367. https://doi.org/10.1016/j.expneurol.2006.04.020.
[96] J. Leijten, J. Seo, K. Yue, G. Trujillo-de Santiago, A. Tamayol, G.U. Ruiz-Esparza, S.R. Shin, R. Sharifi, I. Noshadi, M.M. Álvarez, Y.S. Zhang, A. Khademhosseini, Spatially and temporally controlled hydrogels for tissue engineering, Mater. Sci. Eng. R Reports. 119 (2017) 1–35. https://doi.org/10.1016/j.mser.2017.07.001.
[97] A. Onaciu, R.A. Munteanu, A.I. Moldovan, C.S. Moldovan, I. Berindan-Neagoe, Hydrogels based drug delivery synthesis, characterization and administration, Pharmaceutics. 11 (2019). https://doi.org/10.3390/pharmaceutics11090432.
[98] N. Lorén, J. Hagman, J.K. Jonasson, H. Deschout, D. Bernin, F. Cella-Zanacchi, A. Diaspro, J.G. McNally, M. Ameloot, N. Smisdom, M. Nydén, A.M. Hermansson, M. Rudemo, K. Braeckmans, Fluorescence recovery after photobleaching in material and life sciences: Putting theory into practice, Q. Rev. Biophys. 48 (2015) 323–387. https://doi.org/10.1017/S0033583515000013.
[99] V. Ţucureanu, A. Matei, A.M. Avram, FTIR Spectroscopy for Carbon Family Study, Crit. Rev. Anal. Chem. 46 (2016) 502–520. https://doi.org/10.1080/10408347.2016.1157013.
[100] A. Alizadeh, L. Moradi, M. Katebi, J. Ai, M. Azami, B. Moradveisi, S.N. Ostad, Delivery of injectable thermo-sensitive hydrogel releasing nerve growth factor for spinal cord regeneration in rat animal model, J. Tissue Viability. (2020) 1–8. https://doi.org/10.1016/j.jtv.2020.06.008.
[101] C. Yan, D.J. Pochan, Rheological properties of peptide-based hydrogels for biomedical and other applications, Chem. Soc. Rev. 39 (2010) 3528–3540. https://doi.org/10.1039/b919449p.
[102] K.J. Lampe, R.G. Mooney, K.B. Bjugstad, M.J. Mahoney, Effect of macromer weight percent on neural cell growth in 2D and 3D nondegradable PEG hydrogel culture, J. Biomed. Mater. Res. - Part A. 94 (2010) 1162–1171. https://doi.org/10.1002/jbm.a.32787.
[103] S.K. Seidlits, Z.Z. Khaing, R.R. Petersen, J.D. Nickels, J.E. Vanscoy, J.B. Shear, C.E. Schmidt, The effects of hyaluronic acid hydrogels with tunable mechanical properties on neural progenitor cell differentiation, Biomaterials. 31 (2010) 3930–3940. https://doi.org/10.1016/j.biomaterials.2010.01.125.
[104] B.A.B. Jason C. Dugas, Adiljan Ibrahim, The T3-induced gene KLF9 regulates oligodendrocyte differentiation and myelin regeneration, Mol Cell Neurosci. 176 (2012) 139–148. https://doi.org/10.1016/j.physbeh.2017.03.040.
[105] R.B. Shultz, Z. Wang, J. Nong, Z. Zhang, Y. Zhong, Local delivery of thyroid hormone enhances oligodendrogenesis and myelination after spinal cord injury, J. Neural Eng. 14 (2017). https://doi.org/10.1088/1741-2552/aa6450.
[106] X. Chen, Y. Zhao, X. Li, Z. Xiao, Y. Yao, Y. Chu, B. Farkas, I. Romano, F. Brandi, J. Dai, Functional Multichannel Poly(Propylene Fumarate)-Collagen Scaffold with Collagen-Binding Neurotrophic Factor 3 Promotes Neural Regeneration After Transected Spinal Cord Injury, Adv. Healthc. Mater. 7 (2018) 1–13. https://doi.org/10.1002/adhm.201800315.
[107] Z.Z. Khaing, A. Ehsanipour, C.P. Hofstetter, S.K. Seidlits, Injectable Hydrogels for Spinal Cord Repair: A Focus on Swelling and Intraspinal Pressure, Cells Tissues Organs. 202 (2016) 67–84. https://doi.org/10.1159/000446697.
[108] H.L. Xu, F.R. Tian, C.T. Lu, J. Xu, Z.L. Fan, J.J. Yang, P.P. Chen, Y.D. Huang, J. Xiao, Y.Z. Zhao, Thermo-sensitive hydrogels combined with decellularised matrix deliver bFGF for the functional recovery of rats after a spinal cord injury, Sci. Rep. 6 (2016) 1–15.

https://doi.org/10.1038/srep38332.
[109] L.T.A. Hong, Y.M. Kim, H.H. Park, D.H. Hwang, Y. Cui, E.M. Lee, S. Yahn, J.K. Lee, S.C. Song, B.G. Kim, An injectable hydrogel enhances tissue repair after spinal cord injury by promoting extracellular matrix remodeling, Nat. Commun. 8 (2017) 1–14. https://doi.org/10.1038/s41467-017-00583-8.
[110] H. Ozawa, T. Matsumoto, T. Ohashi, M. Sato, S. Kokubun, Comparison of spinal cord gray matter and white matter softness: Measurement by pipette aspiration method, J. Neurosurg. 95 (2001) 221–224. https://doi.org/10.3171/spi.2001.95.2.0221.
[111] R.J. Oakland, R.M. Hall, R.K. Wilcox, D.C. Barton, The biomechanical response of spinal cord tissue to uniaxial loading, Proc. Inst. Mech. Eng. Part H J. Eng. Med. 220 (2006) 489–492. https://doi.org/10.1243/09544119JEIM135.
[112] M.C. Mosley, H.J. Lim, J. Chen, Y.H. Yang, S. Li, Y. Liu, L.A. Smith Callahan, Neurite extension and neuronal differentiation of human induced pluripotent stem cell derived neural stem cells on polyethylene glycol hydrogels containing a continuous Young's Modulus gradient, J. Biomed. Mater. Res. - Part A. 105 (2017) 824–833. https://doi.org/10.1002/jbm.a.35955.
[113] Q. Chai, Y. Jiao, X. Yu, Hydrogels for Biomedical Applications: Their Characteristics and the Mechanisms behind Them, Gels. 3 (2017) 6. https://doi.org/10.3390/gels3010006.
[114] J. Li, D.J. Mooney, Designing hydrogels for controlled drug delivery, Nat. Rev. Mater. 1 (2016). https://doi.org/10.1038/natrevmats.2016.71.
[115] S.T. Hess, S. Huang, A.A. Heikal, W.W. Webb, Biological and chemical applications of fluorescence correlation spectroscopy: A review, Biochemistry. 41 (2002) 697–705. https://doi.org/10.1021/bi0118512.
[116] T. Canal, N.A. Peppas, Correlation between mesh size and equilibrium degree of swelling of polymeric networks, J. Biomed. Mater. Res. 23 (1989) 1183–1193. https://doi.org/10.1002/jbm.820231007.
[117] N.R. Richbourg, N.A. Peppas, The swollen polymer network hypothesis: Quantitative models of hydrogel swelling, stiffness, and solute transport, Prog. Polym. Sci. 105 (2020) 101243. https://doi.org/10.1016/j.progpolymsci.2020.101243.
[118] B. Chen, J. He, H. Yang, Q. Zhang, L. Zhang, X. Zhang, E. Xie, C. Liu, R. Zhang, Y. Wang, L. Huang, D. Hao, Repair of spinal cord injury by implantation of bFGF-incorporated HEMA-MOETACL hydrogel in rats, Sci. Rep. 5 (2015) 1–10. https://doi.org/10.1038/srep09017.
[119] O. Yom-Tov, L. Neufeld, D. Seliktar, H. Bianco-Peled, A novel design of injectable porous hydrogels with in situ pore formation, Acta Biomater. 10 (2014) 4236–4246. https://doi.org/10.1016/j.actbio.2014.07.006.
[120] U. Freudenberg, A. Hermann, P.B. Welzel, K. Stirl, S.C. Schwarz, M. Grimmer, A. Zieris, W. Panyanuwat, S. Zschoche, D. Meinhold, A. Storch, C. Werner, A star-PEG-heparin hydrogel platform to aid cell replacement therapies for neurodegenerative diseases, Biomaterials. 30 (2009) 5049–5060. https://doi.org/10.1016/j.biomaterials.2009.06.002.
[121] M. Sefidgaran, Hydrogels in Controlled Drug Delivery Systems, 6 (2010) 125–131.
[122] P. Atallah, L. Schirmer, M. Tsurkan, Y.D. Putra Limasale, R. Zimmermann, C. Werner, U. Freudenberg, In situ-forming, cell-instructive hydrogels based on glycosaminoglycans with varied sulfation patterns, Biomaterials. 181 (2018) 227–239. https://doi.org/10.1016/j.biomaterials.2018.07.056.
[123] F. Ganji, S. Vasheghani-Farahani, E. Vasheghani-Farahani, Theoretical Description of Hydrogel Swelling: AReview Fariba, Iran. Polym. J. 7 (2010) 41–48.
[124] F. Lee, J.E. Chung, M. Kurisawa, An injectable hyaluronic acid-tyramine hydrogel system for protein delivery, J. Control. Release. 134 (2009) 186–193. https://doi.org/10.1016/j.jconrel.2008.11.028.

[125] A.E. Mohrman, M. Farrag, R.K. Grimm, N.D. Leipzig, Evaluation of in situ gelling chitosan-PEG copolymer for use in the spinal cord, J. Biomater. Appl. 33 (2018) 435–446. https://doi.org/10.1177/0885328218792824.
[126] H. Kamata, X. Li, U. Il Chung, T. Sakai, Design of Hydrogels for Biomedical Applications, Adv. Healthc. Mater. 4 (2015) 2360–2374. https://doi.org/10.1002/adhm.201500076.
[127] S. Reinicke, J. Schmelz, A. Lapp, M. Karg, T. Hellweg, H. Schmalz, Smart hydrogels based on double responsive triblock terpolymers, Soft Matter. 5 (2009) 2648–2657. https://doi.org/10.1039/b900539k.
[128] D.C. Harsh, S.H. Gehrke, Controlling the swelling characteristics of temperature-sensitive cellulose ether hydrogels, J. Control. Release. 17 (1991) 175–185. https://doi.org/10.1016/0168-3659(91)90057-K.
[129] M.A. Ward, T.K. Georgiou, Thermoresponsive polymers for biomedical applications, Polymers (Basel). 3 (2011) 1215–1242. https://doi.org/10.3390/polym3031215.
[130] K.S. Straley, C.W.P. Foo, S.C. Heilshorn, Biomaterial design strategies for the treatment of spinal cord injuries, J. Neurotrauma. 27 (2010) 1–19. https://doi.org/10.1089/neu.2009.0948.
[131] J. Park, E. Lim, S. Back, H. Na, Y. Park, K. Sun, Nerve regeneration following spinal cord injury using matrix metalloproteinase-sensitive, hyaluronic acid-based biomimetic hydrogel scaffold containing brain-derived neurotrophic factor, J. Biomed. Mater. Res. - Part A. 93 (2010) 1091–1099. https://doi.org/10.1002/jbm.a.32519.
[132] Z. Hassannejad, S.A. Zadegan, A.R. Vaccaro, V. Rahimi-Movaghar, O. Sabzevari, Biofunctionalized peptide-based hydrogel as an injectable scaffold for BDNF delivery can improve regeneration after spinal cord injury, Injury. 50 (2019) 278–285. https://doi.org/10.1016/j.injury.2018.12.027.
[133] H.E. Park, N. Gasek, J. Hwang, D.J. Weiss, P.C. Lee, Effect of temperature on gelation and cross-linking of gelatin methacryloyl for biomedical applications, Phys. Fluids. 32 (2020). https://doi.org/10.1063/1.5144896.
[134] C.A. McKay, R.D. Pomrenke, J.S. McLane, N.J. Schaub, E.K. Desimone, L.A. Ligon, R.J. Gilbert, An injectable, calcium responsive composite hydrogel for the treatment of acute spinal cord injury, ACS Appl. Mater. Interfaces. 6 (2014) 1424–1438. https://doi.org/10.1021/am4027423.
[135] S.M. Moghimi, A.C. Hunter, Poloxamers and poloxamines in nanoparticle engineering and experimental medicine, Trends Biotechnol. 18 (2000) 412–420. https://doi.org/10.1016/S0167-7799(00)01485-2.
[136] D. Liu, T. Jiang, W. Cai, J. Chen, H. Zhang, S. Hietala, H.A. Santos, G. Yin, J. Fan, An In Situ Gelling Drug Delivery System for Improved Recovery after Spinal Cord Injury, Adv. Healthc. Mater. 5 (2016) 1513–1521. https://doi.org/10.1002/adhm.201600055.
[137] S. Lakard, G. Herlem, A. Propper, A. Kastner, G. Michel, N. Vallès-Villarreal, T. Gharbi, B. Fahys, Adhesion and proliferation of cells on new polymers modified biomaterials, Bioelectrochemistry. 62 (2004) 19–27. https://doi.org/10.1016/j.bioelechem.2003.09.009.
[138] A. Hejčl, P. Lesný, M. Přádný, J. Šedý, J. Zámečník, P. Jendelová, J. Michálek, E. Syková, Macroporous hydrogels based on 2-hydroxyethyl methacrylate. Part 6: 3D hydrogels with positive and negative surface charges and polyelectrolyte complexes in spinal cord injury repair, J. Mater. Sci. Mater. Med. 20 (2009) 1571–1577. https://doi.org/10.1007/s10856-009-3714-4.
[139] T. Schackel, P. Kumar, M. Günther, S. Liu, M. Brunner, B. Sandner, R. Puttagunta, R. Müller, N. Weidner, A. Blesch, Peptides and Astroglia Improve the Regenerative Capacity of Alginate Gels in the Injured Spinal Cord, Tissue Eng. - Part A. 25 (2019) 522–537. https://doi.org/10.1089/ten.tea.2018.0082.
[140] N.J. Tester, A.H. Plaas, D.R. Howland, Effect of Body Temperature on Chondroitinase ABC's Ability To Cleave Chondroitin Sulfate Glycosaminoglycans Nicole, J. Neurosci. Res. 85 (2007) 1110–1118. https://doi.org/10.1002/jnr.

[141] M.M. Pakulska, K. Vulic, M.S. Shoichet, Affinity-based release of chondroitinase ABC from a modified methylcellulose hydrogel, J. Control. Release. 171 (2013) 11–16. https://doi.org/10.1016/j.jconrel.2013.06.029.
[142] M.M. Pakulska, C.H. Tator, M.S. Shoichet, Local delivery of chondroitinase ABC with or without stromal cell-derived factor 1α promotes functional repair in the injured rat spinal cord, Biomaterials. 134 (2017) 13–21. https://doi.org/10.1016/j.biomaterials.2017.04.016.
[143] Q. Wang, Y. He, Y. Zhao, H. Xie, Q. Lin, Z. He, X. Wang, J. Li, H. Zhang, C. Wang, F. Gong, X. Li, H. Xu, Q. Ye, J. Xiao, A Thermosensitive Heparin-Poloxamer Hydrogel Bridges aFGF to Treat Spinal Cord Injury, ACS Appl. Mater. Interfaces. 9 (2017) 6725–6745. https://doi.org/10.1021/acsami.6b13155.
[144] P.M. Medberry, Christopher J. Crapo, B.F. Siu, C.A. Carruthers, M.T. Wolf, S.P. Nagarkar, V. Agrawal, K.E. Jones, J. Kelly, S.A. Johnson, S.S. Velankar, S.C. Watkins, M. Modo, S.F. Badylak, Hydrogels Derived from Central Nervous System Extracellular Matrix, Biomaterials. 34 (2013) 1033–1040. https://doi.org/10.1007/s11103-011-9767-z.Plastid.
[145] H.L. Xu, F.R. Tian, J. Xiao, P.P. Chen, J. Xu, Z.L. Fan, J.J. Yang, C.T. Lu, Y.Z. Zhao, Sustained-release of FGF-2 from a hybrid hydrogel of heparin-poloxamer and decellular matrix promotes the neuroprotective effects of proteins after spinal injury, Int. J. Nanomedicine. 13 (2018) 681–694. https://doi.org/10.2147/IJN.S152246.
[146] R.C. Robinson, C. Radziejewski, G. Spraggon, J. Greenwald, M.R. Kostura, L.D. Burtnick, D.I. Stuart, S. Choe, E.Y. Jones, The structures of the neurotrophin 4 homodimer and the brain-derived neurotrophic factor/neurotrophin 4 heterodimer reveal a common Trk-binding site., Protein Sci. 8 (1999) 2589–2597.
[147] I. Elliott Donaghue, C.H. Tator, M.S. Shoichet, Sustained delivery of bioactive neurotrophin-3 to the injured spinal cord, Biomater. Sci. 3 (2015) 65–72. https://doi.org/10.1039/c4bm00311j.
[148] A.H. Sheikh, B. Raghuram, L. Eschen-lippold, D. Scheel, Local delivery of neurotrophin-3 and anti-NogoA promotes repair after spinal cord injury, v (2017) 1–36. https://doi.org/10.2174/138161211796197016.
[149] Y. Cho, R. Shi, R.B. Borgens, Chitosan produces potent neuroprotection and physiological recovery following traumatic spinal cord injury, J. Exp. Biol. 213 (2010) 1513–1520. https://doi.org/10.1242/jeb.035162.
[150] M. Boido, M. Ghibaudi, P. Gentile, E. Favaro, R. Fusaro, C. Tonda-Turo, Chitosan-based hydrogel to support the paracrine activity of mesenchymal stem cells in spinal cord injury treatment, Sci. Rep. 9 (2019) 1–16. https://doi.org/10.1038/s41598-019-42848-w.
[151] J.S. Rao, C. Zhao, A. Zhang, H. Duan, P. Hao, R.H. Wei, J. Shang, W. Zhao, Z. Liu, J. Yu, K.S. Fan, Z. Tian, Q. He, W. Song, Z. Yang, Y.E. Sun, X. Li, NT3-chitosan enables de novo regeneration and functional recovery in monkeys after spinal cord injury, Proc. Natl. Acad. Sci. U. S. A. 115 (2018) E5595–E5604. https://doi.org/10.1073/pnas.1804735115.
[152] B. Ghosh, Z. Wang, J. Nong, M.W. Urban, Z. Zhang, V.A. Trovillion, M.C. Wright, Y. Zhong, A.C. Lepore, Local BDNF delivery to the injured cervical spinal cord using an engineered hydrogel enhances diaphragmatic respiratory function, J. Neurosci. 38 (2018) 5982–5995. https://doi.org/10.1523/JNEUROSCI.3084-17.2018.
[153] E. Vecino, J.C.F. Kwok, The Extracellular Matrix in the Nervous System: The Good and the Bad Aspects, Compos. Funct. Extracell. Matrix Hum. Body. (2016). https://doi.org/10.5772/62527.
[154] C. Tonda-Turo, F. Ruini, M. Ramella, F. Boccafoschi, P. Gentile, E. Gioffredi, G. Falvo D'Urso Labate, G. Ciardelli, Non-covalently crosslinked chitosan nanofibrous mats prepared by electrospinning as substrates for soft tissue regeneration, Carbohydr. Polym. 162 (2017) 82–92. https://doi.org/10.1016/j.carbpol.2017.01.050.
[155] P.G. Popovich, C.A. Tovar, S. Lemesshoe, Q. Yin, L.B. Jakeman, Independent evaluation of the

anatomical and behavioral effects of Taxol in rat models of spinal cord injury, Exp. Neurol. (2015) 97–108. https://doi.org/10.1016/j.expneurol.2014.06.020.Independent.
[156] Q. Wang, H. Zhang, H. Xu, Y. Zhao, Z. Li, J. Li, H. Wang, D. Zhuge, X. Guo, H. Xu, S. Jones, X. Li, X. Jia, J. Xiao, Novel multi-drug delivery hydrogel using scar-homing liposomes improves spinal cord injury repair, Theranostics. 8 (2018) 4429–4446. https://doi.org/10.7150/thno.26717.
[157] G.M. Soliman, A.O. Choi, D. Maysinger, F.M. Winnik, Minocycline block copolymer micelles and their anti-inflammatory effects on microglia, Macromol. Biosci. 10 (2010) 278–288. https://doi.org/10.1002/mabi.200900259.
[158] Z. Zhang, Z. Wang, J. Nong, C.A. Nix, H.-F. Ji, Y. Zhong, Metal ion-assisted self-assembly of complexes for controlled and sustained release of minocycline for biomedical applications, Biofabrication. 7 (2016) 1–25. https://doi.org/10.1088/1758-5090/7/1/015006.Metal.
[159] Z. Wang, J. Nong, R.B. Shultz, Z. Zhang, V.J. Tom, R.K. Ponnappan, Y. Zhong, Local delivery of minocycline from metal ion-assisted self-assembled complexes promotes neuroprotection and functional recovery after spinal cord injury, Biomaterials. 112 (2017) 62–71. https://doi.org/10.1016/j.biomaterials.2016.10.002.
[160] B. Ghosh, J. Nong, Z. Wang, M.W. Urban, N.M. Heinsinger, V.A. Trovillion, M.C. Wright, A.C. Lepore, Y. Zhong, A hydrogel engineered to deliver minocycline locally to the injured cervical spinal cord protects respiratory neural circuitry and preserves diaphragm function, Neurobiol. Dis. 127 (2019) 591–604. https://doi.org/10.1016/j.nbd.2019.04.014.
[161] X. Lu, T.H. Perera, A.B. Aria, L.A.S. Callahan, Polyethylene glycol in spinal cord injury repair: A critical review, J. Exp. Pharmacol. 10 (2018) 37–49. https://doi.org/10.2147/JEP.S148944.
[162] R. Censi, P. Di Martino, T. Vermonden, W.E. Hennink, Hydrogels for protein delivery in tissue engineering, J. Control. Release. 161 (2012) 680–692. https://doi.org/10.1016/j.jconrel.2012.03.002.
[163] S. Ren, Z.H. Liu, Q. Wu, K. Fu, J. Wu, L.T. Hou, M. Li, X. Zhao, Q. Miao, Y.L. Zhao, S.Y. Wang, Y. Xue, Z. Xue, Y.S. Guo, S. Canavero, X.P. Ren, Polyethylene glycol-induced motor recovery after total spinal transection in rats, CNS Neurosci. Ther. 23 (2017) 680–685. https://doi.org/10.1111/cns.12713.
[164] X. Bin Kong, Q.Y. Tang, X.Y. Chen, Y. Tu, S.Z. Sun, Z.L. Sun, Polyethylene glycol as a promising synthetic material for repair of spinal cord injury, Neural Regen. Res. 12 (2017) 1003–1008. https://doi.org/10.4103/1673-5374.208597.
[165] J. Luo, R. Shi, Polyethylene glycol inhibits apoptotic cell death following traumatic spinal cord injury, Brain Res. 1155 (2007) 10–16. https://doi.org/10.1016/j.brainres.2007.03.091.
[166] I. Elliott Donaghue, M.S. Shoichet, Controlled release of bioactive PDGF-AA from a hydrogel/nanoparticle composite, Acta Biomater. 25 (2015) 35–42. https://doi.org/10.1016/j.actbio.2015.08.002.
[167] R.M. Namba, A.A. Cole, K.B. Bjugstad, M.J. Mahoney, Development of porous PEG hydrogels that enable efficient, uniform cell-seeding and permit early neural process extension, Acta Biomater. 5 (2009) 1884–1897. https://doi.org/10.1016/j.actbio.2009.01.036.
[168] S.-Q.K.S.O.D.T. Hagop Kantarjian Guillermo Garcia-Manero Hui Yang, Three-dimensional scaffolding to investigate neuronal derivatives of human embryonic stem cells, Bone. 23 (2005) 1–7. https://doi.org/10.1007/s10544-012-9662-7.Three-dimensional.
[169] X.Q. Zheng, J.F. Huang, J.L. Lin, Y.X. Zhu, M.Q. Wang, M.L. Guo, X.J. Zan, A.M. Wu, Controlled release of baricitinib from a thermos-responsive hydrogel system inhibits inflammation by suppressing JAK2/STAT3 pathway in acute spinal cord injury, Colloids Surfaces B Biointerfaces. 199 (2021) 111532. https://doi.org/10.1016/j.colsurfb.2020.111532.
[170] I. Capila, R.J. Linhardt, Heparin-protein interactions, Angew. Chemie - Int. Ed. 41 (2002) 390–412. https://doi.org/10.1021/j150493a017.

[171] D.R. Coombe, Biological implications of glycosaminoglycan interactions with haemopoietic cytokines, Immunol. Cell Biol. 86 (2008) 598–607. https://doi.org/10.1038/icb.2008.49.
[172] S. Roy, H. Lai, R. Zouaoui, J. Duffner, H. Zhou, L. P Jayaraman, G. Zhao, T. Ganguly, T.K. Kishimoto, G. Venkataraman, Bioactivity screening of partially desulfated low-molecular-weight heparins: A structure/activity relationship study, Glycobiology. 21 (2011) 1194–1205. https://doi.org/10.1093/glycob/cwr053.
[173] O. Ostrovsky, B. Berman, J. Gallagher, B. Mulloy, D.G. Fernig, M. Delehedde, D. Ron, Differential effects of heparin saccharides on the formation of specific fibroblast growth factor (FGF) and FGF receptor complexes, J. Biol. Chem. 277 (2002) 2444–2453. https://doi.org/10.1074/jbc.M108540200.
[174] U. Freudenberg, A. Hermann, P.B. Welzel, K. Stirl, S.C. Schwarz, M. Grimmer, A. Zieris, W. Panyanuwat, S. Zschoche, D. Meinhold, A. Storch, C. Werner, A star-PEG-heparin hydrogel platform to aid cell replacement therapies for neurodegenerative diseases, Biomaterials. 30 (2009) 5049–5060. https://doi.org/10.1016/j.biomaterials.2009.06.002.
[175] M. V. Tsurkan, K. Chwalek, S. Prokoph, A. Zieris, K.R. Levental, U. Freudenberg, C. Werner, Defined polymer-peptide conjugates to form cell-instructive starpeg-heparin matrices in situ, Adv. Mater. 25 (2013) 2606–2610. https://doi.org/10.1002/adma.201300691.
[176] M. V. Tsurkan, K. Chwalek, K.R. Levental, U. Freudenberg, C. Werner, Modular StarPEG-heparin gels with bifunctional peptide linkers, Macromol. Rapid Commun. 31 (2010) 1529–1533. https://doi.org/10.1002/marc.201000155.
[177] A. Watarai, L. Schirmer, S. Thönes, U. Freudenberg, C. Werner, J.C. Simon, U. Anderegg, TGFβ functionalized starPEG-heparin hydrogels modulate human dermal fibroblast growth and differentiation, Acta Biomater. 25 (2015) 65–75. https://doi.org/10.1016/j.actbio.2015.07.036.
[178] L. Schirmer, P. Atallah, C. Werner, U. Freudenberg, StarPEG-Heparin Hydrogels to Protect and Sustainably Deliver IL-4, Adv. Healthc. Mater. 5 (2016) 3157–3164. https://doi.org/10.1002/adhm.201600797.
[179] M. Kassem, M. Kristiansen, B.M. Abdallah, Mesenchymal stem cells: Cell biology and potential use in therapy, Basic Clin. Pharmacol. Toxicol. 95 (2004) 209–214. https://doi.org/10.1111/j.1742-7843.2004.pto950502.x.
[180] S. Wang, X. Qu, R.C. Zhao, Mesenchymal stem cells hold promise for regenerative medicine, Front. Med. China. 5 (2011) 372–378. https://doi.org/10.1007/s11684-011-0164-4.
[181] M. Dominici, K. Le Blanc, I. Mueller, I. Slaper-Cortenbach, F.C. Marini, D.S. Krause, R.J. Deans, A. Keating, D.J. Prockop, E.M. Horwitz, Minimal criteria for defining multipotent mesenchymal stromal cells. The International Society for Cellular Therapy position statement, Cytotherapy. 8 (2006) 315–317. https://doi.org/10.1080/14653240600855905.
[182] R.M. Samsonraj, M. Raghunath, V. Nurcombe, J.H. Hui, A.J. van Wijnen, S.M. Cool, Concise Review: Multifaceted Characterization of Human Mesenchymal Stem Cells for Use in Regenerative Medicine, Stem Cells Transl. Med. 6 (2017) 2173–2185. https://doi.org/10.1002/sctm.17-0129.
[183] A. J. Braga Osorio Gomes Salgado, R. L. Goncalves Reis, N. Jorge Carvalho Sousa, J. M. Gimble, A. J. Salgado, R. L. Reis, N. Sousa, Adipose Tissue Derived Stem Cells Secretome: Soluble Factors and Their Roles in Regenerative Medicine, Curr. Stem Cell Res. Ther. 5 (2010) 103–110. https://doi.org/10.2174/157488810791268564.
[184] S. Lu, C. Lu, Q. Han, J. Li, Z. Du, L. Liao, R.C. Zhao, Adipose-derived mesenchymal stem cells protect PC12 cells from glutamate excitotoxicity-induced apoptosis by upregulation of XIAP through PI3-K/Akt activation, Toxicology. 279 (2011) 189–195. https://doi.org/10.1016/j.tox.2010.10.011.

[185] S.K. Kang, E.S. Jun, Y.C. Bae, J.S. Jung, Interactions between human adipose stromal cells and mouse neural stem cells in vitro, Dev. Brain Res. 145 (2003) 141–149. https://doi.org/10.1016/S0165-3806(03)00224-4.
[186] S.N. Rafiei Alavi, A. Madani Neishaboori, H. Hossein, A. Sarveazad, M. Yousefifard, Efficacy of adipose tissue-derived stem cells in locomotion recovery after spinal cord injury: a systematic review and meta-analysis on animal studies, Syst. Rev. 10 (2021). https://doi.org/10.1186/s13643-021-01771-w.
[187] E.D. Gomes, S.S. Mendes, H. Leite-Almeida, J.M. Gimble, R.Y. Tam, M.S. Shoichet, N. Sousa, N.A. Silva, A.J. Salgado, Combination of a peptide-modified gellan gum hydrogel with cell therapy in a lumbar spinal cord injury animal model, Biomaterials. 105 (2016) 38–51. https://doi.org/10.1016/j.biomaterials.2016.07.019.
[188] E.D. Gomes, S.S. Mendes, R.C. Assunção-Silva, F.G. Teixeira, A.O. Pires, S.I. Anjo, B. Manadas, H. Leite-Almeida, J.M. Gimble, N. Sousa, A.C. Lepore, N.A. Silva, A.J. Salgado, Co-Transplantation of Adipose Tissue-Derived Stromal Cells and Olfactory Ensheathing Cells for Spinal Cord Injury Repair, Stem Cells. 36 (2018) 696–708. https://doi.org/10.1002/stem.2785.
[189] E.D. Gomes, B. Ghosh, R. Lima, M. Goulão, T. Moreira-Gomes, J. Martins-Macedo, M.W. Urban, M.C. Wright, J.M. Gimble, N. Sousa, N.A. Silva, A.C. Lepore, A.J. Salgado, Combination of a Gellan Gum-Based Hydrogel With Cell Therapy for the Treatment of Cervical Spinal Cord Injury, Front. Bioeng. Biotechnol. 8 (2020) 1–14. https://doi.org/10.3389/fbioe.2020.00984.
[190] C.C. Chen, S.F. Yang, I.K. Wang, S.Y. Hsieh, J.X. Yu, T.L. Wu, W.J. Huang, M.H. Su, H.L. Yang, P.C. Chang, A.C. Teng, C. Chia-Yi, S.L. Liang, The Long-Term Efficacy Study of Multiple Allogeneic Canine Adipose Tissue-Derived Mesenchymal Stem Cells Transplantations Combined With Surgery in Four Dogs With Lumbosacral Spinal Cord Injury, Cell Transplant. 31 (2022). https://doi.org/10.1177/09636897221081487.
[191] F. Mussano, T. Genova, M. Corsalini, G. Schierano, F. Pettini, D. Di Venere, S. Carossa, Cytokine, Chemokine, and Growth Factor Profile Characterization of Undifferentiated and Osteoinduced Human Adipose-Derived Stem Cells, Stem Cells Int. 2017 (2017). https://doi.org/10.1155/2017/6202783.
[192] D.W. Greening, R.J. Simpson, Understanding extracellular vesicle diversity–current status, Expert Rev. Proteomics. 15 (2018) 887–910. https://doi.org/10.1080/14789450.2018.1537788.
[193] A.O. Pires, B. Mendes-Pinheiro, F.G. Teixeira, S.I. Anjo, S. Ribeiro-samy, E.D. Gomes, S.C. Serra, N.A. Silva, B. Manadas, A.J. Salgado, Unveiling the Differences of Secretome of Human Bone Marrow Mesenchymal Stem Cells, Adipose Tissue derived Stem Cells and Human Umbilical Cord Perivascular Cells: A Proteomic Analysis, Stem Cells Dev. 25 (2016) 1073–1083. https://doi.org/10.1089/scd.2016.0048.
[194] R.C. Assunção-Silva, B. Mendes-Pinheiro, P. Patrício, L.A. Behie, F.G. Teixeira, L. Pinto, A.J. Salgado, Exploiting the impact of the secretome of MSCs isolated from different tissue sources on neuronal differentiation and axonal growth, Biochimie. 155 (2018) 83–91. https://doi.org/10.1016/j.biochi.2018.07.026.
[195] M.I. Guillén, J. Platas, M.D. Pérez del Caz, V. Mirabet, M.J. Alcaraz, Paracrine anti-inflammatory effects of adipose tissue-derived mesenchymal stem cells in human monocytes, Front. Physiol. 9 (2018) 1–10. https://doi.org/10.3389/fphys.2018.00661.
[196] C.A. Ribeiro, J.S. Fraga, M. Grãos, N.M. Neves, R.L. Reis, J.M. Gimble, N. Sousa, A.J. Salgado, The secretome of stem cells isolated from the adipose tissue and Wharton jelly acts differently on central nervous system derived cell populations, Stem Cell Res. Ther. 3 (2012) 18. https://doi.org/10.1186/scrt109.
[197] S.C. Serra, J.C. Costa, R.C. Assunção-Silva, F.G. Teixeira, N.A. Silva, S.I. Anjo, B. Manadas, J.M. Gimble, L.A. Behie, A.J. Salgado, Influence of passage number on the impact of the secretome of

adipose tissue stem cells on neural survival, neurodifferentiation and axonal growth, Biochimie. 155 (2018) 119–128. https://doi.org/10.1016/j.biochi.2018.09.012.
[198] L.A. Rocha, E.D. Gomes, J.L. Afonso, S. Granja, F. Baltazar, N.A. Silva, M.S. Shoichet, R.A. Sousa, D.A. Learmonth, A.J. Salgado, In vitro Evaluation of ASCs and HUVECs Co-cultures in 3D Biodegradable Hydrogels on Neurite Outgrowth and Vascular Organization, Front. Cell Dev. Biol. 8 (2020) 1–14. https://doi.org/10.3389/fcell.2020.00489.
[199] E. Szekiova, L. Slovinska, J. Blasko, J. Plsikova, D. Cizkova, The neuroprotective effect of rat adipose tissue-derived mesenchymal stem cell-conditioned medium on cortical neurons using an in vitro model of SCI inflammation, Neurol. Res. 40 (2018) 258–267. https://doi.org/10.1080/01616412.2018.1432266.
[200] H. Valadi, K. Ekström, A. Bossios, M. Sjöstrand, J.J. Lee, J.O. Lötvall, Exosome-mediated transfer of mRNAs and microRNAs is a novel mechanism of genetic exchange between cells, Nat. Cell Biol. 9 (2007) 654–659. https://doi.org/10.1038/ncb1596.
[201] B. Mead, S. Tomarev, Bone Marrow-Derived Mesenchymal Stem Cells-Derived Exosomes Promote Survival of Retinal Ganglion Cells Through miRNA-Dependent Mechanisms, Stem Cells Transl. Med. (2017) 1273–1285. https://doi.org/10.1002/sctm.12056.
[202] Y. Rong, W. Liu, J. Wang, J. Fan, Y. Luo, L. Li, F. Kong, J. Chen, P. Tang, W. Cai, Neural stem cell-derived small extracellular vesicles attenuate apoptosis and neuroinflammation after traumatic spinal cord injury by activating autophagy, Cell Death Dis. 10 (2019). https://doi.org/10.1038/s41419-019-1571-8.
[203] A.G. Pinho, J.R. Cibrão, R. Lima, E.D. Gomes, S.C. Serra, J. Lentilhas-Graça, C. Ribeiro, S. Lanceros-Mendez, S.F.G. Teixeira, S. Monteiro, N.A. Silva, A.J. Salgado, Immunomodulatory and regenerative effects of the full and fractioned adipose tissue derived stem cells secretome in spinal cord injury, Exp. Neurol. 351 (2022) 113989. https://doi.org/10.1016/j.expneurol.2022.113989.
[204] E. Thomas Pashuck, M.M. Stevens, Designing regenerative biomaterial therapies for the clinic, Sci. Transl. Med. 4 (2012). https://doi.org/10.1126/scitranslmed.3002717.
[205] Z. Nazemi, M.S. Nourbakhsh, S. Kiani, Y. Heydari, M.K. Ashtiani, H. Daemi, H. Baharvand, Co-delivery of minocycline and paclitaxel from injectable hydrogel for treatment of spinal cord injury, J. Control. Release. 321 (2020) 145–158. https://doi.org/10.1016/j.jconrel.2020.02.009.
[206] K. Yamane, T. Mazaki, Y. Shiozaki, A. Yoshida, K. Shinohara, M. Nakamura, Y. Yoshida, D. Zhou, T. Kitajima, M. Tanaka, Y. Ito, T. Ozaki, A. Matsukawa, Collagen-Binding Hepatocyte Growth Factor (HGF) alone or with a Gelatin-furfurylamine Hydrogel Enhances Functional Recovery in Mice after Spinal Cord Injury, Sci. Rep. 8 (2018) 1–12. https://doi.org/10.1038/s41598-018-19316-y.
[207] B. Ghosh, Z. Wang, J. Nong, M.W. Urban, Z. Zhang, V.A. Trovillion, M.C. Wright, Y. Zhong, A.C. Lepore, Local BDNF delivery to the injured cervical spinal cord using an engineered hydrogel enhances diaphragmatic respiratory function, J. Neurosci. 38 (2018) 5982–5995. https://doi.org/10.1523/JNEUROSCI.3084-17.2018.
[208] J.M. Kwiecien, L. Zhang, J.R. Yaron, L.N. Schutz, C.J. Kwiecien-Delaney, E.A. Awo, M. Burgin, W. Dabrowski, A.R. Lucas, Local Serpin Treatment via Chitosan-Collagen Hydrogel after Spinal Cord Injury Reduces Tissue Damage and Improves Neurologic Function, J. Clin. Med. 9 (2020) 1221. https://doi.org/10.3390/jcm9041221.
[209] C. Wang, Z. Gong, X. Huang, J. Wang, K. Xia, L. Ying, J. Shu, C. Yu, X. Zhou, F. Li, C. Liang, Q. Chen, An injectable heparin-Laponite hydrogel bridge FGF4 for spinal cord injury by stabilizing microtubule and improving mitochondrial function, Theranostics. 9 (2019) 7016–7032. https://doi.org/10.7150/thno.37601.
[210] A. Guijarro-Belmar, M. Viskontas, Y. Wei, X. Bo, D. Shewan, W. Huang, Epac2 Elevation Reverses Inhibition by Chondroitin Sulfate Proteoglycans In Vitro and Transforms Postlesion Inhibitory

Environment to Promote Axonal Outgrowth in an Ex Vivo Model of Spinal Cord Injury, J. Neurosci. 39 (2019) 8330–8346. https://doi.org/10.1523/JNEUROSCI.0374-19.2019.

[211] Y.Z. Zhao, X. Jiang, J. Xiao, Q. Lin, W.Z. Yu, F.R. Tian, K.L. Mao, W. Yang, H.L. Wong, C.T. Lu, Using NGF heparin-poloxamer thermosensitive hydrogels to enhance the nerve regeneration for spinal cord injury, Acta Biomater. 29 (2016) 71–80. https://doi.org/10.1016/j.actbio.2015.10.014.

CHAPTER II

Sustained Release of hASCs Secretome from StarPEG-GAG Hydrogels promotes neuronal differentiation of hNPCS and neurite outgrowth in organotypic spinal cord slices

This chapter is part of published work in an international peer reviewed journal:

Sustained Release of Human Adipose Tissue Stem Cell Secretome from Star-Shaped Poly (ethylene glycol) Glycosaminoglycan Hydrogels Promotes Motor Improvements after Complete Transection in Spinal Cord Injury Rat Model

Deolinda Silva; Lucas Schirmer; Tiffany S. Pinho; Passant Atallah; Jorge R. Cibrão; Rui Lima; João Afonso; Sandra B-Antunes; Cláudia R. Marques; João Dourado; Uwe Freudenberg; Rui A. Sousa; Carsten Werner; António J. Salgado

Advanced Healthcare Materials

2023

Sustained Release of hASCs Secretome from StarPEG-GAG Hydrogels promotes neuronal differentiation of hNPCS and neurite outgrowth in organotypic spinal cord slices

Deolinda Silva [1,2,3]; Lucas Schirmer [4]; Tiffany S. Pinho[1,2,3]; Passant Atallah [4]; Jorge R. Cibrão[1,2]; Rui Lima[1,2]; João Afonso[1,2]; Sandra B-Antunes[1,2,3]; Cláudia R. Marques[1,2]; João Dourado[5]; Uwe Freudenberg[4]; Rui A. Sousa [3]; Carsten Werner [4,6*]; António J. Salgado[1,2*]

[1] Life and Health Sciences Research Institute (ICVS), School of Medicine, University of Minho, Campus de Gualtar, 4710-057 Braga, Portugal;

[2] ICVS/3B's – PT Government Associated Laboratory, Braga/Guimarães, Portugal;

[3]Stemmatters, Biotecnologia e Medicina Regenerativa SA, Guimarães, Portugal;

[4]Leibniz Institute of Polymer Research Dresden (IPF), Max Bergmann Center of Biomaterials Dresden (MBC), Dresden, Germany;

[5]School of Medicine, University of Minho, Campus de Gualtar, 4710-057 Braga, Portugal

[6]Technische Universität Dresden, Center for Regenerative Therapies Dresden (CRTD), Dresden, Germany;

*These authors shared senior authorship

Corresponding author

António Salgado – asalgado@med.uminho.pt

Abstract

Inducing tissue regeneration after a spinal cord injury (SCI) is critical for motor and sensory recovery. In this regard, ASC transplantation has been demonstrated to be a promising tool in the field. Several studies have revealed their role in promoting motor recovery, primarily by reducing the inflammatory response following lesion. Most importantly, those effects are thought to be modulated through bioactive molecules secreted by them. This shifted the spotlight on cell-free therapy for secretome. However, their administration is a source of concern. Using starPEG-Hep hydrogels as delivery systems, we aimed to develop a platform to load and release the hASCs secretome for an extended period of time at lesion site. In the present work, we show that secretome is continuously released for 10 days. Furthermore, a wide range of molecules were detected to be released in a time-dependent manner. Cytokines and angiogenic factors were primarily released after 2 days, while neuroregulatory growth factors were released between 2 and 10 days. Additionally, the secretome released from starPEG-Hep hydrogels could promote higher neuronal differentiation into immature (DCX) and mature (MAP2) neurons.

Finally, secretome released from hydrogels promoted robust neurite outgrowth in spinal cord slice organotypic cultures. Overall, the data presented here strongly supports the use of hASCs secretome in CNS injuries due to their ability to modulate regenerative processes. Local treatment can also be extended and potentiated by using as drug delivery systems.

Keywords

Spinal cord injury

Hydrogels

Secretome

Delivery systems

StarPEG

Heparin

1. Introduction

Central nervous system (CNS) has a low regenerative capacity. In spinal cord injury (SCI) axons fail to regrow either by the inhibitory environment at lesion site [1] or the glial scar formation [2] that acts as a barrier for regenerative processes. Furthermore, molecules released from the components of glial scar or myelin debris create an inhibitory environment for growth cone formation and axonal elongation [3]. The major challenge in regenerative medicine is to develop therapies that could overcome these events and induce tissue regeneration. In this sense, several approaches have been used as neurotrophic factors. They have the ability to support survival, growth or induce neuronal differentiation [4]. Brain derived neurotrophic factor (BDNF) has a critical role in promoting axonal growth and guidance [5]. Moreover, its overexpression in bone marrow stromal cells (BMSCs) promoted higher host axonal growth in an SCI animal model [6]. GDNF can also have a neuroprotective role in decreasing dopaminergic loss in Parkinson's disease model [7]. Other strategies tried to induce regeneration by administering drugs such as methylprednisolone (MPSS) which is an anti-inflammatory agent that could improve motor outcomes in SCI patients [8]. Minocycline (MH) is also used due to their potential to inhibit microglia activation, proliferation, reduce excitotoxicity and neuronal death [9].

However, several restrictions are raised in regarding to their administration. Due to the existence of blood brain barrier (BBB), systemically administered molecules may have difficulty passing through this barrier and acting in tissue, as the need of high dose may cause off-target systemic effects and fast diffusion to other organs [10]. Indeed, some drugs that reach clinical trials, fail their progression to clinics due to severe side effects caused [11]. In addition, molecules can have short half-life or be more prone to enzymatic degradation. This has led to the development of different administration routes, namely as intracerebral or intracranial [12] application using catheters or minipumps [13,14]. Nevertheless, these approaches have also been demonstrated has being invasive and could promote further damage in the tissue. Thus, with the advent of delivery strategies the design of biohybrid matrices has been shown to be capable of slow and controlled target release inducing desired regenerative processes, with appropriate dose. Therefore, biomaterials have emerged has suitable candidates to local deliver of therapeutic agents, in particular hydrogels. They can be divided into natural or synthetic materials. Natural materials include agarose [15], gellan gum [16], or alginate [17], which have the advantage of good biocompatibility and degradability. However, in recent years the interest in synthetic materials, like polyethylene glycol (PEG) [18], poloxamers [19] or HEMA [20], is concerned with the easy modulation of mechanical properties in order to improve their use for biomedical implantation. Freudenberg et al., for example, developed a hybrid material based on star-shaped poly (ethylene glycol) (starPEG) and heparin, which physical and

bimolecular characteristics can be gradually and independently modulated [21]. The degree of crosslinking during meshwork structure development can easily control mechanical stiffness, mesh size, and swelling degree [22]. As heparin inclusion plays a vital role in delivery techniques, this opens up new opportunities for the use of hydrogels as acceptable matrices for regenerative therapies. Heparin is a linear structure containing sulfate groups at N-, 2-O-, 6-O- position, resulting in high density charges. Spatial distribution of sulfate units gives rise to strong electrostatic interactions with molecular biological molecules, modulating their localization and activity in living tissues [23,24]. Thus, heparin could form these interactions with a wide range of positively charged molecules, including growth factors, cytokines, and chemokines, through affinity-based interactions that control their release rate and exert a protective effect. Affinity-based release systems have been demonstrated to be effective in releasing FGF-2 [21], TGF-ß [25], SDF-1 [26], GDNF [27] and IL-4 [28]. Following this concept, new strategies can be developed in order to sustainably release adipose tissue derived stem cell (ASCs) secretome. ASCs secretome is composed of a wide range of molecules such as growth factors, cytokines and chemokines [29,30] that can exert beneficial effects in regenerative processes. For instance, can increase metabolic viability and neuronal density in hippocampal neurons [31], induce differentiation of human neural progenitor cells (hNPCs) [32], axonal growth in dorsal root ganglia (DRGs) explants [30,32,33] or protect PC12 cells from excitotoxicity agents [34] and ultimately induce motor recovery after SCI [35]. Regenerative capacity of hASCs secretome is mainly attributed to molecules such as BDNF, GDNF, VEGF, ß-NGF, FGF-ß and SCF known for their potential role in favor those processes [36,37].

As a result, loading hASCs secretome in starPEG-Hep hydrogels could be a more holistic method to successfully deliver hASCs secretome *in vivo*. Herein we characterized the mechanical properties of starPEG-Hep hydrogels and evaluate their potential in promoting controlled and prolonged release of hASCs secretome. Additionally, *in vitro* experiments evaluated their potential in inducing neuronal differentiation in hNPCs and neurite outgrowth in organotypic spinal cord slices. Altogether, data presented here aims to evaluate the potential of this therapeutic approach for further *in vivo* inducing regeneration in SCI animal models.

2. Materials and Methods

2.1. Synthesis of hydrogel precursors, starPEG, heparin maleimide

Amine end-functionalized 4-arm starPEG (MW 10,000, USA), Heparin (MW 15,000, Merck, Germany) were synthesized as previously described [21,22]. Hydrogel formation was obtained by dissolving the maleimide functionalized heparin and thiol end-functionalized 4-arm starPEG in PBS on ice with an appropriate molar ratio. Briefly, 1.5mM heparin dissolved in PBS was mixed with an equal volume of starPEG solution in the concentration of 1.1mM to 2.2mM to produce hydrogels in the crosslinking range of 0.75-1.5 (molar ratio of starPEG to heparin). Michael type click reaction between the maleimide moieties of heparin with thiol-functionalized starPEG groups occurs within seconds of mixing the two solutions. To adjust the polymerization time, the pH of starPEG buffer solution was slightly decreased and adjusted between 5 and 7, to allow a polymerization time for at least 20s ensuring efficient mixing of all hydrogel components.

2.2. Characterization of starPEG-GAG hydrogel properties

2.2.1. Rheological measurements

For rheological measurements, hydrogels with different molar ratio (0.75-1.5) were prepared. Briefly, 67 µL of hydrogel were prepared and allowed to polymerize between two hydrophobic Sigmacote coverslips (Merck, Germany) of defined diameter (D_i = 9 mm). After polymerization, discs were hydrated in PBS. Then, oscillating measurements on swollen gel disks were carried out on a rotational rheometer (ARES LN2; TA Instruments, Germany), with plate-plate geometry (plate diameter 25 mm; gap width, 1.2-1.5 mm). Frequency sweeps were performed at 25°C with a shear frequency range of 10^{-1}-10^{2} rad s^{-1} and a strain amplitude of 2%. Mean values of the storage modulus were calculated. Experiments were performed in triplicate. The gel volumetric swelling of the gels was determined by the following equation 1: where d_0 is the diameter of the unswollen gel disk and d is the diameter after swollen gel for 24 h in PBS.

$$Q = (\frac{d}{d_0})^3$$ Equation 1

2.2.2. Mesh size

The mesh size of a hydrogel is defined as the distance between two entanglement points (ξ) and vary with the different molar ratio in a hydrogel network [38]. It was calculated from the storage modulus G' based on rubber elasticity theory [39] using following equation 2, where G' is the storage modulus, N_A the Avogadro constant, R the molar gas constant, and T the temperature:

$$\xi = \left(\frac{G'N_A}{RT}\right)^{-\frac{1}{3}}$$ Equation 2

2.3. Secretome collection

2.3.1. Cell isolation and culture

The hASCs were obtained from lipoaspirates from consenting donors under a protocol approved and reviewed by an institutional board of LaCell LLC. Cells were isolated according to the protocol described by Dubois et al. [40] and maintained in culture, at 37 °C and 5% CO2, in α-MEM (Invitrogen, USA), with 10% Fetal Bovine Serum (FBS, Biochrom AG, Germany) and 1% antibiotic/antimycotic solution – penicillin/streptomycin (pen/strep; Invitrogen, USA). Medium was changed every 2/3 days until reach 85% confluence, afterwards cells were enzymatically detached and seeded onto new cell culture flasks.

2.3.2. Secretome collection

For secretome collection, hASCs were seeded at a density of 4000 cells/cm^2 in cell culture flasks with alpha minimum essential medium (α-MEM), as described above. The medium was harvested 72 hours after culture and the cells were washed four times with PBS without Ca^{2+}/Mg^{2+} (Merk, Germany). The cells were then placed 24 hours in Neurobasal medium (ThermoFisher, USA) with 1% pen/strep or Neurobasal

A (ThermoFisher, USA) with 1% kanamycin, depending on which cultures the secretome will be applied. It was further centrifuged (249g, Megafuge 1.0R, Heraeus, Germany) for 5 minutes to remove any cell debris. Then, hASCs secretome was concentrated (100x) by centrifugation (3000g) using 5kDa cut-off concentrator (Vivaspin, GE Healthcare, UK) and frozen at -80°C until used.

2.4. Loading of hASCs secretome in starPEG-GAG hydrogels

2.4.1. Characterization of secretome release by immunofluorescence

For fluorescence release experiments, secretome was previously labeled using a FluoReporter FITC protein labeling Kit (ThermoFisher, USA). FITC (fluorescein isothiocyanate) dye will bind to primary amine bonds of proteins forming a dye-protein conjugate, which is detected by fluorescence emission at 518nm, respectively. Briefly, secretome was labeled according to manufacturer's procedure at a labeling ratio 1:2 protein dye.

For gel formation, labeled secretome (10 µL) was mixed with heparin (5µL) and starPEG (5µL) and allowed to polymerize inside low protein binding tubes. Secretome was allowed to release from hydrogels into PBS supplemented with BSA (1%, 300 µL). Samples from released secretome were collected at defined intervals (0, 3h and 1, 2, 3, 4, 5, 6, 7, 10), and replaced by equal volume of fresh medium. The release samples were stored at -80°C until analyzed by measuring fluorescence intensity on a Varioskan flash plate reader (ThermoFisher).

2.4.2. Characterization of secretome release by multiplex assay

As for previous release assay, concentrated secretome (10 µL) was mixed with heparin (5 µL) and starPEG (5 µL) and allowed to polymerize inside low protein binding tubes. Secretome was allowed to release from hydrogels at room temperature into PBS supplemented with BSA (1%, 150µL). Samples were collected at defined intervals (0, 3h and 1, 3, 5, 7, 10 days), and replaced by equal volume of fresh medium. The release samples were stored at -80°C until analyzed by Human Premixed Multi-Analyte kit (R&D Systems, Minneapolis, USA) according to manufacturer's instructions.

2.4.3. Characterization of secretome release by array membranes

To obtain samples for these experiments, secretome (15 µL) was mixed with heparin (7.5 µL) and then loaded into starPEG (7.5 µL) into 24-well plate. Secretome was allowed to release by adding Neurobasal medium (1 mL, ThermoFisher, USA) supplemented with 1% penicillin/streptomycin (ThermoFisher, USA). Samples were collected at defined time points (two and ten days) and replaced by an equal volume of fresh medium. The released samples were stored at -80°C until analyzed by Human Neuro Discovery Array C1 (C-Series RayBiotech, USA) and Human Cytokine Antibody Array C5 (C-Series RayBiotech, USA). For secretome analysis, after blocking the membrane for 30 min at RT, released samples (1 mL) were incubated in each well overnight at 4°C. After washing five times, the membranes were incubated with a biotinylated antibody cocktail for 2 h at RT. Then membranes were incubated with HRP-Streptavidin for 2 h at RT and analyzed by chemiluminescence detection in Sapphire Biomolecular Imager (Azure Biosystems, USA). Analysis of the membranes was performed in AzureSpot Analysis software (Azure Biosystems, USA) where the relative intensity of each spot was measured. Afterward, quantification was done by subtracting the background in each spot and normalizing it to positive control in each membrane.

2.5. Bioactivity of released secretome in *in vitro* cultures

2.5.1. Neural progenitor cells (hNPCs) growth and incubation with released secretome

To study the potential of secretome released from starPEG-Hep hydrogels in promoting neuronal differentiation hNPCs were used. hNPCs were kindly gifted from Prof. Leo A. Behie (University of Calgary, Canada). Cells were isolated from the telencephalon region of a 10 week post-conception fetus, as described previously [41]. Ethical guidelines were previously established and approved by the Conjoint Health Research Ethics Board (CHREB, University of Calgary, Canada; ID: E-18786). Cells were thawed and cultured in suspension as neurospheres in Complete NeuroCult™ Proliferation Medium (Stem Cell Technologies, California) for 3 days. After that, neurospheres were mechanically triturated using a 200 µL micropipette by pipetting up and down 50-100 times in a firm consistent rhythm until obtaining a single cell suspension. At the end, viable cells were counted and cells seeded (density of $1x10^4$ viable cells/cm^2) in fresh medium. hNPCs were maintained in culture for 10-14 days until obtain neurospheres with approximately 100 µm diameter, adding medium every two days as suggested in reference protocol (StemCells Technologies, California). For differentiation assays, neurospheres were mechanically dissociated as previously described and plated in 24-well plates in coverslips coated with poly-D-Lysine (100 µg/mL; Merck, USA) and laminin (10 µg/mL; Merck, USA) using 60,000 cells per well. After seeding

hNPCs on the bottom, hydrogels were prepared and pipetted onto the insert membrane as illustrated in Figure II.1A. Briefly, concentrated secretome (15µL) collected in Neurobasal A was mixed with Heparin (7.5µL) and starPEG (7.5µL) and pipetted per well. NbA supplemented with 1% kanamycin and 1 % GlutaMAX (Gibco, USA) (basal medium) was added as negative control, and the same amount of loaded secretome diluted in this medium added as a free condition. Additionally, NbA supplemented with B27 (2%, ThermoFisher, USA), FGF-2 (0.05%; R&D Systems, USA), kanamycin (1%) and GlutaMAX (1%) was used as positive control. Cultures were maintained for 5 days.

2.5.2. Spinal cord slices isolation and incubation with released secretome

Organotypic spinal cord slice cultures were prepared from Wistar Han rats of postnatal day 7 (P7). Briefly, pups were decapitated, the spinal cord exposed, and the thoracic segment removed and placed in ice-cold high glucose (6mg/mL) Hanks' Balanced Salt Solution (HBSS) without Ca^{2+} and Mg^{2+}(ThermoFisher, USA) with 1 % pen/strep for some time. Under sterile conditions, meninges and roots were removed to ensure the cleaning of the tissue. Then spinal cord was sectioned in a McIlwain Tissue Chopper (Gomshall, UK), transversal segments with 350 µm thickness and placed in cold HBSS. Rat tail type I collagen (3.4 mg/mL, BD Biosciences, USA) was prepared by adding Basal Eagle's medium (10x, Gibco, USA) in a proportion of collagen (450µL) to basal medium (50µL) and sodium bicarbonate solution (7.5%, 2µL) [42]. Single drops (30µL) were placed on 24-well plate and incubated at 37°C and 5% CO_2 for approximately 1h to promote collagen gel formation. Then, viable slices were deposited on top of collagen drops. Additionally, drops of starPEG hydrogel loading secretome (30µL) were allowed to polymerized and release secretome in the same well as illustrated in Figure II.1B. Afterwards, Neurobasal medium supplemented with B27 (2%, ThermoFisher, USA), glucose (2%, 300mg, Merck, USA), L-Glutamine (1%, ThermoFisher, USA) and 1% pen/strep. A total of 200µL was added to each well and medium changed after 2 days and the cultures maintained at 37°C and 5% CO_2.

2.5.3. Immunocytochemistry

hNPCs and Spinal Cord slices were fixed with 4% paraformaldehyde (PFA; Merck, Portugal) for 20 and 45 min at RT, respectively, to retain antigenicity of the target molecules and preserve cell morphology. For hNPCs, permeabilization was performed using 0.3% Triton X-100 in PBS (PBS-T; Merck, USA) for five min, followed by blocking of non-specific binding sites using PBS with newborn calf serum (10 %, NBCS, Biochrom, Germany) or 1h. In case of spinal cord slices permeabilization and blocking were performed

using phosphate-buffered saline (PBS) with Triton X-100 (0.5%, PBS-T, Merck, USA) NBCS (10%) for 1 h at RT. hNPCs were incubated with the following primary antibodies: rabbit anti-doublecortin (DCX, , 1:300, Abcam, UK) for immature neurons and anti-microtubule associated protein-2 (MAP-2, 1:500, Merck, USA) for more mature neurons, diluted in PBS with NBCS (10%) for 1h at RT, while slices incubated with anti-neurofilament (NF, 1:200; Merck, USA) in PBS-T 0.5% +10% NBCS for 48h at 4 °C. After washing 3x with PBS with NBCS (0.5%), cells were incubated with secondary antibodies Alexa Fluor 488 goat anti-rabbit (1:1000; Thermo) and Alexa Fluor 594 goat anti-mouse (1:1000; ThermoFisher, USA) for DCX and MAP-2 detection, respectively, for 1 h 30 at RT. Spinal cord slices were incubated with Alexa Fluor 488 goat anti-mouse (1:1000; ThermoFisher, USA) for 24h at 4 °C. Cell nuclei were stained with 4-6-diamidino-2-phenylindoledhydrochloride (DAPI, 1:1000; ThermoFisher, California) for five and 30 min at RT, hNPCs and spinal cord slices, respectively. Imaging was performed with a fluorescence microscope (BX61, Olympus, Germany) for hNPCS and with a confocal point-scanning microscope Olympus FV1000 for spinal cord slices.

2.5.4. Neuronal differentiation analysis

Cell counts were performed under blinded conditions using Image J (NIH) software for quantification. Ten representative fields per condition were selected and analyzed. The number of positive cells for DCX and MAP-2 were counted per field and normalized to a total number of cells in each field stained with DAPI. Results are presented as a percentage of differentiated cells.

2.5.5. Neurite extension analysis

To quantify the area occupied by neurites, Fiji software was used. Firstly, the scale was defined, and the total slice area was measured, using the proper drawing tools. Then applying the threshold contrast was possible to emphasize the neurite identification. Using the function "Analyze particles," the total area occupied by neurite was calculated. The results were then normalized to the total area of the slice and presented as a percentage of neurite area.

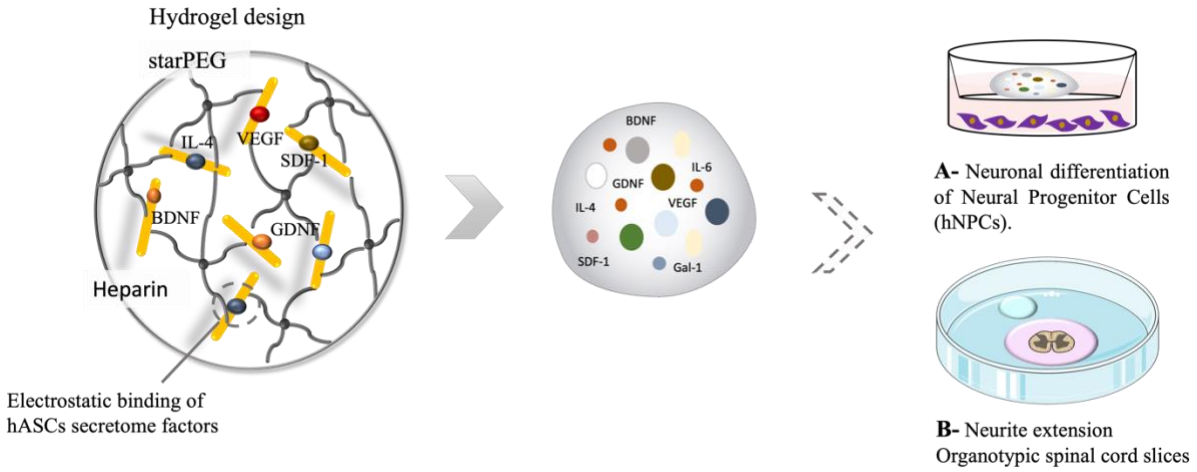

Figure II. 1 Schematic representation of *in vitro* cultures to evaluate the bioactivity of hASCs secretome released from starPEG-Hep hydrogels. Capacity to promote differentiation of human Neural Progenitor Cells (hNPCs) (**A**) and neurite outgrowth in organotypic spinal cord slices (**B**) were performed under described conditions.

2.6. Statistical Analysis

Data regarding neurodifferentiation of hNPCs was analyzed using Mixed ANOVA to compare the mean values of five groups. When evaluating the neurite outgrowth in spinal cord slices one-way ANOVA was performed. A pairwise comparison between groups based on estimated marginal means using Turkey's correction was performed. The significance value was set as $p \leq 0.05$ for all statistical tests and graphs are presented as mean ± SEM. For all data normality was assessed using Shapiro-Wilk statistical tests and taking into account the measures of skewness and kurtosis. Moreover, is important to highlight that for repeated measures ANOVA distribution can be approximately normal distributed [43]. IBM SPSS® Statistics version 27 for IOS (IBM Co., USA) was used to perform all statistical analysis. For graphical representations GraphPad Prism ver.8.4.3 (GraphPad Software, La Jolla, USA) was used.

3. Results

3.1. Physical characterization of *in-situ* forming hydrogels

Hydrogels were formed by desulfated heparin derivatives bearing six maleimide groups and thiol-terminated starPEG. Hydrogels were characterized with respect to their physicochemical network properties, such as stiffness, mesh size and swelling (Figure II. 2 and Supplementary Table II. S1). The physical properties of hydrogels can be modulated by the number of starPEG molecules reacting with

heparin maleimide group, changing the degree of crosslinking, and by the solid content [22]. Increasing the crosslinking degree from 0.75 to 1 and 1.5, hydrogels increase their storage modulus from 1.01 ± 0.13 to 2.69 ± 0.30 to 7.14 ± 0.97 kPa, respectively (Figure II.2A), which range from soft to stiff materials. On the other hand, mesh size and swelling degree decrease with increased solid content, or a higher number of starPEG molecules in solution (Figure II. 2B and C). To notice, the modulation of physical properties is extremely important for further implantation *in vivo.*

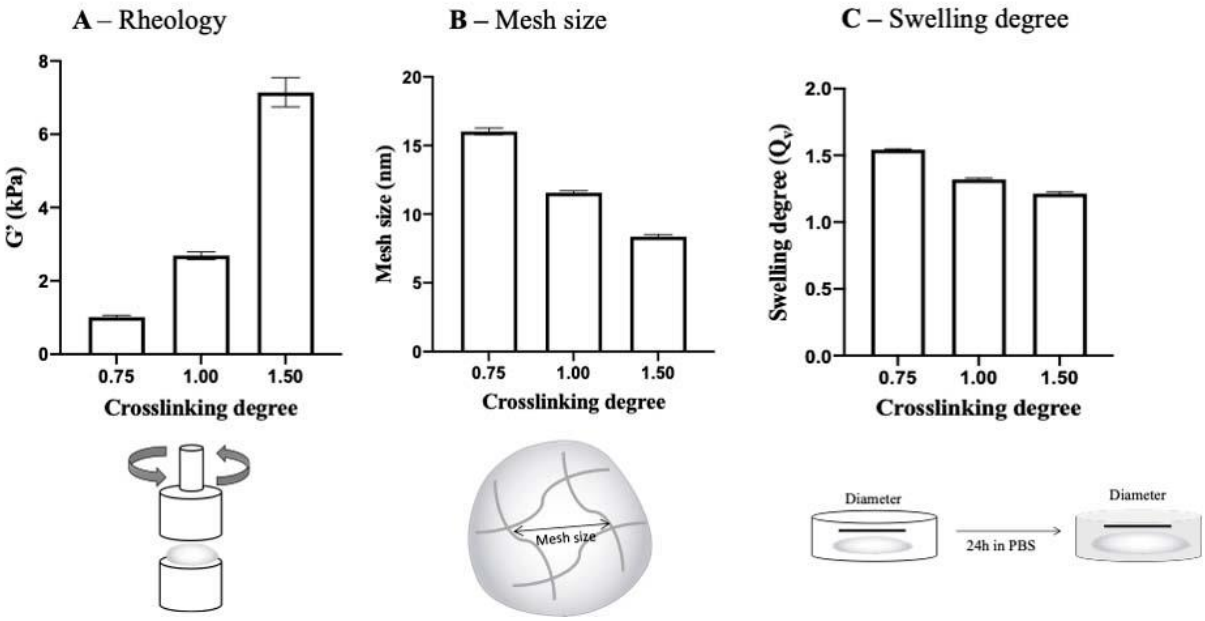

Figure II. 2 Physical characterization of starPEG-Hep hydrogels. At different crosslinking degrees (starPEG/Hep molar ratio) hydrogels characteristics such as stiffness (**A**), mesh size (**B**) and swelling degree (**C**) were measured. Hydrogels can vary from soft to stiff materials, decrease mesh size and swelling degree with increased crosslinking degree. Measurements are plotted as mean ± SEM, corresponding to 9 replicates

3.2. Characterization of secretome released from starPEG-Hep hydrogels

In the context of SCI, administering a therapy is still a concern, considering the administration route and associated problems, such as toxic side effects promoted by high doses or the rapid clearance by the fluids at injury site. Moreover, the enzymatic degradation at the injury site can compromise the bioactivity of drugs and molecules [44].

To minimize these problems, starPEG-GAG hydrogels can be easily integrated at the lesion site and bind, protect, and sustainably deliver the secretome of ASCs. As the secretome of ASCs has already been characterized to be composed of a wide range of signaling factors [29,30,45], our approach capitalize from the high number of binding sites within the starPEG-Hep hydrogels that allow for independent release of multiple factors [46]. Several release assays were conducted to evaluate the release profile of the hASCs secretome from starPEG-Hep hydrogels. In a first approach, the secretome was labeled with a FITC dye that binds to amine groups of proteins, enabling their detection by fluorescence intensity. Then, the labeled secretome was loaded into starPEG-Hep hydrogels with an efficiency of immobilization of about 95% and incubated in phosphate buffered saline (PBS) with 1% bovine serum albumin (BSA). To characterize the release of the secretome, samples from the supernatant that have been in contact with the hydrogel were collected over ten days, revealing a controlled and prolonged release profile (Figure II. 3A). Briefly, after a burst release during the first day (approximately 45%) the hydrogel showed a cumulative release of the secretome until ten days, reaching approximately 70% of release at that time point of the experiment. Over the following 9 days, a sustained release of the secretome was detected. Regarding multiplex results, Gal-1 was detected to be continuously released for the entire time of the experiment (Figure II. 3B).

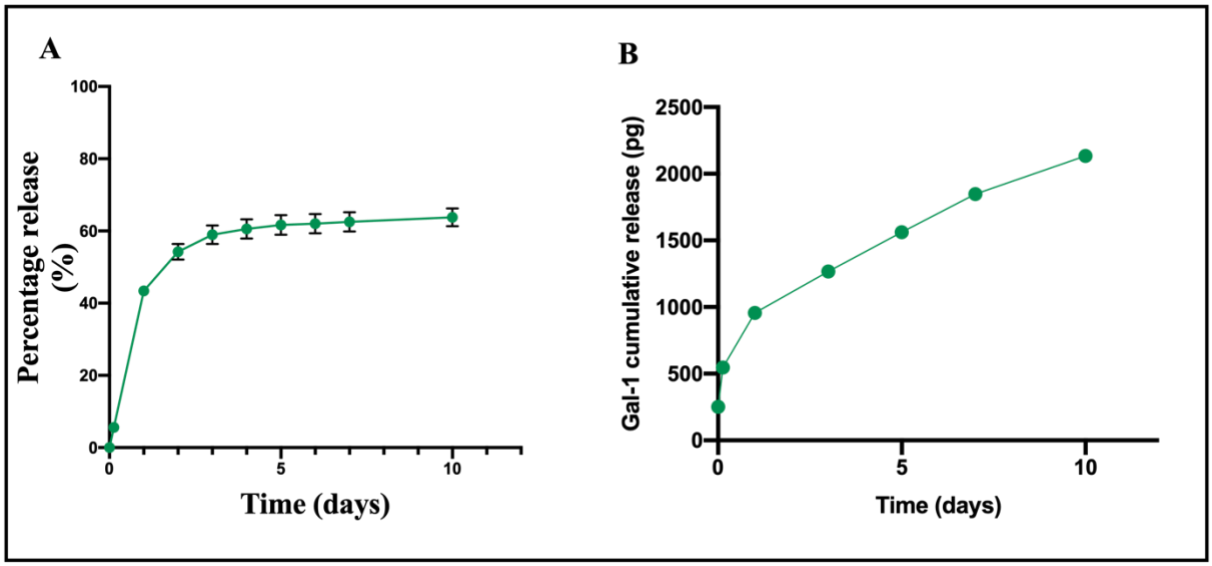

Figure II. 3 Cumulative release of hASCs secretome from starPEG-Hep hydrogels. **A**, Prior of loading in starPEG-Hep hydrogels, secretome was labeled with a FITC dye and samples collected at 0 and 3h, 1, 2, 3, 4, 5, 6, 7 and 10 days. Secretome was detected by fluorescence absorbance and percentage of cumulative release calculated over time. **B**, For Multiplex assay, samples were collected at 0, 3h, 1,3,5,7,10 days and Gal-1 was detected to be controlled and prolonged released over that time. Values

are plotted as mean ± SEM from 2 independent experiment white four replicates each (**A**), and one independent experiment (**B**).

Though these results have shown the potential of the hydrogel as a good release system, secretome is composed of a wide range of proteins, cytokines growth factors and other molecules [29]. In order to decipher more closely which components of the secretome were being released from starPEG-Hep hydrogels, membrane-based protein arrays were used (Figure II 4A and B). For this purpose, samples of released secretome were collected only at 2 and 10 days and evaluated separately using Human Neuro Discovery Array C1 and Human Cytokine Antibody Array C5 (Figure II. 4 A-D), allowing the detection of known ASCs released neurotrophic factors and cytokines after two and ten days, respectively. Each dot was quantified and normalized to the positive controls to determine the relative amount released at different time points. The full array of molecules detected, and their relative expression can be found in Supplementary Figures II. S1 and S2. Membrane arrays revealed a different release profile of neuroinflammatory and angiogenic factors (Figure II. 4C) from neuroregulatory molecules (Figure II. 4D). In fact, cytokines that play a role in modulating the immune response such as IL-1α, IL-1ß, IL-2, IL-3 and IL-4, or factors involved in angiogenesis like angiogenin or VEGF had a burst release after two days. Despite that, the cumulative release observed after ten days evidenced their continuous and extended release. In contrast, growth factors that promote neuronal growth and survival like BDNF, ß-NGF, HB-EGF are mainly released from two to ten days, indicating overall an instant release of immune modulating factors and slightly delayed but therefore more prolonged release of neuro-regulating factors. Moreover, it was possible to detect a wide range of molecules present in the secretome of hASCs that were continuously released from hydrogels such as FGF, TGF-ß, HGF, NT-3, NT-4, IL-16 (Supplementary Figure II. S1 and S2). Altogether, these results support and explain the cumulative release profile presented in Figure II. 3A. While Figure II. 3A shows the total release of the secretome, membrane-based protein arrays show which of these factors are released over time. The burst release results from high amounts of neuroinflammatory and angiogenic factors released in the first days, while the continuous and prolonged release until ten days is driven mainly by neuroregulatory growth factors.

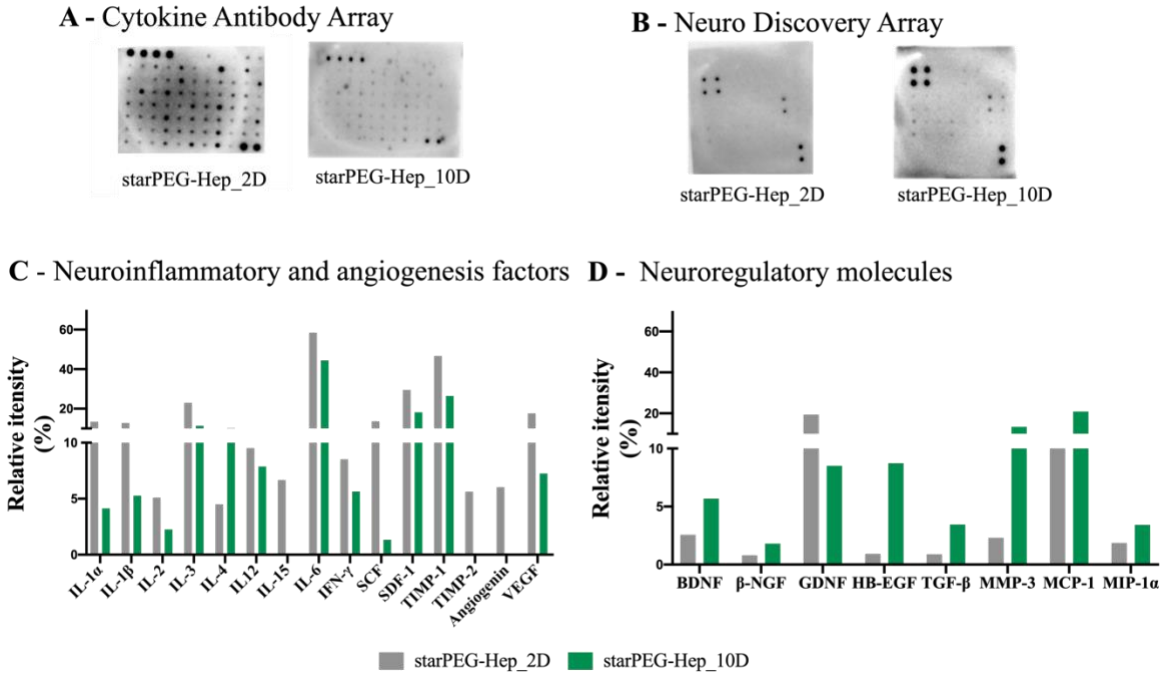

Figure II. 4 Evaluation of hASCs secretome release profile from starPEG-Hep hydrogels using membrane-based protein arrays. **A** and **B** show the membranes of Cytokines Antibody arrays and Neuro Discovery arrays, respectively. **C**, Relative intensity of factors involved in neuroinflammatory and angiogenesis, such as IL-4, tissue inhibitor of metalloproteinase (TIMP)-1, and VEGF, present a higher release in the first two days. On the opposite neuroregulatory molecules (**C**) like BDNF, β-NGF, or TGF-β are mainly released within two to ten days of release. Values are presented as relative intensity, in percentage, for the positive control in each membrane.

3.3. hASCs secretome released from starPEG-Hep hydrogels promote differentiation of hNPCs

Testing of the bioactivity of the developed hydrogel system then followed through the evaluation of the differentiation of hNPCs. For this goal, hNPCs were seeded as a single monolayer of adherent cells on precoated coverslips with poly-D-Lysin and laminin, after which secretome-loaded starPEG-Hep (starPEG-Hep+sec) hydrogels were placed on an insert, above the cell layer. After 5 days in culture, differentiation of hNPCs was assessed by immunocytochemistry analysis for doublecortin positive cells (DCX^+) and microtubule-associated protein positive cells ($MAP2^+$), staining immature and mature neurons, respectively. Fluorescence microscopy imagens showed hNPCs differentiation (Figure II. 5A). Statistical analysis showed that there was an effect of factor treatment ($F(4, 474) = 57.87$, $p<0.0001$, $\eta^2_{partial} = 0.33$),

and the differentiation condition (F (1, 474) = 153.66, p<0.0001, $\eta^{2}_{partial}$ = 0.25), and the interaction between this two factors (F(4, 474) = 40.15, p<0.0001, $\eta^{2}_{partial}$ = 0.25). As shown in Figure II. 5B, hASCs secretome released from starPEG-Hep hydrogels present significative higher percentage of DCX^{+} cells when compared with hydrogel loading the vehicle in which secretome was collected (Neurobasal A) (starPEG-Hep+NbA) (n = 120; 25.47±17.90 vs n = 99; 9.08± 12.66; p<0.0001) or the vehicle alone (n = 80; 17.57±15.37; p<0.0001). No statistical differences were observed when comparing with control (n = 100; 24.77±13.87; p = 0.72) or free secretome (n = 80;28.78±9.97; p = 0.11), which was in contact with cells for the entire experiment. The same tendency is observed regarding the staining for mature neurons ($MAP2^{+}$). Cells treated with secretome released from starPEG-Hep hydrogels promoted a higher differentiation for $MAP2^{+}$ cells (Figure II. 5C) compared to cells treated with the vehicle released from the hydrogel (n = 120;30.75±19.80 vs n = 99;10.43±13.23; p<0.0001) and cells treated only with vehicle (n = 80; 17.95±15.01; p<0.0001). Significance was also observed when comparing with control (n = 100; 44.78±13.34; p<0.0001) or free secretome (n = 80; 36.72±11.74; p = 0.007). All statistical values are presented in Supplementary Table II. S2.

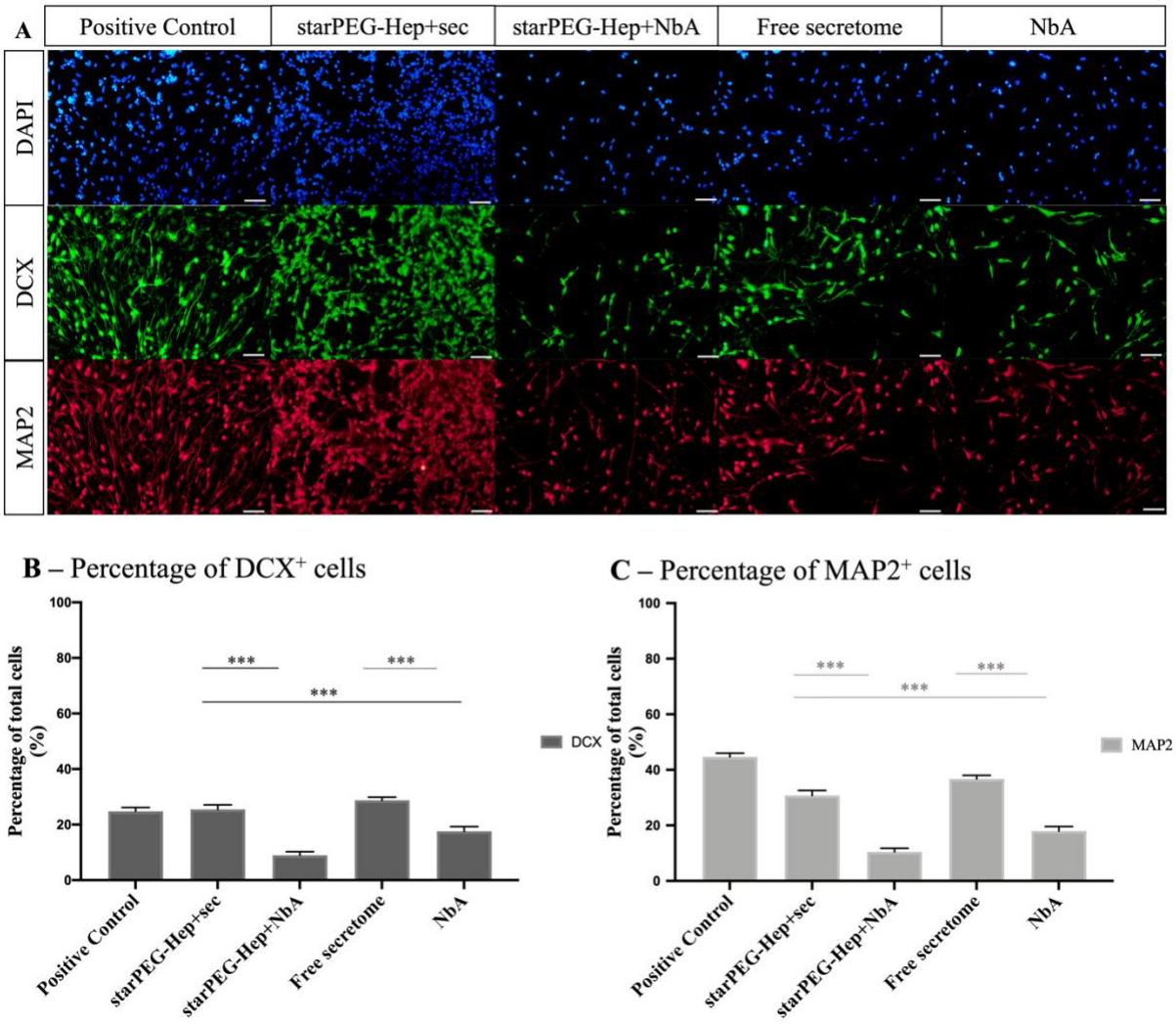

Figure II. 5 Effect of hASCs secretome released from starPEG-Hep hydrogels in hNPCs differentiation *in vitro*. **A**, Representative micrographs of hNPCs differentiation in immature (DCX) and mature (MAP2) neurons when exposed to control, secretome or NbA released from starPEG-Hep hydrogels, free secretome or NbA conditions. Nuclei are stained with DAPI and neurons with MAP2 and DCX. **B-C**, Quantification of the percentage of DCX^+, $MAP2^+$ cells from total cells, respectively. Results represented three independent experiments with 8/12 replicates in a total of ten representative fields per replicate. Repeated measures ANOVA; $^{***}p < 0.0001$. Error bars represented mean ± SEM. Scale bar: 50 μm. MAP2 microtubule associated protein 2, DCX doublecortin, DAPI 4',6'-diamino-2-fenil-indol

3.4. hASCs secretome promotes neurite outgrowth in organotypic cultures

Given the generally low regenerative capacity observed in the context of SCI, it is of the utmost importance to develop therapies that can promote better regeneration. Bearing this in mind, organotypic spinal cord slice cultures were used as a more representative assay to evaluate the potential of hASCs secretome in promoting axonal or neurite outgrowth. After seven days in culture, the secretome effect was evaluated by staining slices with neurofilament (NF) antibody (Figure II.6). Quantification was performed by normalizing the total area occupied by the neurite to the total slice area. Statistical analysis evidenced the effect of the treatment ($F(3.65) = 12.22$, $p<0.001$). Indeed, as shown in Figure II.6B the percentage of relative neurofilament area was significantly higher in the presence of starPEG-Hep+sec when compared with starPEG-Hep+Nb ($n = 16$; 25.70 ± 12.04 vs $n = 17$; 18.04 ± 8.47; $p = 0.039$). Statistical significance was also detected when compared with control group ($n=19$; 12.73 ± 2.58; $p< 0.001$) and to free secretome ($n = 17$; 10.71 ± 5.72; $p< 0.001$, Table II. S3 Supplementary Information).

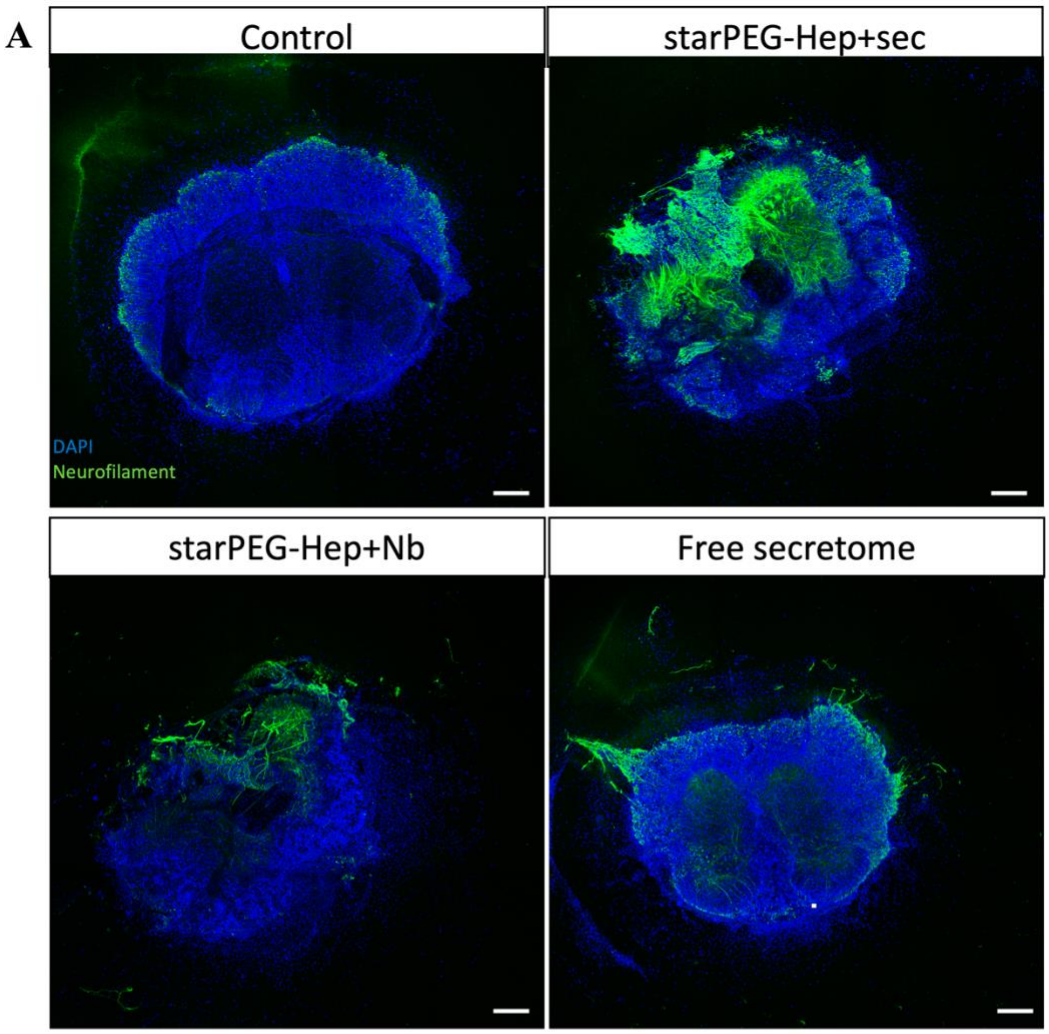

B – Quantification of neurite area

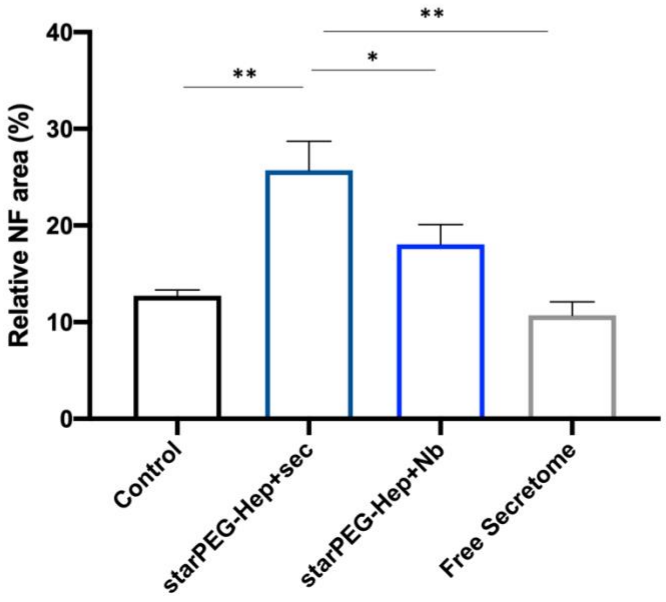

Figure II. 6 Effect of hASCs secretome released from starPEG-Hep hydrogels in promoting neurite outgrowth in organotypic *in vitro* cultures. **A**, Representative micrographs of spinal cord slices when exposed to control, secretome- or vehicle in which secretome was collected (Nb)-loaded starPEG-Hep hydrogels, free secretome conditions. Nuclei were stained with DAPI and neurites with anti-Neurofilament. **B,** Quantification of the percentage of area occupied by neurofilament normalized to total slice area. Results represented four independent experiments with 16/19 replicates. One-way ANOVA; * $p < 0.05$; ** $p < 0.001$. Error bars represent mean ± SEM. Scale bar: 100 μm. DAPI 4',6'-diamino-2-fenil-indol; NF - Neurofilament

4. Discussion

Design a local therapy for SCI is still a challenge in the field. Local or systemic treatment have been shown to be inefficient, either by rapid clearance or off-target effects [47,48]. In this sense, hydrogels flourished as suitable platforms not only to locally promote a controlled and prolonged release, but also to protect molecules from enzymatic degradation [49,50]. StarPEG-Hep hydrogels can act as affinity-based systems, in which molecules establish electrostatic interactions with heparin and control their dissociation rate and biological action [21,51]. Since cell-based therapy has gained a lot of attention mainly because of the potential of secreted factors that modulate regenerative processes, withstand their deliver to restore SC normal function appears as promising approach [29,36,52].

In this work, using starPEG-Hep hydrogels, our main goal was to promote a sustainable release of hASCs secretome. StarPEG-GAG hydrogels are well characterized and have been presented as good matrices for *in vivo* implantation [21,53,54]. Herein we showed that mechanical properties of these materials can easily be modulated by adjusting the number of starPEG molecules reacting with heparin, resulting in soft to stiff materials, which was demonstrated previously [22,51]. This control over material stiffness is highly important in SCI, where the material's mechanical properties should mimic the spinal cord's soft tissue [55]. In this manner, the low stiffness hydrogels were selected to be used in this work, mainly due to its similar stiffness to neuronal tissue and its ability to allow axons to grow throughout the material [56]. Furthermore, mesh size and swelling degree decrease with increased crosslinking degree (Figure II. 2B and C, Table II.S1 Supporting Information). The mesh size will allow the diffusion of molecules through the material [57]. Hydrogels injected at the spinal cord may swell around twice the initial volume to avoid additional pressure or lesion in the tissue [58,59]. In accordance, starPEG-Hep hydrogels have a low swelling degree, between 1.2 to 1.5, which will ensure no damage to the tissue. Besides this, by

incorporating heparin, these polymers can be used as drug delivery systems. The highly negative charge of this glycosaminoglycan allows the formation of electrostatic interactions with positively charged molecules, such as proteins, growth factors, cytokines, and chemokines [23,24]. Through this affinity-based interactions, molecules are release throughout time, in a time-dependent release process. Actually, several studies have shown that these hydrogels can effectively release a wide range of molecules such as VEGF[54] and FGF-2 [60], IL-4 [28] and TGFß [25]. Secretome of ASCs has already been characterized by our and other groups showing to be composed of growth factors, cytokines and chemokines [29,30,45]. Due to the particular properties mentioned above, we hypothesized that starPEG-Hep hydrogels could be a promising choice for delivering hASCs secretome within SCI sites. In fact, we have shown a controlled and prolonged release of secretome over 10 days, in which Galectin-1(Gal-1) was detected to be continuously released. Pires et al. already mentioned that hASCs secrete this molecule that as a role in the anti-apoptotic processes [29] and have a neuroregenerative effect by binding to NRP-1 and promote axonal growth [61]. Multiplex limiar detection reveals to be very low. To overcome this issue, we used membrane-based protein arrays to reveal which secretome molecules were being released.

Membrane-based protein arrays detect multiple protein levels with high sensitivity and specificity in a single experiment. The technology is based on the sandwich immunoassay, in which each dot in the membrane represents a single factor and signals are detected using chemiluminescence [62].For this purpose, samples of released secretome were collected only at two an ten days and evaluated separately. This allows to determine whether all factors are released after two days or if they are delayed until the end of the experiment. This could also be useful in determining which processes are being addressed by the protein release for biological purposes. Membrane arrays revealed that the burst release, presented in Figure II. 3A, results from high amounts of neuroinflammatory and angiogenic factors released in the first days, while the continuous and prolonged release until ten days is driven mainly by neuroregulatory growth factors. This pattern may also indicate the different affinity of various proteins to heparin which control the overall release characteristics [63]. This profile is in line with other approaches that used hydrogels as affinity-based delivery systems incorporating heparin to deliver fibroblast growth factor (FGF-2) [64,65], and was effective in promoting their prolonged release and improved functional recovery after SCI in animal models.

Bioactivity of developed systems then followed, through the evaluation of the differentiation of hNPCs and the capacity to induce neurite outgrowth in organotypic spinal cord slices. The results demonstrated that secretome released from hydrogels can increase the percentage of DCX^+ (immature neurons) and $MAP2^+$

(mature neurons) cells (Figure II. 5) when compared with hydrogel loading the vehicle or the vehicle alone. Importantly, these levels are similar to free secretome, which was in contact with cells during 5 days of the experiment. In part, this showed that secretome is efficiently being released from hydrogels and that it leads to similar differentiation levels of free secretome. With this, we have shown that starPEG-Hep hydrogels are suitable for sustainably releasing a wide range of molecules, that are closely implicated in regenerative processes such as BDNF and NGF, which are known to be involved in the survival, proliferation and differentiation of hNPCs through the extracellular signal-regulated kinase (ERK) pathway[66,67]. Additionally, TIMP-1, highly released by starPEG-Hep+sec hydrogels, is also involved in the differentiation of oligodendrocyte progenitor cells (OPCs) by activating the protein kinase B (Akt) pathway [68]. These results are also in line with our previous work, where we showed the effects of hASCs secretome in inducing proliferation and metabolic activity of hippocampal neurons [69], promoting differentiation of hNPCs and neurite outgrowth of DRG explants [32]. The secretome's role in modulating regenerative processes may rely on initial inflammatory activity created by the early release of pro-inflammatory cytokines, such as IL-1α, IL-1β or IL-2 (Figure II. 4C), which are required to activate elements of innate response and may be involved in the proliferation and differentiation of reparative cells [70,71]. On the other hand, the time-dependent release of anti-inflammatory cytokines, IL-10 and pro-regenerative molecules such as BDNF, NGF or even TGF-β (Figure II. 4D) helps to restrict the immune response while also triggering axonal sprouting and regeneration [72].

Accordingly, secretome released from starPEG-Hep hydrogels also promoted higher neurite area when compared with hydrogel loading the vehicle, vehicle only or the free secretome in organotypic spinal cord cultures (Figure II.6). The observed effect can be attributed to the released signaling mediators, such as BDNF, which induces outgrowth of cortical and hippocampal neurons [5] as well as supports axonal growth [6]. Neurite extension in organotypic spinal cord slices could be caused by the growth factors released during the first days, such as GDNF, FGF-2 and NT-3 supporting neurogenesis, axonal growth, and cell metabolism [67,73,74]. However main effects may be most likely governed by factors released from two to ten days, such as BDNF and NGF, as the medium was changed after 48 h, in an attempt to recapitulate the rapid clearance by the fluid at the SCI lesion site [75]. Other highly released factors can also influence these processes, such as IL-6, which can enhance sprouting and functional recovery, as observed in lesioned hippocampal slices associated with a high level of growth associated protein (GAP)-43 expression, a protein associated with axonal growth [76], or by activating mitogen-activated protein kinase (MAPK) signaling pathway inducing regeneration [77]. Apart from specific well-known molecules related to the beneficial effects of the secretome in *in vitro* and *in vivo* cultures, stomal cell-derived factor

(SDF)-1, previously shown to be sustainably released from starPEG-Hep hydrogels [26], has been associated with tissue protection, namely when mesenchymal stem cells (MSCs) overexpress this factor after myocardial infarction leading to the preservation of cardiac tissue [78].

Altogether, these results emphasize the potential of starPEG-Hep hydrogels as a release system for a broad spectrum of the neuroregenerative signaling mediators of the hASCs secretome that can induce neural differentiation and neurite outgrowth. Furthermore, the promising avenue in promoting an extended release of secretome from starPEG-Hep hydrogels holds up not only for the action of single factors, but most likely for the balance between pro-inflammatory and pro-regenerative factors that are being released in an optimal time-dependent frame that favor the processes of regeneration path, when compared with free secretome condition.

5. Conclusions

As far as we know, this is the first time that an efficient hydrogel capable of loading and releasing hASCs secretome for an extended period of time has been reported (10 days). Furthermore, starPEG-Hep have been shown to have the ability to easily modulate mechanical properties such as stiffness in order to optimize their *in vivo* implantation. The cumulative release profile of hASCs secretome allows for the detection of a diverse range of molecules such as cytokines (IL-4, IL-2) and growth factors (BDNF, ß-NGF) that are released at different rates over time. When compared to starPEG-Hep+NbA or NbA, the hASCs secretome released from starPEG-Hep hydrogel promoted significant hNPC differentiation in immature (DCX) and mature (MAP2) neurons in *in vitro* cultures. When organotypic spinal cord slices were treated with starPEG-Hep+sec, neurite extension was also found to be greater. Similarly, demonstrating secretome controlled and extended release can influence disease severity, aiding in motor and autonomic recovery.

Acknowledgments

This work was supported by Prémios Santa Casa Neurociências–Prize Melo e Castro for Spinal Cord Injury Research (MC-04/17; MC-18-2021) and the Portuguese Foundation for Science and Technology (Ph.D. Fellowship to D.S (PD/BDE/135567/2018 and COVID/BDE/152051/2022); T. S. P. (PD/BDE/143150/2019); J.R.C (SFRH/BD/145860/2019); J.A (2021.08337.BD); S.B.-A ((PD/BDE/135568/2018). This work was funded by national funds and FEDER, through the Foundation for Science and Technology (FCT), under the scope of the projects UIDB/50026/2020; UIDP/50026/2020; POCI-01-0145-FEDER-029206; POCI-01-0145-FEDER-031392; PTDC/ MED-NEU/31417/2017; NORTE-01-0145-FEDER-029968; POCI-01-0145-FEDER-029751; POCI-01-0145-FEDER-032619. This work has been funded by ICVS Scientific Microscopy Platform, a member of the national infrastructure PPBI - Portuguese Platform of Bioimaging (PPBI-POCI-01-0145-FEDER-022122. This work has also been developed under the scope of the project NORTE-01-0145- FEDER-000013 and NORTE-01-0145-FEDER-000023, supported by the Northern Portugal Regional Operational Programme (NORTE 2020), under the Portugal 2020 Partnership Agreement, through the European Regional Development Fund (FEDER). Work supported by the Portuguese Foundation for Science and Technology (FCT): projects UID/FIS/04650/2020, PTDC/EMD-EMD/28159/2017, and PTDC/BTM-MAT/28237/2017.

Dr. Jeff Gimble and LaCell, Inc. kindly provided the adipose tissue-derived stem cells used in this study. Nelly Rein for her technical advice and support in working with the hydrogel material.

Author contributions

D.S designed and performed most of the experiments, collected and analyzed the data, and drafted the manuscript. T.S.P, J.C.R, R.L, J.A, S.B-A, C.R.M, JD helped *in vitro* and animal experiments. P.A, L.S helped in designing experiments. U. F. and C.W provided hydrogel materials. A.J.S conceived and financially support the study, participated in its design and coordination. L.S, U. F., C.W., A.J. S. critically read the manuscript. Supervision: R.A.S, U. F., C.W., A.J.S. All authors read and approved the final manuscript.

Conflict of Interest

The authors declare that they have no known competing financial interests or personal relationships that could have appeared to influence the work reported in this paper.

Data availability

The data that supports this study is available from the authors upon reasonable request.

References

[1] S. David, A.J. Aguayo, Axonal elongation into peripheral nervous system "bridges" after central nervous system injury in adult rats, Science (80-.). 214 (1981) 931–933. https://doi.org/10.1126/science.6171034.

[2] J. Silver, Jerry; Miller, Regeneration beyond the glial scar, Sci. Rep. 9 (2018) 1–10. https://doi.org/10.1016/j.physbeh.2017.03.040.

[3] G. Yiu, Z. He, Glial inhibition of CNS axon regeneration Glenn, Net Rev Neurosci. 7 (2006) 617–627. https://doi.org/10.1038/nrn1956.Glial.

[4] C.C. Stichel, H.W. Müller, Experimental strategies to promote axonal regeneration after traumatic central nervous system injury, Prog. Neurobiol. 56 (1998) 119–148. https://doi.org/10.1016/S0301-0082(98)00033-1.

[5] L.F. Martins, R.O. Costa, J.R. Pedro, P. Aguiar, S.C. Serra, F.G. Teixeira, N. Sousa, A.J. Salgado, R.D. Almeida, Mesenchymal stem cells secretome-induced axonal outgrowth is mediated by BDNF, Sci. Rep. 7 (2017) 4153. https://doi.org/10.1038/s41598-017-03592-1.

[6] P. Lu, L.L. Jones, M.H. Tuszynski, BDNF-expressing marrow stromal cells support extensive axonal growth at sites of spinal cord injury, Exp. Neurol. 191 (2005) 344–360. https://doi.org/10.1016/j.expneurol.2004.09.018.

[7] M.M. Migliore, R. Ortiz, S. Dye, R.B. Campbell, M.M. Amiji, B.L. Waszczak, Neurotrophic and neuroprotective efficacy of intranasal GDNF in a rat model of Parkinson's disease, Neuroscience. 274 (2014) 11–23. https://doi.org/10.1016/j.neuroscience.2014.05.019.

[8] M.B. Bracken, M.J. Shepard, T.R. Holford, L. Leo-Summers, E.F. Aldrich, M. Fazl, M. Fehlings, D.L. Herr, P.W. Hitchon, L.F. Marshall, R.P. Nockels, V. Pascale, P.L. Perot, J. Piepmeier, V.K.H. Sonntag, F. Wagner, J.E. Wilberger, H.R. Winn, W. Young, Administration of methylprednisolone for 24 or 48 hours or tirilazad mesylate for 48 hours in the treatment of acute spinal cord injury: Results of the Third National Acute Spinal Cord Injury randomized controlled trial, J. Am. Med. Assoc. 277 (1997) 1597–1604. https://doi.org/10.1097/00132586-199808000-00011.

[9] V.W. Yong, J. Wells, F. Giuliani, S. Casha, C. Power, L.M. Metz, The promise of minocycline in neurology, Lancet Neurol. 3 (2004) 744–751. https://doi.org/10.1016/S1474-4422(04)00937-8.

[10] T. Hachiya, Y. Ochi, M. Yoshimura, T. Miyazaki, Serum T3 Level in the Patients with Hyperthyroidism After Therapy, Endocrinol. Jpn. 22 (1975) 255–260. https://doi.org/10.1507/endocrj1954.22.255.

[11] Z. Liu, Y. Yang, L. He, M. Pang, C. Luo, B. Liu, L. Rong, High-dose methylprednisolone for acute traumatic spinal cord injury: A meta-analysis, Neurology. 93 (2019) e841–e850. https://doi.org/10.1212/WNL.0000000000007998.

[12] F.G. Teixeira, M.M. Carvalho, K.M. Panchalingam, A.J. Rodrigues, B. Mendes-pinheiro, S.I. Anjo, B. Manadas, L.A. Behie, N. Sousa, A.J. Salgado, Impact of the Secretome of Human Mesenchymal Stem Cells on Brain Structure and Animal Behavior in a Rat Model of Parkinson's Disease, Stem Cells Transl. Med. (2017) 634–646. https://doi.org/10.5966/sctm.2016-0071.

[13] K.A. Follett, R.L. Boortz-Marx, J.M. Drake, S. DuPen, S.J. Schneider, M.S. Turner, R.J. Coffey, Prevention and management of intrathecal drug delivery and spinal cord stimulation system infections, Anesthesiology. 100 (2004) 1582–1594. https://doi.org/10.1097/00000542-200406000-00034.

[14] L.L. Jones, M.H. Tuszynski, Chronic intrathecal infusions after spinal cord injury cause scarring and compression, Microsc. Res. Tech. 54 (2001) 317–324. https://doi.org/10.1002/jemt.1144.

[15] B. Ghosh, Z. Wang, J. Nong, M.W. Urban, Z. Zhang, V.A. Trovillion, M.C. Wright, Y. Zhong, A.C. Lepore, Local BDNF delivery to the injured cervical spinal cord using an engineered hydrogel

enhances diaphragmatic respiratory function, J. Neurosci. 38 (2018) 5982–5995. https://doi.org/10.1523/JNEUROSCI.3084-17.2018.
[16] E.D. Gomes, S.S. Mendes, H. Leite-Almeida, J.M. Gimble, R.Y. Tam, M.S. Shoichet, N. Sousa, N.A. Silva, A.J. Salgado, Combination of a peptide-modified gellan gum hydrogel with cell therapy in a lumbar spinal cord injury animal model, Biomaterials. 105 (2016) 38–51. https://doi.org/10.1016/j.biomaterials.2016.07.019.
[17] Z. Nazemi, M.S. Nourbakhsh, S. Kiani, Y. Heydari, M.K. Ashtiani, H. Daemi, H. Baharvand, Co-delivery of minocycline and paclitaxel from injectable hydrogel for treatment of spinal cord injury, J. Control. Release. 321 (2020) 145–158. https://doi.org/10.1016/j.jconrel.2020.02.009.
[18] G.E. Rooney, A.M. Knight, N.N. Madigan, L. Gross, B. Chen, C.V. Giraldo, S. Seo, J.J. Nesbitt, M. Dadsetan, M.J. Yaszemski, A.J. Windebank, Sustained delivery of dibutyryl cyclic adenosine monophosphate to the transected spinal cord via oligo [(polyethylene glycol) fumarate] hydrogels, Tissue Eng. - Part A. 17 (2011) 1287–1302. https://doi.org/10.1089/ten.tea.2010.0396.
[19] A.S. Samaddar, P. Chatterjee, A. Roy, Thermosensitive heparin-poloxamer hydrogels enhance the effects of GDNF on neuronal circuit remodelling and neuroprotection after spinal cord injury, Microbiol. Res. 2 (2018) 1–38. https://doi.org/10.1016/j.micres.2018.11.005.
[20] B. Chen, J. He, H. Yang, Q. Zhang, L. Zhang, X. Zhang, E. Xie, C. Liu, R. Zhang, Y. Wang, L. Huang, D. Hao, Repair of spinal cord injury by implantation of bFGF-incorporated HEMA-MOETACL hydrogel in rats, Sci. Rep. 5 (2015) 1–10. https://doi.org/10.1038/srep09017.
[21] U. Freudenberg, A. Hermann, P.B. Welzel, K. Stirl, S.C. Schwarz, M. Grimmer, A. Zieris, W. Panyanuwat, S. Zschoche, D. Meinhold, A. Storch, C. Werner, A star-PEG-heparin hydrogel platform to aid cell replacement therapies for neurodegenerative diseases, Biomaterials. 30 (2009) 5049–5060. https://doi.org/10.1016/j.biomaterials.2009.06.002.
[22] M. V. Tsurkan, K. Chwalek, S. Prokoph, A. Zieris, K.R. Levental, U. Freudenberg, C. Werner, Defined polymer-peptide conjugates to form cell-instructive starpeg-heparin matrices in situ, Adv. Mater. 25 (2013) 2606–2610. https://doi.org/10.1002/adma.201300691.
[23] O. Ostrovsky, B. Berman, J. Gallagher, B. Mulloy, D.G. Fernig, M. Delehedde, D. Ron, Differential effects of heparin saccharides on the formation of specific fibroblast growth factor (FGF) and FGF receptor complexes, J. Biol. Chem. 277 (2002) 2444–2453. https://doi.org/10.1074/jbc.M108540200.
[24] F. Peysselon, S. Ricard-Blum, Heparin-protein interactions: From affinity and kinetics to biological roles. Application to an interaction network regulating angiogenesis, Matrix Biol. 35 (2014) 73–81. https://doi.org/10.1016/j.matbio.2013.11.001.
[25] A. Watarai, L. Schirmer, S. Thönes, U. Freudenberg, C. Werner, J.C. Simon, U. Anderegg, TGFβ functionalized starPEG-heparin hydrogels modulate human dermal fibroblast growth and differentiation, Acta Biomater. 25 (2015) 65–75. https://doi.org/10.1016/j.actbio.2015.07.036.
[26] S. Prokoph, E. Chavakis, K.R. Levental, A. Zieris, U. Freudenberg, S. Dimmeler, C. Werner, Sustained delivery of SDF-1α from heparin-based hydrogels to attract circulating pro-angiogenic cells, Biomaterials. 33 (2012) 4792–4800. https://doi.org/10.1016/j.biomaterials.2012.03.039.
[27] K. Schurig, A. Zieris, A. Hermann, U. Freudenberg, S. Heidel, M. Grimmer, A. Storch, C. Werner, Neurotropic growth factors and glycosaminoglycan based matrices to induce dopaminergic tissue formation, Biomaterials. 67 (2015) 205–213. https://doi.org/10.1016/j.biomaterials.2015.07.029.
[28] L. Schirmer, P. Atallah, C. Werner, U. Freudenberg, StarPEG-Heparin Hydrogels to Protect and Sustainably Deliver IL-4, Adv. Healthc. Mater. 5 (2016) 3157–3164. https://doi.org/10.1002/adhm.201600797.

[29] A.O. Pires, B. Mendes-Pinheiro, F.G. Teixeira, S.I. Anjo, S. Ribeiro-samy, E.D. Gomes, S.C. Serra, N.A. Silva, B. Manadas, A.J. Salgado, Unveiling the Differences of Secretome of Human Bone Marrow Mesenchymal Stem Cells, Adipose Tissue derived Stem Cells and Human Umbilical Cord Perivascular Cells: A Proteomic Analysis, Stem Cells Dev. 25 (2016) 1073–1083. https://doi.org/10.1089/scd.2016.0048.

[30] S.C. Serra, J.C. Costa, R.C. Assunção-Silva, F.G. Teixeira, N.A. Silva, S.I. Anjo, B. Manadas, J.M. Gimble, L.A. Behie, A.J. Salgado, Influence of passage number on the impact of the secretome of adipose tissue stem cells on neural survival, neurodifferentiation and axonal growth, Biochimie. 155 (2018) 119–128. https://doi.org/10.1016/j.biochi.2018.09.012.

[31] C.A. Ribeiro, J.S. Fraga, M. Grãos, N.M. Neves, R.L. Reis, J.M. Gimble, N. Sousa, A.J. Salgado, The secretome of stem cells isolated from the adipose tissue and Wharton jelly acts differently on central nervous system derived cell populations, Stem Cell Res. Ther. 3 (2012) 18. https://doi.org/10.1186/scrt109.

[32] R.C. Assunção-Silva, B. Mendes-Pinheiro, P. Patrício, L.A. Behie, F.G. Teixeira, L. Pinto, A.J. Salgado, Exploiting the impact of the secretome of MSCs isolated from different tissue sources on neuronal differentiation and axonal growth, Biochimie. 155 (2018) 83–91. https://doi.org/10.1016/j.biochi.2018.07.026.

[33] E.D. Gomes, S.S. Mendes, R.C. Assunção-Silva, F.G. Teixeira, A.O. Pires, S.I. Anjo, B. Manadas, H. Leite-Almeida, J.M. Gimble, N. Sousa, A.C. Lepore, N.A. Silva, A.J. Salgado, Co-Transplantation of Adipose Tissue-Derived Stromal Cells and Olfactory Ensheathing Cells for Spinal Cord Injury Repair, Stem Cells. 36 (2018) 696–708. https://doi.org/10.1002/stem.2785.

[34] S. Lu, C. Lu, Q. Han, J. Li, Z. Du, L. Liao, R.C. Zhao, Adipose-derived mesenchymal stem cells protect PC12 cells from glutamate excitotoxicity-induced apoptosis by upregulation of XIAP through PI3-K/Akt activation, Toxicology. 279 (2011) 189–195. https://doi.org/10.1016/j.tox.2010.10.011.

[35] A.G. Pinho, J.R. Cibrão, R. Lima, E.D. Gomes, S.C. Serra, J. Lentilhas-Graça, C. Ribeiro, S. Lanceros-Mendez, S.F.G. Teixeira, S. Monteiro, N.A. Silva, A.J. Salgado, Immunomodulatory and regenerative effects of the full and fractioned adipose tissue derived stem cells secretome in spinal cord injury, Exp. Neurol. 351 (2022) 113989. https://doi.org/10.1016/j.expneurol.2022.113989.

[36] A. J. Braga Osorio Gomes Salgado, R. L. Goncalves Reis, N. Jorge Carvalho Sousa, J. M. Gimble, A. J. Salgado, R. L. Reis, N. Sousa, Adipose Tissue Derived Stem Cells Secretome: Soluble Factors and Their Roles in Regenerative Medicine, Curr. Stem Cell Res. Ther. 5 (2010) 103–110. https://doi.org/10.2174/157488810791268564.

[37] J. Rehman, D. Traktuev, J. Li, S. Merfeld-Clauss, C.J. Temm-Grove, J.E. Bovenkerk, C.L. Pell, B.H. Johnstone, R. V. Considine, K.L. March, Secretion of Angiogenic and Antiapoptotic Factors by Human Adipose Stromal Cells, Circulation. 109 (2004) 1292–1298. https://doi.org/10.1161/01.CIR.0000121425.42966.F1.

[38] Q. Chai, Y. Jiao, X. Yu, Hydrogels for Biomedical Applications: Their Characteristics and the Mechanisms behind Them, Gels. 3 (2017) 6. https://doi.org/10.3390/gels3010006.

[39] M. Rubinstein, R.H. Colby, Polymer physics, 2003.

[40] S.G. Dubois, E.Z. Floyd, S. Zvonic, G. Kilroy, X. Wu, S. Carling, Y.D.C. Halvorsen, E. Ravussin, J.M. Gimble, Isolation of human adipose-derived stem cells from biopsies and liposuction specimens, Methods Mol. Biol. 449 (2008) 69–79. https://doi.org/10.1007/978-1-60327-169-1_5.

[41] F.G. Teixeira, K.M. Panchalingam, S.I. Anjo, B. Manadas, R. Pereira, N. Sousa, A.J. Salgado, L.A. Behie, Do hypoxia/normoxia culturing conditions change the neuroregulatory profile of Wharton Jelly mesenchymal stem cell secretome?, Stem Cell Res. Ther. 6 (2015) 1–14. https://doi.org/10.1186/s13287-015-0124-z.

[42] A. Tucker, Cranial motor axons respond differently to the floor plate and sensory ganglia in collagen gel co-cultures, Eur. J. Neurosci. 8 (1996) 906–916. https://doi.org/10.1111/j.1460-9568.1996.tb01577.x.
[43] LUND ADAM, L. MARK, Laerd Statistics, (n.d.). https://statistics.laerd.com/spss-tutorials/one-way-anova-repeated-measures-using-spss-statistics.php (accessed January 6, 2022).
[44] J.E. Springer, R.D. Azbill, S.E. Kennedy, J. George, J.W. Geddes, Rapid calpain I activation and cytoskeletal protein degradation following traumatic spinal cord injury: Attenuation with riluzole pretreatment, J. Neurochem. 69 (1997) 1592–1600. https://doi.org/10.1046/j.1471-4159.1997.69041592.x.
[45] R. Vawda, A. Badner, J. Hong, M. Mikhail, R. Dragas, K. Xhima, A. Jose, M.G. Fehlings, Harnessing the Secretome of Mesenchymal Stromal Cells for Traumatic Spinal Cord Injury: Multicell Comparison and Assessment of in Vivo Efficacy, Stem Cells Dev. 29 (2020) 1429–1443. https://doi.org/10.1089/scd.2020.0079.
[46] A. Zieris, K. Chwalek, S. Prokoph, K.R. Levental, P.B. Welzel, U. Freudenberg, C. Werner, Dual independent delivery of pro-angiogenic growth factors from starPEG-heparin hydrogels, J. Control. Release. 156 (2011) 28–36. https://doi.org/10.1016/j.jconrel.2011.06.042.
[47] D. Dooley, E. Lemmens, P. Ponsaerts, S. Hendrix, Interleukin-25 is detrimental for recovery after spinal cord injury in mice, J. Neuroinflammation. 13 (2016) 1–6. https://doi.org/10.1186/s12974-016-0566-y.
[48] H.J. Lee, J.S. Ryu, P.J. Vig, Current strategies for therapeutic drug delivery after traumatic CNS injury, Ther. Deliv. 10 (2019) 251–263. https://doi.org/10.4155/tde-2019-0006.
[49] G. Perale, F. Rossi, E. Sundstrom, S. Bacchiega, M. Masi, G. Forloni, P. Veglianese, Hydrogels in spinal cord injury repair strategies, ACS Chem. Neurosci. 2 (2011) 336–345. https://doi.org/10.1021/cn200030w.
[50] D. Silva, R.A. Sousa, A.J. Salgado, Hydrogels as delivery systems for spinal cord injury regeneration, Mater. Today Bio. 9 (2021) 100093. https://doi.org/10.1016/j.mtbio.2021.100093.
[51] P. Atallah, L. Schirmer, M. Tsurkan, Y.D. Putra Limasale, R. Zimmermann, C. Werner, U. Freudenberg, In situ-forming, cell-instructive hydrogels based on glycosaminoglycans with varied sulfation patterns, Biomaterials. 181 (2018) 227–239. https://doi.org/10.1016/j.biomaterials.2018.07.056.
[52] A.G. Pinho, J.R. Cibrão, N.A. Silva, S. Monteiro, A.J. Salgado, Cell secretome: Basic insights and therapeutic opportunities for CNS disorders, Pharmaceuticals. 13 (2020) 1–18. https://doi.org/10.3390/ph13020031.
[53] U. Freudenberg, Y. Liang, K.L. Kiick, C. Werner, Glycosaminoglycan-based biohybrid hydrogels: a sweet and smart choice for multifunctional biomaterials, Adv. Mater. 28 (2016) 8861–8891. https://doi.org/10.1016/j.physbeh.2017.03.040.
[54] U. Freudenberg, A. Zieris, K. Chwalek, M. V. Tsurkan, M.F. Maitz, P. Atallah, K.R. Levental, S.A. Eming, C. Werner, Heparin desulfation modulates VEGF release and angiogenesis in diabetic wounds, J. Control. Release. 220 (2015) 79–88. https://doi.org/10.1016/j.jconrel.2015.10.028.
[55] R.D. Bartlett, D. Eleftheriadou, R. Evans, D. Choi, J.B. Phillips, Mechanical properties of the spinal cord and brain: Comparison with clinical-grade biomaterials for tissue engineering and regenerative medicine, Biomaterials. 258 (2020) 120303. https://doi.org/10.1016/j.biomaterials.2020.120303.
[56] A.P. Balgude, X. Yu, A. Szymanski, R. V. Bellamkonda, Agarose gel stiffness determines rate of DRG neurite extension in 3D cultures, Biomaterials. 22 (2001) 1077–1084. https://doi.org/10.1016/S0142-9612(00)00350-1.

[57] Z.Z. Khaing, A. Ehsanipour, C.P. Hofstetter, S.K. Seidlits, Injectable Hydrogels for Spinal Cord Repair: A Focus on Swelling and Intraspinal Pressure, Cells Tissues Organs. 202 (2016) 67–84. https://doi.org/10.1159/000446697.

[58] M.C. Jimenez Hamann, E.C. Tsai, C.H. Tator, M.S. Shoichet, Novel intrathecal delivery system for treatment of spinal cord injury, Exp. Neurol. 182 (2003) 300–309. https://doi.org/10.1016/S0014-4886(03)00040-2.

[59] P. V. Turner, T. Brabb, C. Pekow, M.A. Vasbinder, Administration of substances to laboratory animals: Routes of administration and factors to consider, J. Am. Assoc. Lab. Anim. Sci. 50 (2011) 600–613.

[60] A. Zieris, S. Prokoph, K.R. Levental, P.B. Welzel, M. Grimmer, U. Freudenberg, C. Werner, FGF-2 and VEGF functionalization of starPEG-heparin hydrogels to modulate biomolecular and physical cues of angiogenesis, Biomaterials. 31 (2010) 7985–7994. https://doi.org/10.1016/j.biomaterials.2010.07.021.

[61] H.R. Quintá, J.M. Pasquini, G.A. Rabinovich, L.A. Pasquini, Glycan-dependent binding of galectin-1 to neuropilin-1 promotes axonal regeneration after spinal cord injury, Cell Death Differ. 21 (2014) 941–955. https://doi.org/10.1038/cdd.2014.14.

[62] R.P. Huang, W. Yang, D. Yang, L. Flowers, I.R. Horowitz, X. Cao, R. Huang, The promise of cytokine antibody arrays in the drug discovery process, Expert Opin. Ther. Targets. 9 (2005) 601–615. https://doi.org/10.1517/14728222.9.3.601.

[63] U. Freudenberg, P. Atallah, Y.D.P. Limasale, C. Werner, Charge-tuning of glycosaminoglycan-based hydrogels to program cytokine sequestration., Faraday Discuss. 219 (2019) 244–251. https://doi.org/10.1039/c9fd00016j.

[64] H.L. Xu, F.R. Tian, J. Xiao, P.P. Chen, J. Xu, Z.L. Fan, J.J. Yang, C.T. Lu, Y.Z. Zhao, Sustained-release of FGF-2 from a hybrid hydrogel of heparin-poloxamer and decellular matrix promotes the neuroprotective effects of proteins after spinal injury, Int. J. Nanomedicine. 13 (2018) 681–694. https://doi.org/10.2147/IJN.S152246.

[65] H.L. Xu, F.R. Tian, C.T. Lu, J. Xu, Z.L. Fan, J.J. Yang, P.P. Chen, Y.D. Huang, J. Xiao, Y.Z. Zhao, Thermo-sensitive hydrogels combined with decellularised matrix deliver bFGF for the functional recovery of rats after a spinal cord injury, Sci. Rep. 6 (2016) 1–15. https://doi.org/10.1038/srep38332.

[66] J. Langhnoja, L. Buch, P. Pillai, Potential role of NGF, BDNF, and their receptors in oligodendrocytes differentiation from neural stem cell: An in vitro study, Cell Biol. Int. 45 (2021) 432–446. https://doi.org/10.1002/cbin.11500.

[67] S.Q. Chen, Q. Cai, Y.Y. Shen, X.Y. Cai, H.Y. Lei, Combined use of NGF/BDNF/bFGF promotes proliferation and differentiation of neural stem cells in vitro, Int. J. Dev. Neurosci. 38 (2014) 74–78. https://doi.org/10.1016/j.ijdevneu.2014.08.002.

[68] A.M. Nicaise, K.M. Johnson, C.M. Willis, R.M. Guzzo, S.J. Crocker, TIMP-1 Promotes Oligodendrocyte Differentiation Through Receptor Mediated Signaling, Mol Neurobiol. 56 (2019) 3380–3392. https://doi.org/10.1007/s12035-018-1310-7.TIMP-1.

[69] C.A. Ribeiro, A.J. Salgado, J.S. Fraga, N.A. Silva, R.L. Reis, N. Sousa, The secretome of bone marrow mesenchymal stem cells-conditioned media varies with time and drives a distinct effect on mature neurons and glial cells (primary cultures), J. Tissue Eng. Regen. Med. 5 (2011) 668–672. https://doi.org/10.1002/term.365.

[70] S.A. Eming, T.A. Wynn, P. Martin, Inflammation and metabolism in tissue repair and regeneration, Science (80-.). 1356 (2017) 1026–1030. https://doi.org/10.1126/science.aam7928.

[71] N.G. Frangogiannis, The Inflammatory Response in Tissue Repair, in: J.-M. Cavaillon, M. Singer (Eds.), Inflamm. From Mol. Cell. Mech. to Clin., Weinheim,G, Weinheim,Germany: John Wiley and Sons, 2017: pp. 1517–1537.

[72] L.I. Benowitz, P.G. Popovich, Inflammation and axon regeneration, Curr. Opin. Neurol. 24 (2011) 577–583. https://doi.org/10.1097/WCO.0b013e32834c208d.

[73] L. Crigler, R.C. Robey, A. Asawachaicharn, D. Gaupp, D.G. Phinney, Human mesenchymal stem cell subpopulations express a variety of neuro-regulatory molecules and promote neuronal cell survival and neuritogenesis, Exp. Neurol. 198 (2006) 54–64. https://doi.org/10.1016/j.expneurol.2005.10.029.

[74] K.M. Keefe, I.S. Sheikh, G.M. Smith, Targeting neurotrophins to specific populations of neurons: NGF, BDNF, and NT-3 and their relevance for treatment of spinal cord injury, Int. J. Mol. Sci. 18 (2017) 1–17. https://doi.org/10.3390/ijms18030548.

[75] H.J. Lee, J.S. Ryu, P.J. Vig, Current strategies for therapeutic drug delivery after traumatic CNS injury, Ther. Deliv. 10 (2019) 251–263. https://doi.org/10.4155/tde-2019-0006.

[76] D. Hakkoum, L. Stoppini, D. Muller, Interleukin-6 promotes sprouting and functional recovery in lesioned organotypic hippocampal slice cultures, J. Neurochem. 100 (2007) 747–757. https://doi.org/10.1111/j.1471-4159.2006.04257.x.

[77] F.Y.H. Teng, B.L. Tang, Axonal regeneration in adult CNS neurons - Signaling molecules and pathways, J. Neurochem. 96 (2006) 1501–1508. https://doi.org/10.1111/j.1471-4159.2006.03663.x.

[78] M. Zhang, N. Mal, M. Kiedrowski, M. Chacko, A.T. Askari, Z.B. Popovic, O.N. Koc, M.S. Penn, SDF-1 expression by mesenchymal stem cells results in trophic support of cardiac myocytes after myocardial infarction, FASEB J. 21 (2007) 3197–3207. https://doi.org/10.1096/fj.06-6558com.

Supplementary Information

Supplementary Table II. S1 Characterization of starPEG-Hep hydrogels. Hydrogels with crosslinking degree of 0.75, 1 and 1.5 were characterized in relation to their stiffness, mesh size and swelling degree.

Characteristics	Crosslinking degree		
	0.75	1	1.5
Stiffness (kPa)	1.01 ± 0.13	2.69 ± 0.30	7.14 ± 0.97
Mesh size (nm)	16.02 ± 0.72	11.55 ± 0.42	8.36 ± 0.38
Swelling degree (Q_v)	1.54 ± 0.01	1.32 ± 0.01	1.21 ± 0.02

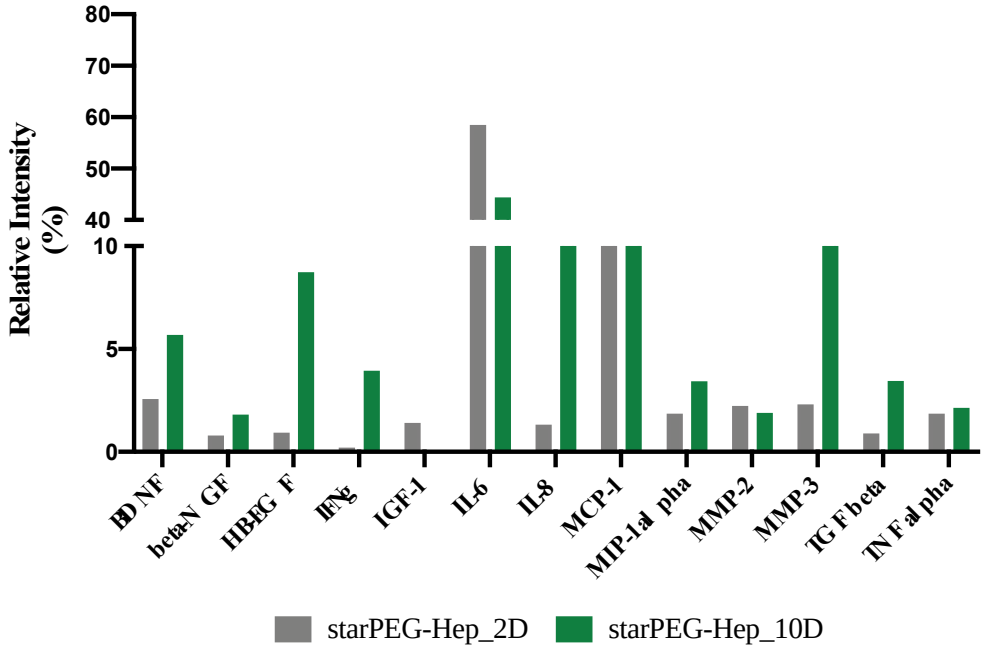

Supplementary Figure II. S1 Characterization of hASCs secretome released from starPEG-Hep hydrogels at tow and twn days using Membrane-based protein array RayBio ® C-Series Human Neuro Discovery array C1 Kit.

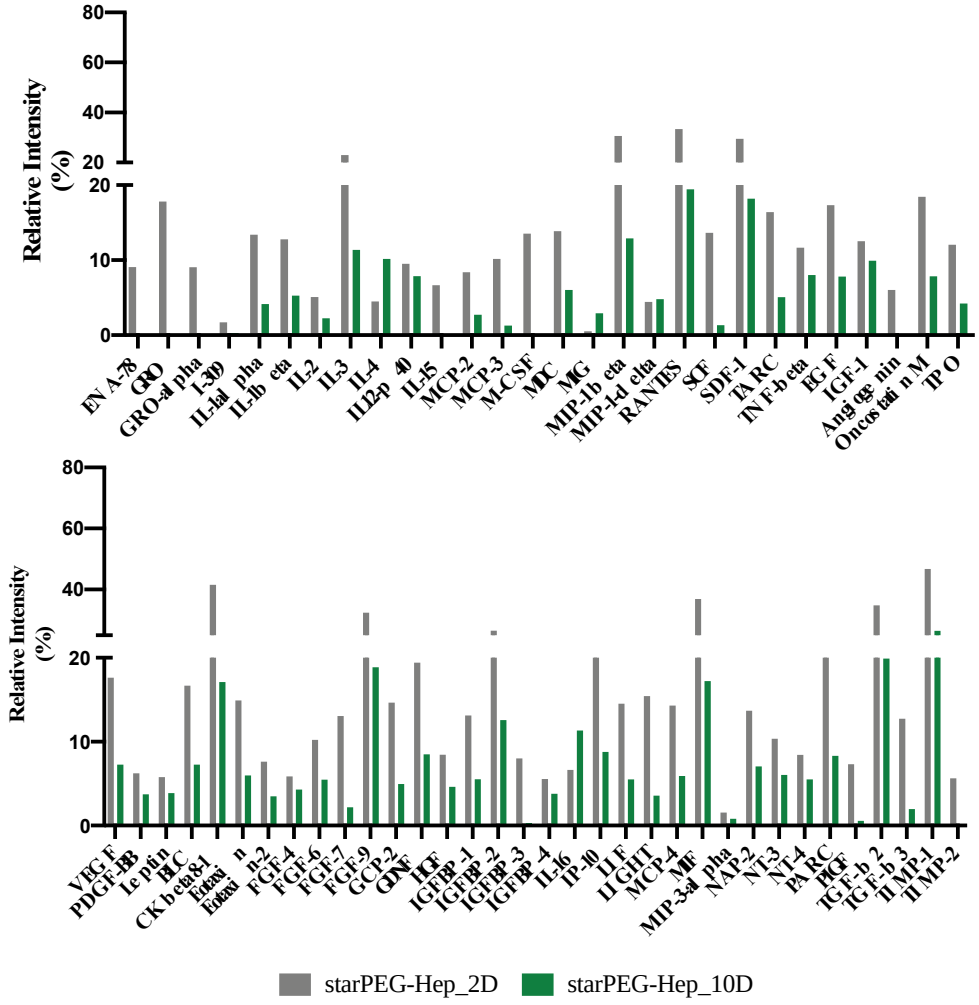

Supplementary Figure II. S2 Characterization of hASCs secretome released from StarPEG-Hep hydrogels at 2 and 10 days using Membrane-based protein array RayBio ®C-Series Human Cytokine Discovery array C5 Kit.

Supplementary Table II. S2 Pairwise comparisons between groups using Tukey's correction for the percentage of hNPCs differentiated in immature (DCX^+) and mature ($MAP2^+$) neurons.

NPCs differentiation			
DCX			
Comparison between groups	Mean Difference	SEM	*p*-Value
Positive Control vs starPEG-Hep+sec	-0.70	1.96	0.72
Positive Control vs starPEG-Hep+NbA	15.68	2.05	<0.0001
Positive Control vs Secretome	-4.00	2.17	0.066
Positive Control vs NbA	7.2	2.17	<0.001
starPEG-Hep+sec vs starPEG-Hep+NbA	16.38	1.97	<0.0001
starPEG-Hep+Sec vs Secretome	-3.30	2.18	0.11
starPEG-Hep+Sec vs NbA	7.90	2.09	<0.0001

starPEG-Hep+NbA vs Secretome	-19.69	2.18	<0.0001
starPEG-Hep+NbA vs NbA	-8.48	2.18	<0.0001
Secretome vs NbA	11.21	2.29	<0.0001
MAP2			
Positive Control vs starPEG-Hep+secretome	13.94	2.06	<0.0001
Positive Control vs starPEG-Hep+NbA	34.29	2.16	<0.0001
Positive Control vs Secretome	7.96	2.29	<0.001
Positive Control vs NbA	26.74	2.29	<0.0001
starPEG-Hep+sec vs starPEG-Hep+NbA	20.32	2.07	<0.0001
starPEG-Hep+Sec vs Secretome	-5.97	2.2	0.007
starPEG-Hep+Sec vs NbA	12.80	2.2	<0.0001
starPEG-Hep+NbA vs Secretome	-26.29	2.29	<0.0001
starPEG-Hep+NbA vs NbA	-7.52	2.29	0.001
Secretome vs NbA	18.77	2.41	<0.0001

Supplementary Table II. S3 Multiple comparisons between groups using Tukey's correction for the percentage of neurofilament are in organotypic spinal cord slices cultures.

Neurite outgrowth in organotypic cultures			
Comparison between groups	Mean Difference	SEM	*p*-Value
Control vs starPEG-Hep+sec	-12.97	2.65	<0.001
Control vs starPEG-Hep+Nb	-5.31	2.61	0.275
Control vs Secretome	2.03	2.61	1
starPEG-Hep+sec vs starPEG-Hep+Nb	7.66	2.72	0.039
starPEG-Hep+Sec vs Secretome	14.99	2.72	<0.001
starPEG-Hep+Nb vs Secretome	7.33	2.68	0.048

CHAPTER III

---

hASCs Secretome Released from StarPEG-GAG Hydrogels Promotes Motor Improvements after Complete Transection in Spinal Cord Injury Rat Model

This chapter is part of published work in an international peer reviewed journal:

Sustained Release of Human Adipose Tissue Stem Cell Secretome from Star-Shaped Poly (ethylene glycol) Glycosaminoglycan Hydrogels Promotes Motor Improvements after Complete Transection in Spinal Cord Injury Rat Model

Deolinda Silva; Lucas Schirmer; Tiffany S. Pinho; Passant Atallah; Jorge R. Cibrão; Rui Lima; João Afonso; Sandra B-Antunes; Cláudia R. Marques; João Dourado; Uwe Freudenberg; Rui A. Sousa; Carsten Werner; António J. Salgado

Advanced Healthcare Materials

2023

hASCs Secretome Released from StarPEG-GAG Hydrogels Promotes Motor Improvements after Complete Transection in Spinal Cord Injury Rat Model

Deolinda Silva [1,2,3]; Lucas Schirmer [4]; Tiffany S. Pinho[1,2,3]; Passant Atallah [4]; Jorge R. Cibrão[1,2]; Rui Lima[1,2]; João Afonso[1,2]; Sandra B-Antunes[1,2,3]; Cláudia R. Marques[1,2]; João Dourado[5]; Uwe Freudenberg[4]; Rui A. Sousa [3]; Carsten Werner [4,6*]; António J. Salgado[1,2*]

[1] Life and Health Sciences Research Institute (ICVS), School of Medicine, University of Minho, Campus de Gualtar, 4710-057 Braga, Portugal;

[2] ICVS/3B's – PT Government Associated Laboratory, Braga/Guimarães, Portugal;

[3]Stemmatters, Biotecnologia e Medicina Regenerativa SA, Guimarães, Portugal;

[4]Leibniz Institute of Polymer Research Dresden (IPF), Max Bergmann Center of Biomaterials Dresden (MBC), Dresden, Germany;

[5]School of Medicine, University of Minho, Campus de Gualtar, 4710-057 Braga, Portugal

[6]Technische Universität Dresden, Center for Regenerative Therapies Dresden (CRTD), Dresden, Germany;

*These authors shared senior authorship

Corresponding author

António Salgado – asalgado@med.uminho.pt

Abstract

Adipose tissue-derived stem cells (ASCs) have been trialed in cell transplantation to assist regenerative processes, particularly those occurring at spinal sord injury (SCI). Their beneficial effects are mainly attributed to intense paracrine activity (secretome) capable of inducing axonal growth, reducing inflammation, promoting cell survival and vascular remodeling. Importantly also promote motor recovery after SCI in animal models. However, when secretome is administered locally it has revealed a low regenerative efficiency due to a an accelerated clearance from the injury site. Following previous results, in the present report we evaluated if hASCs secretome loaded in starPEG-Hep hydrogels is able to modulate the pathophysiology of SCI and induce motor gains, in a complete transection SCI rat model. Secretome loaded hydrogels were able to significantly improve motor function by reducing the percentage of ameboid microglia and systemically elevated levels of anti-inflammatory cytokines. Delivery of ASC-derived secretome from starPEG-Hep hydrogels may therefore offer unprecedented options for regenerative therapy of SCI.

Keywords

Spinal cord injury
Hydrogels
Secretome
Delivery systems
StarPEG
Heparin
Regeneration

1. Introduction

Spinal cord injury (SCI) have been known as “an ailment not to be treated” since ancient Egyptian times, about 2500 years B.C.E [1]. However, even thousands of years later, no effective cure exists. SCI incidence is approximately 54 cases per one million people, or about 17,700 new cases per year in the United States alone [2]. As a severely disabling condition, SCI encompasses a detrimental impact on the quality of life of patients afflicted. The disease affects both motor and sensory functions in the body. Although physical disabilities are the major incapacitating alterations, patients are further burdened by the emerging psychological and financial concerns [3,4].

SCI pathophysiology comprehends three main phases: the primary injury starts when a mechanical impact compresses, contuses or lacerates the spinal sord, disrupting ascending and descending tracts [5]. Massive amounts of inflammatory cells infiltrate the injured tissue, leading to the release of pro-inflammatory cytokines initiating the second phase [6]. In addition, cell death and damage to spinal neurons and axons also occur [5,7]. A chronic or third phase is then established, with a cystic cavity formed and surrounded by reactive astrocytes. Furthermore, the demyelination of white matter together with grey matter dissolution creates an inhibitory environment for the regenerative process [8]. The complexity of these cascade of events makes developing regenerative approaches for SCI far more complex when compared to other trauma-related injuries.

Cell based therapies have opened a window of new possible therapeutic approaches that have been studied in both preclinical and clinical applications [9–12]. In particularly, adipose tissue-derived stem cells (ASCc) can provide protection, survival an differentiation of neural cells and support neuroregeneration with their beneficial immunomodulatory profile [13–15]. In addition, the implantation of ASCs in a contusion mice model enhanced functional recovery, reduced inflammation, and preserved neural tissue [10]. Moreover, our group showed that the transplantation of a combination of ASCs and olfactory ensheathing cells (OECs) within a gellan gum hydrogel improved motor function by reducing inflammatory cells in the lumbar [16] and thoracic hemisection SCI rat model [9]. Likewise, this approach was capable of increasing diaphragmatic activity and partially restoring sensory function in C2 hemisection SCI in rats [17].

The impact of cell transplantation on regenerative processes is mainly conveyed through their secreted bioactive molecules (secretome), including soluble proteins (cytokines, growth factors, and chemokines) and a vesicular fraction (exosomes), both of which have neuroprotective, neuroregenerative and immunomodulatory capabilities [13,18]. Thus, ASCs-derived secretome has been shown to protect pheochromocytoma (PC12) cells from glutamate excitotoxicity and apoptosis by reducing the levels of

cleaved-caspase-3 [14]. Regarding inflammation, the ASCs secretome is able to reduce the release of pro-inflammatory tumor necrosis factor-α (TNF-α) after exposure to an inflammatory stimulus, as well as to induce actively macrophages (M2) polarization and the secretion of anti-inflammatory cytokines IL-10 and transforming growth factor (TGFβ1) [19]. Furthermore, the ASCs secretome was shown to be capable of promoting neuronal survival and differentiation[20,21], axonal outgrowth in dorsal root ganglia (DRG) explants [9,22] and also tissue vascularization [23].

Based on these positive effects on neuroregeneration, our group recently showed that ASCs secretome can promote functional recovery in an SCI mice model by multiple systemic injections [24]. The beneficial effects have only been observed by systemic administration in this study, whereas the action of local injection was greatly diminished due to its quick clearance of the secretome from the target site. However, systemic administration also presents some disadvantages, frequently associated with rapid diffusion through the body and off-target effects [25]. Other strategies involve catheter implantation or mini pumps, which come with the downside of the additional risk of infections at the delivery site [26,27].

Taking all of the previous into account, new methods of sustained administration must be developed, such as hydrogels. Indeed, in recent years several studies have demonstrated the ability of hydrogels to serve as delivery platforms for a variety of therapeutic agents for a plethora of disable conditions. In an SCI rat model, elastic poly(sebacoyl diglyceride) coated with isoleucine-lysine-valine-alanine-valine-serine (PSeD-IKVAV) hydrogel loading neural stem cells (NSCs) promoted improved motor function while reducing inflammation and cell death [28]. Pan and coworkers also demonstrated that the release of human periodontal ligament stem cells (hPDLSCs) from a thermosensitive hydrogel overexpressing platelet-derived growth factor-BB (PDGF-BB) supported bone regeneration [29]. Hydrogels have also been identified as promising candidates for chemotherapeutic drug delivery as an alternative to conventional methods [30]. Overall, these findings strongly support the development and application of hydrogels as delivery systems. In fact, the ability of hydrogels to act as release systems is directly related to their ability to integrate at lesion sites, to support tissue regeneration, and to load and release a wide range of small molecules or biological compounds [31–34]. In particular, the viscoelasticity, cell compatibility and biofunctionalization of hydrogels can support the treatment of SCI [35].

Poly(ethylene glycol) (PEG) is a biocompatible synthetic polymer that has been widely used to design hydrogels that allow axonal growth, vascularization, and infiltration of glial cells [36], promotes functional recovery and reduced cystic cavity [37]. Moreover, these hydrogels can be easily functionalized with cell-instructive peptides, such as Arg-Glys-Asp (RGD), to improve cell loading and survival [38]. The physical and chemical characteristics of PEG-based hydrogels, such as their inert characteristics avoiding the

interactions with proteins, are favorable to create a permissive environment to drive the diffusion of molecules which confers an advantage of using them as encapsulating platforms [39]. For instance the controlled delivery of brain-derived neurotrophic factor (BDNF) and glial-derived neurotrophic factor (GDNF) from PEG-based hydrogels into the brain have been beneficial to reduce microglial response [40], as the local delivery of neurotrophin-3 (NT-3) in SCI induced axonal growth and functional recovery [32]. However, hydrogels lacking affinity sites for cytokines and growth factors can hardly provide long term release. To overcome this limitation, biohybrid hydrogels made of starPEG (star-shaped PEG) and the glycosaminoglycan (GAG) heparin (Hep)have been produced and demonstrated to enable the sustained release of various growth factors [41–43]. In this system the anionic charge arising from the high density of sulfate moieties on heparin results in a high affinity for a broad range of growth factors, cytokines, and chemokines mainly due to electrostatic interactions [44]. This effect has been previously utilized to modulate the release of multiple growth factors such as FGF-2 and vascular endothelial growth factor (VEGF) [45] or cytokines, such as IL-4 [46] in a controlled and sustained manner over weeks. Additionally, these matrices can be applied as *in situ* forming hydrogels, which allow for the injection in a liquid state at the injury site, and posterior fast polymerization due to a Michael type reaction [47].

We have demonstrated in chapter II that starPEG-Hep hydrogel is efficient in promoting controlled release of hASCs secretome and its effective in modulate regenerative processes. Herein, we accessed the potential of this release system in promoting regeneration after a complete transection in an SCI rat model (Figure III.1). Histological analysis was conducted in an attempt to decipher which molecular mechanisms were underlying motor function. Moreover, the systemic inflammation was evaluated through a defined panel of cytokines in three different stages of lesion (acute, intermediate and chronic).

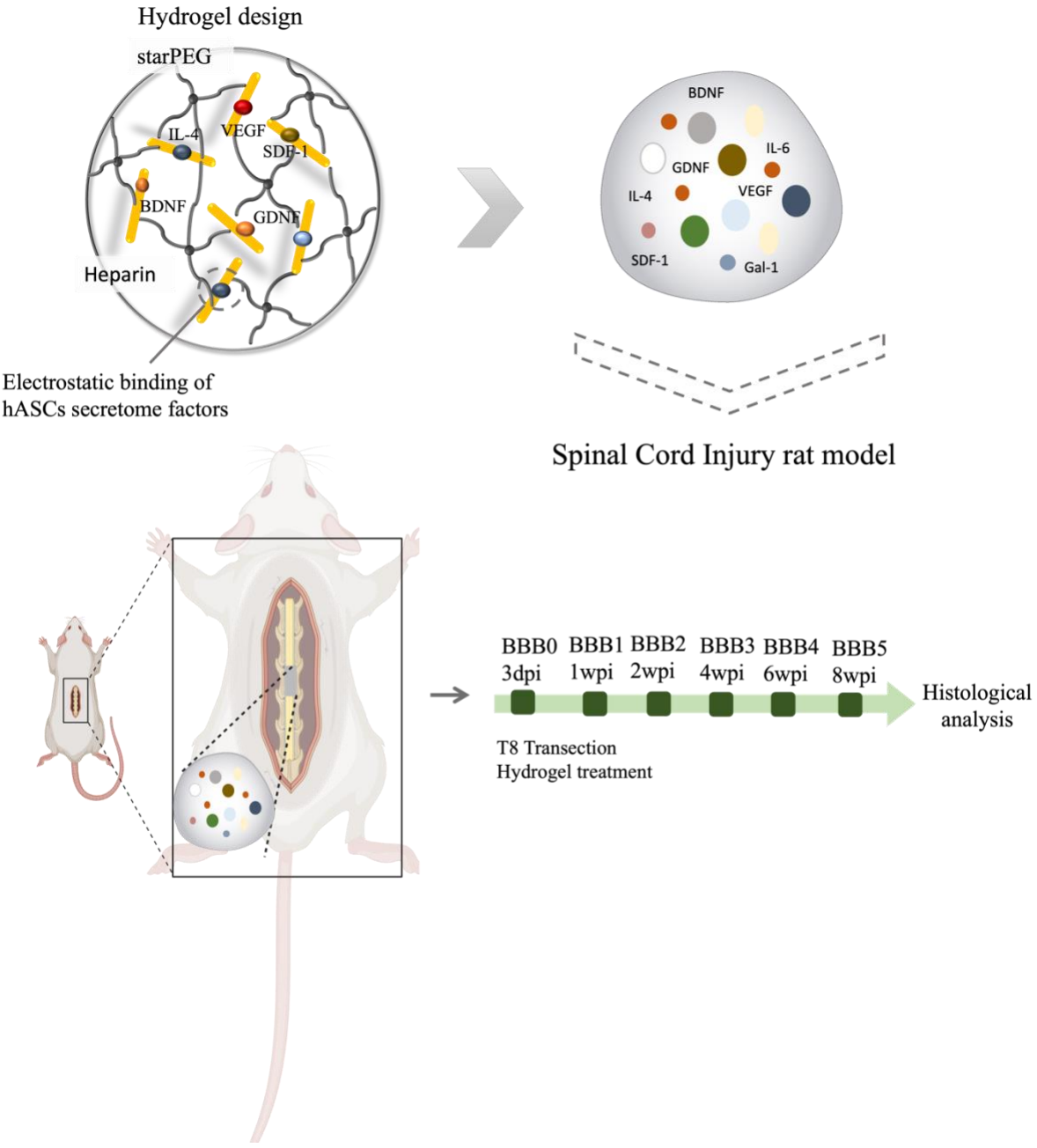

Figure III. 1 Schematic representation of our biomaterial concept and in vivo model that were used to evaluate the bioactivity of human adipose-tissue derived stem cells (hASCs) secretome released from starPEG-Hep hydrogels injected right before lesion. Recovery of thoracic (T8) level transected rats by secretome-loaded starPEG-Hep hydrogels was analyzed.

2. Materials and Methods

2.1. Secretome collection

2.1.1. Cell isolation and culture

The hASCs were obtained from lipoaspirates from consenting donors under a protocol approved and reviewed by an institutional board of LaCell LLC. Cells were isolated according to the protocol described by Dubois et al. [48] and maintained in culture, at 37 °C and 5% CO2, in α-MEM (Invitrogen, USA), with 10% Fetal Bovine Serum (FBS, Biochrom AG, Germany) and 1% antibiotic/antimycotic solution – penicillin/streptomycin (pen/strep; Invitrogen, USA). Medium was changed every 2/3 days until reach 85% confluence, afterwards cells were enzymatically detached and seeded onto new cell culture flasks.

2.1.2. Secretome collection

For secretome collection, hASCs were seeded at a density of 4000 cells/cm^2 in cell culture flasks with alpha minimum essential medium (α-MEM), as described above. The medium was harvested 72 hours after culture and the cells were washed four times with PBS without Ca^{2+}/Mg^{2+} (Merk, Germany). The cells were then placed 24 hours in Neurobasal A medium (ThermoFisher, USA) with 1% kanamycin, being this medium harvested at the end of that time (conditioned medium). It was further centrifuged (249g, Megafuge 1.0R, Heraeus, Germany) for 5 minutes to remove any cell debris. Then, hASCs secretome was concentrated (100x) by centrifugation (3000g) using 5kDa cut-off concentrator (Vivaspin, GE Healthcare, UK) and frozen at -80°C until used.

2.2. In vivo proof of concept

2.2.1. Study Design

The goal of this study was to evaluate the capacity of a secretome release system, based on the use of starPEG-Hep hydrogel in promoting regeneration in an SCI animal model. Thus, regenerative processes were assessed by functional recovery and histological alterations. Animals were randomly treated and all data collection (behavior and histology) was obtained in blinded conditions. All procedures were carried out in accordance with EU directive 2010/63/EU and were approved by the ethical committee in life and health sciences (ID: SECVS116/2016, University of Minho, Braga, Portugal).

2.2.2. Animals and groups

In this *in vivo* study, Wistar Han female rats (8-11 weeks old, weighing 170g-190g) were used. Animals were kept in light and temperature-controlled cages and fed *ad libitum* with a standard diet. The handling of the animals was carried out five days before the surgery. The animals were divided into five different groups according to the treatment/procedure instituted: 1) Animals subjected to SCI that were injected with starPEG-Hep loading secretome (starPEG-Hep+sec) (n = 7); 2) SCI animals treated with starPEG-Hep hydrogel and vehicle (NbA) (starPEG-Hep+NbA)(n = 4); or 3) SCI animals treated with secretome locally (n = 7); 4)SCI animals treated only with vehicle (NbA) (n = 6); and 5) Animals with laminectomy only (SHAM) (n = 7).

2.2.3. Spinal Cord Injury Surgery

For surgery, animals were previously anesthetized with an intraperitoneal injection of a mixture (1:5:1) of ketamine (100 mg/mL, Ketamidor/Richter Pharma, Austria) and medetomidine hydrochloride (1 mg/mL, Seedorm/ProdivetZN, Portugal). After anesthesia, the animals' fur was shaved and the skin disinfected with 70% ethanol and chlorhexidine. The incision was made in the dorsal midline, between T7 and T13, with subsequent retraction of the paravertebral muscles. A laminectomy (removal of the spinous processes to expose the spinal cord) was performed at T8 level and a total spinal cord transection was performed at this level. After administering the respective treatment, the paravertebral muscles and the skin were sutured with Vicryl sutures (Johnson and Johnson, USA). After surgery, all rats were kept under heat lamps and received daily post-operative care, during the first week, of vitamins (10 mL/Kg, Duphalyte,Pfizer, USA), 0.9% NaCl, the analgesic butorphanol (Butomidor, Richter Pharma AG, Austria), the antibiotic enrofloxacin (5mg/mL, Baytril, Bayer, Germany) and atipamezole (5mg/mL, Tipafar, ProdivetZN, Portugal) to reverse anesthesia (given on the first day only). In addition, manual bladder emptying was performed twice a day. The animals were examined for symptoms of disease and urinary infections detected during the eight weeks of study were treated with antibiotic enrofloxacin oral solution (Baytril, Bayer, Germany) and evaluated potential adverse reactions to treatment.

2.2.4. Hydrogel preparation

Amine end-functionalized 4-arm starPEG (MW 10,000, USA), Heparin (MW 15,000, Merck, Germany) and RGD (990 g/mol, Peptides International) were synthesized as previously described [41,47]. Hydrogel

formation was obtained by dissolving the maleimide functionalized heparin and thiol end-functionalized 4-arm starPEG in PBS on ice with an appropriate molar ratio. Briefly, 1.5mM heparin dissolved in PBS was mixed with an equal volume of starPEG solution in the concentration of 1.1mM to produce hydrogels in the crosslinking of 0.75 (molar ratio of starPEG to heparin).

For *in vivo* application heparin, starPEG and RGD were dissolved as previously described and filtered using low protein binding 0.2 µm filter (Acrodisc, PALL, USA) to ensure sterile conditions of the materials prior to injecting. Briefly, hASCs secretome (5 µL collected in NbA) were mixed with an equal amount of heparin/RGD and starPEG (2.5 µL).

2.2.5. Behavioral Analysis

2.2.5.1 *Locomotor rating*

The Basso, Beattie, Bresnahan Locomotor Rating Scale (BBB) [49] was employed to evaluate motor behavior and recovery. The test was performed for four minutes for two blinded researchers starting three days after surgery and performed 1, 2, 4, 6 weeks up to a total of eight weeks. Locomotion of the affected hindlimbs was rated in a score of 0 if no movement was observed, 1 to 8 indicates some movement of joints without weight support. From 9 to 20 animals are capable of weight support, have coordinated steps and trunk stability and finally, a 21 score corresponds to a normal animal with perfect movements. To attribute the final score to each animal the average score of both hindlimbs was made and plotted over eight weeks of behavior analysis.

2.2.5.2. Motor Swimming test (MST)

Animals have a natural capability to swim and the buoyancy provided by the water enables rats to perform locomotor movements without having to totally support their body weight. MST was performed once at 8 weeks post-injury where animals were placed in a quadrangular pool (water temperature 24-25°C) and had to reach the platform to get out of the water. After a short training trial, all trials were recorded by a video camera. To access locomotor activity, the velocity of the animals from one side of the pool to reach the platform was measured by using 3 trials per animal. Values were extracted using Ethovision XT 13 software (Noldus, Wageningen, Netherlands) and values of 3 trials averaged for each animal. Animals that weren't capable to perform the test, either if they don't have motivation to swim or needed more than 3 min to perform all trials were excluded.

2.2.5.3. Von Frey

Loss or gain of sensitivity in the hindlimbs of the lesioned animals were assessed through mechanical allodynia that measures the evoked pain using Von Frey test. In this test monofilaments are applied in the center of the hindlimbs by the up-down method [50]. Once at a time, animals are placed in the Von Frey apparatus and left for some time undisturbed to be acquainted, then a monofilament (2.0g) is applied to the hindlimb center, once at a time, for no more than 4s. If the animals reacted, withdrew the paw, was considered a positive response and a monofilament of a lower force was applied; if no reaction was observed negative response was considered and consequently a monofilament of a high force is applied [51]. The test is finished if the extreme monofilament was reached or 4 measurements around the turning point were obtained. The range of VF monofilaments used was the following: 0.4, 0.6, 1.0, 2.0, 4.0, 6.0, 8.0, 15.0g. The assessment was performed twice at 2- and 6-weeks post-injury.
The measurement used was the 50% threshold, that is an approximation of the monofilament that causes pain or sensitivity, for that the following equation 1 was used:

$$50\%g\ \_treshold = \frac{\left(10^{Xf+K.\delta}\right)}{10000} \qquad \text{Equation 1}$$

where Xf=value (in log units) of the final VF monofilament; K=tabular value corresponding to pattern of positive and negative responses; δ=mean difference (in log units) between stimuli (0.224).

2.2.6. Immunohistochemistry

2.2.6.1. Histological Analysis

Eight-weeks post-injury, rats were deeply anesthetized by an intraperitoneal injection of sodium pentobarbital (200 mg/mL, Euthasol, Ecuphar, Spain) and perfused through the ascending aorta with NaCl (0.9 %; 100mL) followed by PFA (4 %; 100mL). A rough dissection of the spine and spinal cord was performed, centered on the site of transection and the tissues were fixed in 4 % PFA overnight at 4°C. A more detailed dissection of the spinal cord was then done, and the tissues were carefully placed on a solution of sucrose (30 % (w/v)) on the next day. Afterwards, 1.5 cm length of spinal cord tissues, centered on the lesion, were involved in optimal cutting temperature compound (OCT, ThermoFisher, USA), frozen

with liquid nitrogen and stored at -20 °C. Later, longitudinal sections of 20 µm thickness were performed using a Leica CM1900 cryostat.

2.2.6.2. Immunohistochemistry

Spinal cord longitudinal sections were initially permeabilized with PBS-T (0.2 %) for 10 min. Then, the slides were blocked with a solution of NBCS (5 %) in PBS-T (0,2%) for 30 min. After that, the samples were incubated overnight with the following primary antibodies: rabbit anti-rat GFAP for astrocytes (1:200, Dako Denmark, Glostrup, Denmark), mouse anti-neurofilament (NF, 1:200, Merck, USA), rabbit anti-Iba-1 (1:1000, Wako, Japan), mouse anti-SMI-71 (1:200, Biolegend, USA). On the next day, samples were incubated for 2 h with the respective secondary antibodies: Alexa Fluor 594 goat anti-rabbit for GFAP, Alexa Fluor 488 goat anti-mouse for NF, Alexa Fluor 488 goat anti-rabbit for Iba-1, Alexa Fluor 594 goat anti-mouse for SMI-71 (all from Invitrogen, USA). All samples were counterstained with DAPI (1:1000, Life Technologies) for 10 min. Between steps, three washes with PBS were performed. Finally, the slides were mounted in Immu-Mount® (ThermoFisher, USA) and observed at a fluorescence microscope, Olympus Widefield Inverted Microscope IX81. All images were treated using Fiji software.

2.2.7. Immunofluorescence Analysis

For immunofluorescence analysis, images of the longitudinal section were obtained for each animal as a mosaic of all tissue, 4-6 micrographs per animal. Then images were open with Fiji software and scale was determined first. For GFAP and NF analysis the positive area for each marker was calculated. For that a section of 2000µm was delineated for rostral, epicenter and caudal part of the spinal cord. Following, imagens were converted to 8 bits and processed in the command “make binary”. Finally, after applying the threshold command, using the menu “analyze particles”, the program automatically calculated the positive area occupied for each marker, using the dark background as contrast. The positive area of each marker was normalized to the area of the tissue for each region. For Iba-1 the immunofluorescence quantification was performed by measuring the total ameboid area and normalized to the total area of the spinal cord segment. For SMI-71 analysis a 1500µm region rostral and caudal to the lesion were selected and vessels analyzed using Angio Tool software as previously described [52] three parameters where selected, vessel area, vessel length, average vessel length.

2.2.8. Serum collection and analysis by Neuro array membrane

Rat blood was collected directly from the tail vein at 48h and four weeks post-injury and from the heart at sacrifice. Blood was allowed to coagulate for approximately 15min and centrifuged at 15330 g for 15min. Serum was collected and stored at -80°C until use. For each group a pool of serum was made and analyzed using Rat Cytokine Array C2 (C-Series RayBiotech, USA) according to the manufacture's instructions. Analysis of the membranes was performed in AzureSpot Analysis software (Azure Biosystems, USA) where the relative intensity of each spot was measured. Afterwards, to quantify the relative intensity of each spot corresponding to a different protein, the background was subtracted, and intensity normalized to positive controls.

2.3. Statistical Analysis

Data regarding BBB and Von Frey test were analyzed using Mixed ANOVA to compare the mean values of five groups. When evaluating the velocity in MST, the ameboid area of Iba-1 and positive area of NF, GFAP and SMI-71 one-way ANOVA was performed. A pairwise comparison between groups based on estimated marginal means using Turkey's correction was performed. The significance value was set as $p \leq 0.05$ for all statistical tests and graphs are presented as mean ± SEM. For all data normality was assessed using Shapiro-Wilk statistical tests and taking into account the measures of skewness and kurtosis. Moreover, it is important to highlight that ANOVA distribution can be approximately normal distributed [53]. IBM SPSS® Statistics version 27 for IOS (IBM Co., USA) was used to perform all statistical analysis. For graphical representations GraphPad Prism ver.8.4.3 (GraphPad Software, La Jolla, USA) was used.

3. Results

3.1. hASCs secretome released from starPEG-Hep hydrogels promotes motor recovery in an SCI animal model.

The secretome of hASCs has previously been shown to induce regeneration after SCI in animal models [24,54]. Herein we aimed to develop a hydrogel system capable of controlled and prolonged release of secretome at the injury site in order to potentiate its effect. Considering the pro-regenerative capacity

shown in *in vitro* studies (Chapter II) we explored the potential of the released secretome in promoting motor improvements after a complete transection in a rat model. Animals were divided into five groups: SCI treated with starPEG-Hep hydrogel loading secretome (starPEG-Hep+sec; n = 7); SCI treated with starPEG-Hep loading Neurobasal A (starPEG-Hep+NbA; n = 4); SCI treated with secretome locally (Secretome; n = 7); SCI treated with Neurobasal A (NbA; n = 6); and non-injured animals (laminectomy – SHAM; n = 7). Complete transection was performed at T8 level and animals were immediately treated after lesion.

Motor recovery was evaluated every two weeks until eight weeks post-injury by BBB test. Animal treated with starPEG-Hep+sec displayed improved motor outcomes compared with other groups, Figure III.2. In addition, SHAM animals did not present motor deficits during that time. Statistical analysis revealed an effect of factor time (weeks $F(5, 130) = 33.54$ $p<0.0001$, $\eta^2_{partial} = 0.56$), and treatment $F(4, 26) = 948.54$ $p<0.0001$, $\eta^2_{partial} = 0.99$) and the interaction between these two factors ($F(20, 130) = 3.90$ $p<0.0001$, $\eta^2_{partial} = 0.38$). In particular, the mean BBB score was significantly improved by starPEG-Hep+sec treatment at two, six- and eight weeks post-injury (wpi). Moreover, at two and six wpi, animals treated with starPEG-Hep+sec showed improved motor function when compared with animals treated with only secretome (2wpi: 2 ± 2 vs 0.71 ±0.57; p = 0.032; 6wpi: 3.5 ± 2.25 vs 1.29 ± 0.95; p = 0.004). Notably, at eight wpi animals treated with starPEG-Hep+sec showed statistically significant improvements compared with starPEG-Hep+NbA (4.07 ± 2.24 vs 2.00 ± 0.82; p = 0.012), animals treated with only secretome (1.86 ± 0.85, p = 0.002) and animals lesioned treated with vehicle (2.25 ± 0.69; p = 0.013). Interestingly, comparing the group treated with starPEG-Hep+sec with free secretome, a difference of approximately two points in BBB scale was reported clearly showing a beneficial effect of the hydrogel-based release. All statistical data is presented in Supplementary Table III.S1.

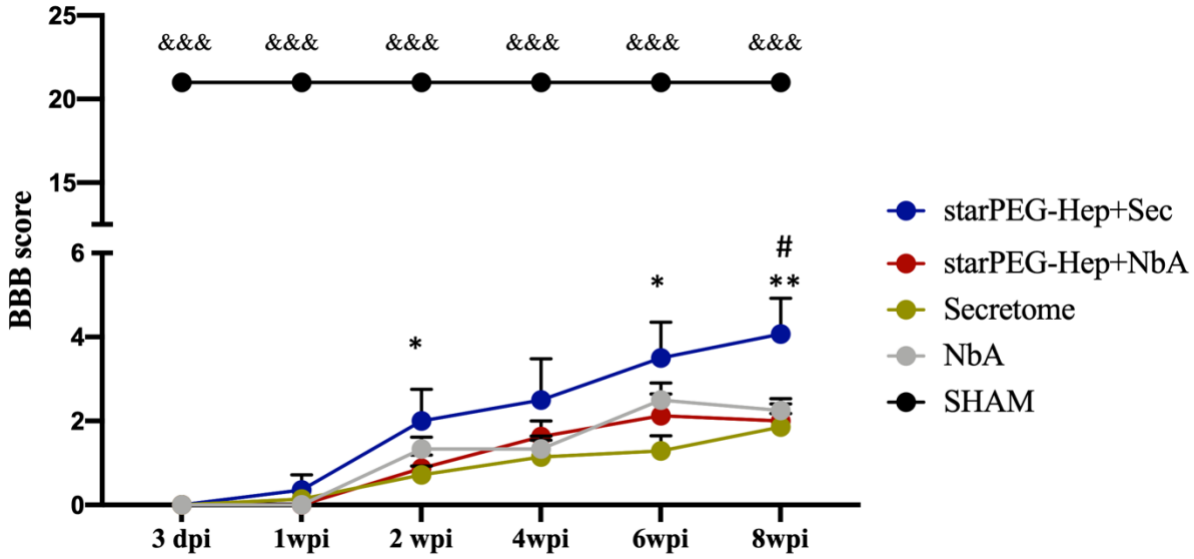

Figure III. 2 Evaluation of motor performance in SCI rats by BBB test for eight weeks post-injury. Animals treated with secretome presented improved motor recovery eight weeks after treatment. Mixed ANOVA; (*) represented differences between starPEG-Hep+sec and Secretome, (#) differences between starPEG-Hep+sec vs starPEG-Hep+NbA and NbA, and (&) differences between SHAM group and all other; * and # $p < 0.05$; **$p < 0.001$ and &&& $p < 0.0001$. Error bars represented mean ± SEM.

The BBB score of animals treated with starPEG-Hep+sec indicates that animals could perform extensive movements of two joints (such as ankle, knee or hip), while animals treated with starPEG-Hep+NbA or NbA were only able to perform extensive movement of one joint and slight movement of the third. Finally, animals treated with secretome only performed slight movements of hindlimbs joints.

Other motor tests were performed for motor recovery or sensorial function after injury. Regarding the MST, animals treated with starPEG-Hep+sec were able to perform the task at a higher velocity when compared with animals treated with starPEG-Hep+NbA (9.68±3.85 vs 5.34±1.08), Secretome (8.88±1.97) or NbA (8.24±3.65), Figure III.3A. While animals treated with starPEG-Hep+NbA had the lowest velocity. Nevertheless, no statistical significance was observed among groups and all were slower than SHAM animals, as shown in Supplementary Table III.S2.

Sensorial function was evaluated by performing Von Frey test, in which different force filaments were applied to the hindlimbs. Then, results were evaluated as a 50% chance of being the final response filament. For the left hindlimb animals treated with starPEG-Hep+sec showed slightly less sensitivity when compared with starPEG-Hep+NbA (4.53±2.68 vs 3.75±2.26), secretome (4.45±4.86) or NbA (3.37± 1.49) at two wpi. However, a slight increase in sensitivity was observed at six wpi (4.08±4.43) when compared with other groups (starPEGHep+NbA 6.90± 5.87; Secretome 4.84±4.55, NbA 4.33±3.91) as

shown in Figure III.3B. For right hindlimb, animals treated with starPEG-Hep+sec (4.53±3.38) also showed less sensitivity at two wpi when compared with other groups (starPEG-Hep+NbA 2.30±0.98, secretome 2.61±0.72, NbA 4.13±1.75). This tendency is maintained at six weeks after lesion (starPEG-Hep+sec 6.42±6.01, starPEG-Hep+NbA 3.82±2.33, secretome 5.37±5.48, NbA 3.25 ±1.78) (Figure III.3C). Though, no statistical difference was observed among treated groups and all were statistical different from SHAM animals (Supplementary Table III.S3).

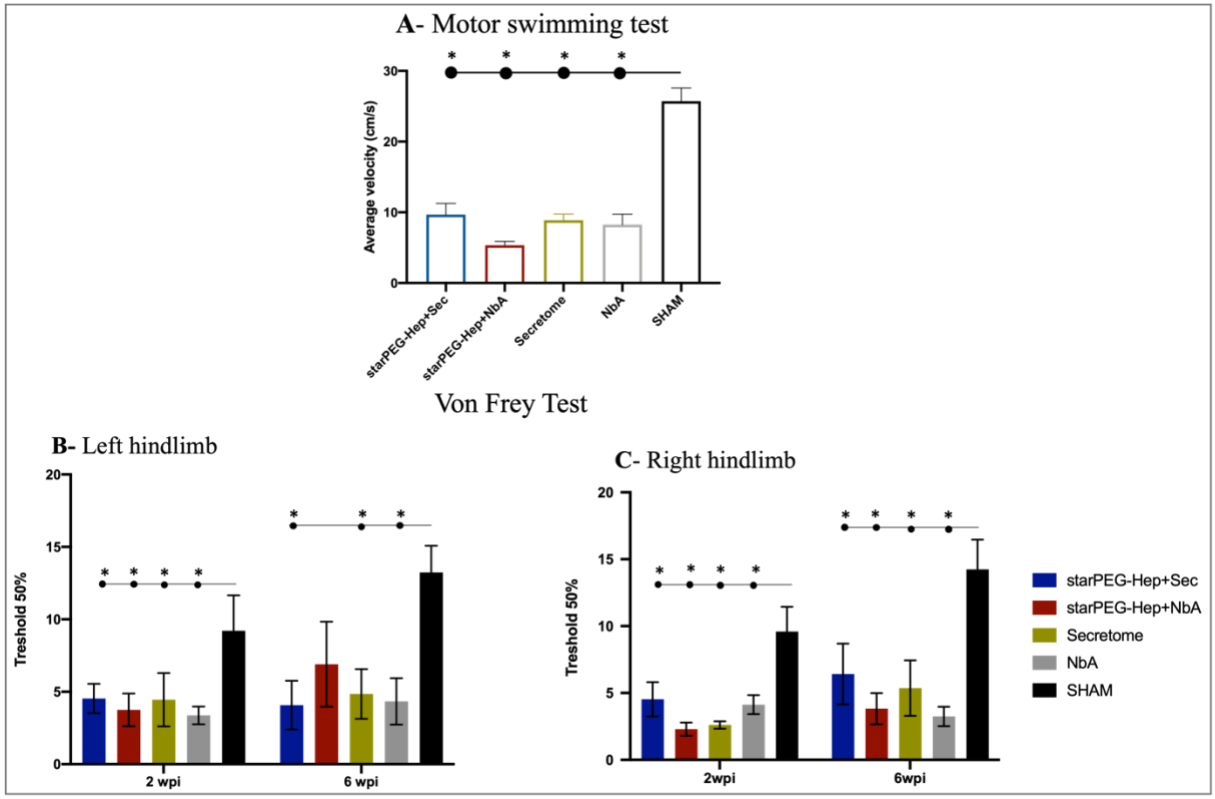

Figure III. 3 Evaluation of motor recovery after SCI rat model. **A**, Average velocity in Motor swimming test performed 8 weeks after lesion. Von Frey test evaluated sensorial recovery 2 and 6 weeks after lesion in left (**B**) and right (**C**) hindlimb. A – ANOVA B-C Mixed Anova (*) represents differences between SHAM group and all other; $p < 0.001$. Error bars represented mean ± SEM

3.2. hASCs secretome released from starPEG-Hep hydrogels decreases the inflammation in an SCI model

Eight weeks after spinal cord transection, animals were sacrificed and the spinal cords processed for histological analysis. Neuroinflammation in tissue was evaluated through immunostaining with Iba-1. In this sense, area of ameboid microglia, a phenotype associated higher inflammation, was quantified Figure III.4. Statistical analysis showed that there was a significant effect in Iba-1 staining ($F(4.30) = 96.90$, $p<0.0001$). Animals treated with starPEG-Hep+sec presented a significantly reduced area of ameboid microglia ($p = 0.019$) when compared with animals treated with secretome only ($n = 7$; 38.88 ± 7.44 vs $n=7$; 48.59 ± 5.05) or NbA ($n = 6$; 49.28 ± 4.32; $p = 0.015$; Figure III.4C). On the other way, no differences were reported regarding comparison with animals treated with starPEG-Hep+NbA ($n = 4$; 44.43 ± 7.77, $p = 0.49$). All statistical comparisons between groups are presented in Supplementary Table III.S4.

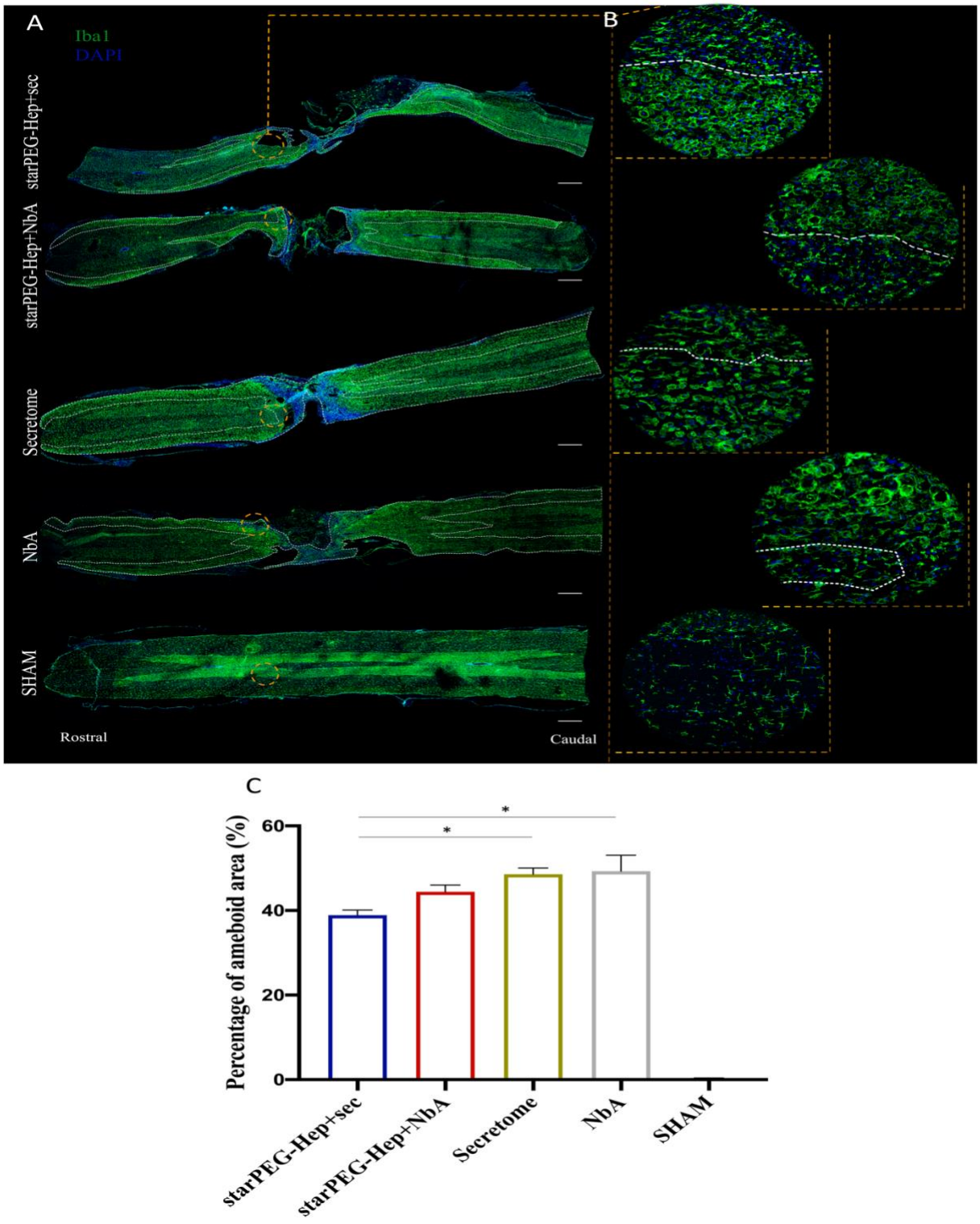

Figure III. 4 Representative confocal microscopy images of longitudinal sections of spinal cord tissue for Iba1 staining. **A**, delineated ameboid area in animals treated with starPEG-Hep+sec, starPEG-Hep+NbA, Secretome, NbA and SHAM eight weeks after lesion. **B**, Magnification of tissue stained with anti-Iba1 and considered ameboid area. **C**, quantification of ameboid area in all groups. Ameboid area

was normalized to total area of the tissue and plotted as percentage. One-way ANOVA; * $p < 0.05$. Error bars represented mean ± SEM. Scale bar: 100 μm.

Other markers were used to access astrocytes (glial fibrillary acidic protein (GFAP)) and axonal regeneration/preservation (NF), which are displayed in Figure III.5. A decrease in the percentage of GFAP positive area at rostral, epicenter, and caudal regions was also observed in animals treated with starPEG-Hep+sec compared with animals treated with secretome and NbA (Figure III.5B). A similar trend occurs for NF-positive area. While a slight increase in NF positive area in starPEG-Hep+sec is observed at the epicenter region, a decrease is noticed at rostral and caudal regions with all other groups (Figure III.5C). Nevertheless, no significant differences were observed among treated animals for both markers (Supplementary Table III.S5)

SMI-71 is an antibody that allows to assess blood brain barrier integrity (BBB). In this study, we evaluated the presence of vessels in rostral and caudal regions, right after and before lesion, respectively (Figure III.6). An increase in vessel area was observed in animals treated with starPEG-Hep+sec and secretome (0.10 ± 0.02) when comparing with starPEG-Hep+NbA or NbA (Figure III.6B). Regarding vessel length, animals treated with starPEG-Hep+sec continue to have higher vessels in comparison to other treated groups, as displayed in Figure III.6C. However, vessels are quite similar, among treated groups, considering average vessel length (Figure III.6C). Nonetheless, no statistical significance was observed in all three referred parameters, (Supplementary Table III.S6).

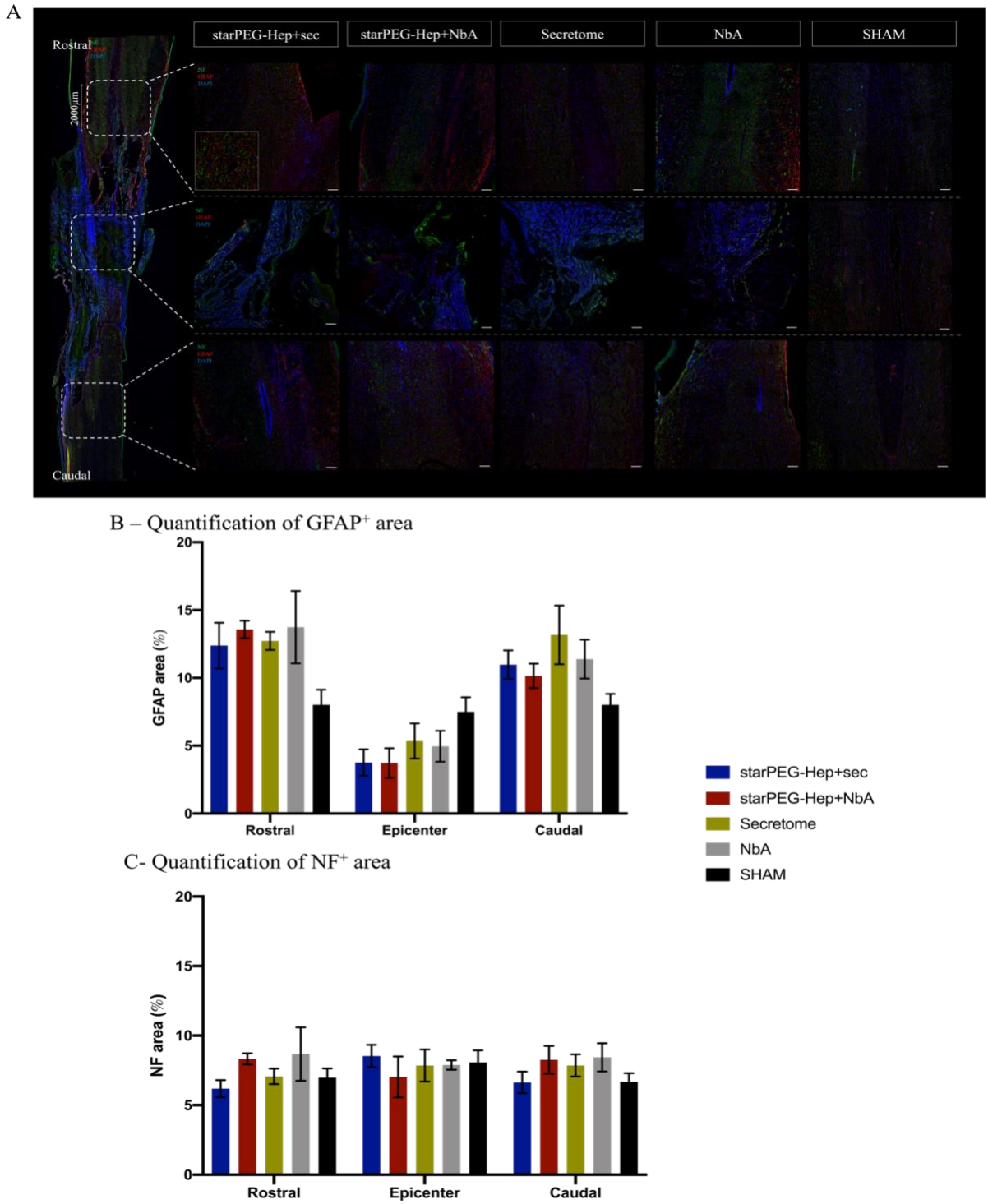

Figure III. 5 Representative confocal microscopy images of longitudinal sections of spinal cord tissue for GFAP and NF staining. **A**, delineated selected areas at rostral, epicenter and caudal regions in animals treated with starPEG-Hep+secretome, starPEG-Hep+NbA, Secretome, NbA and SHAM, 8 weeks after lesion. **B**, Quantification of GFAP positive area in three different regions. **C**, Quantification of NF positive area in three different regions. One-Way ANOVA, Error bars represented mean ± SEM. Scale bar: 100 µm. GFAP – Glial Fibrillary acidic protein, NF – Neurofilament, DAPI 4',6'-diamino-2-fenil-indol

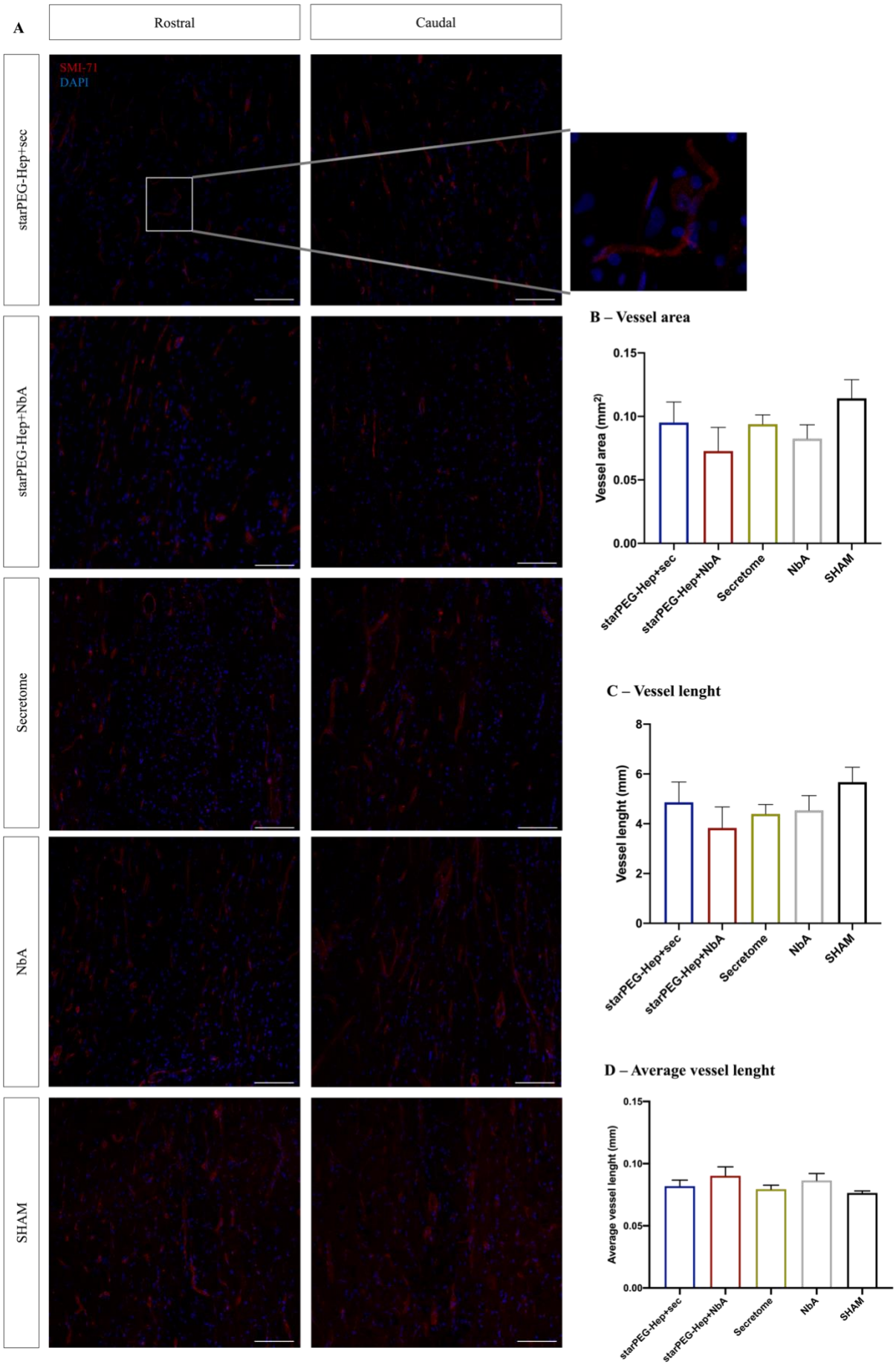
A
Rostral
Caudal
SMI-71
DAPI
starPEG-Hep+sec
starPEG-Hep+NbA
Secretome
NbA
SHAM
B – Vessel area
Vessel area (mm²)
0.15
0.10
0.05
0.00
starPEG-Hep+sec
starPEG-Hep+NbA
Secretome
NbA
SHAM
C – Vessel lenght
Vessel lenght (mm)
8
6
4
2
0
starPEG-Hep+sec
starPEG-Hep+NbA
Secretome
NbA
SHAM
D – Average vessel lenght
Average vessel lenght (mm)
0.15
0.10
0.05
0.00
starPEG-Hep+sec
starPEG-Hep+NbA
Secretome
NbA
SHAM

Figure III. 6 SMI-71 quantification in SCI rat model eight weeks after lesion. **A**, Representative confocal microscopy images of selected areas at rostral and caudal regions in animals treated with starPEG-Hep+sec, starPEG-Hep+NbA, Secretome, NbA and SHAM eight weeks after lesion. **B**, Quantification of SMI-71 vessel area, **C**, Quantification of SMI-71 vessel length, **D**, Quantification of SMI-71 average vessel length. One-Way ANOVA, Error bars represented mean ± SEM. Scale bar: 100 μm.SMI-71 – Anti Blood Brain Barrier, DAPI 4',6'-diamino-2-fenil-indol

SCI is characterized by an exacerbation of inflammatory response, which could be one of the causes of the massive damage to the tissue after lesion. After we observed an attenuation of inflammation characterized by the reduction of ameboid microglia in the damage tissue of animals treated with hydrogel and secretome, we evaluated if the same could be observed systemically. For this purpose, animal serum was collected at three different time points (48h, four and eight wpi) and the expression of cytokines was evaluated by a cytokine array. Molecular analyses of sera at 48h post-lesion are presented in Figure III.7B, where the expression of a heatmap (Figure III. 7A). Animals treated with starPEG-Hep+sec have an increase in IL-10 compared with animals treated with hydrogel only, secretome or NbA, and a decrease of inflammatory cytokine monocyte chemoattractant protein (MCP-1) compared with other groups. Moreover, cluster of differentiation 89 (CD86), a classically (M1) marker, presented values similar to SHAM animals at this time point.

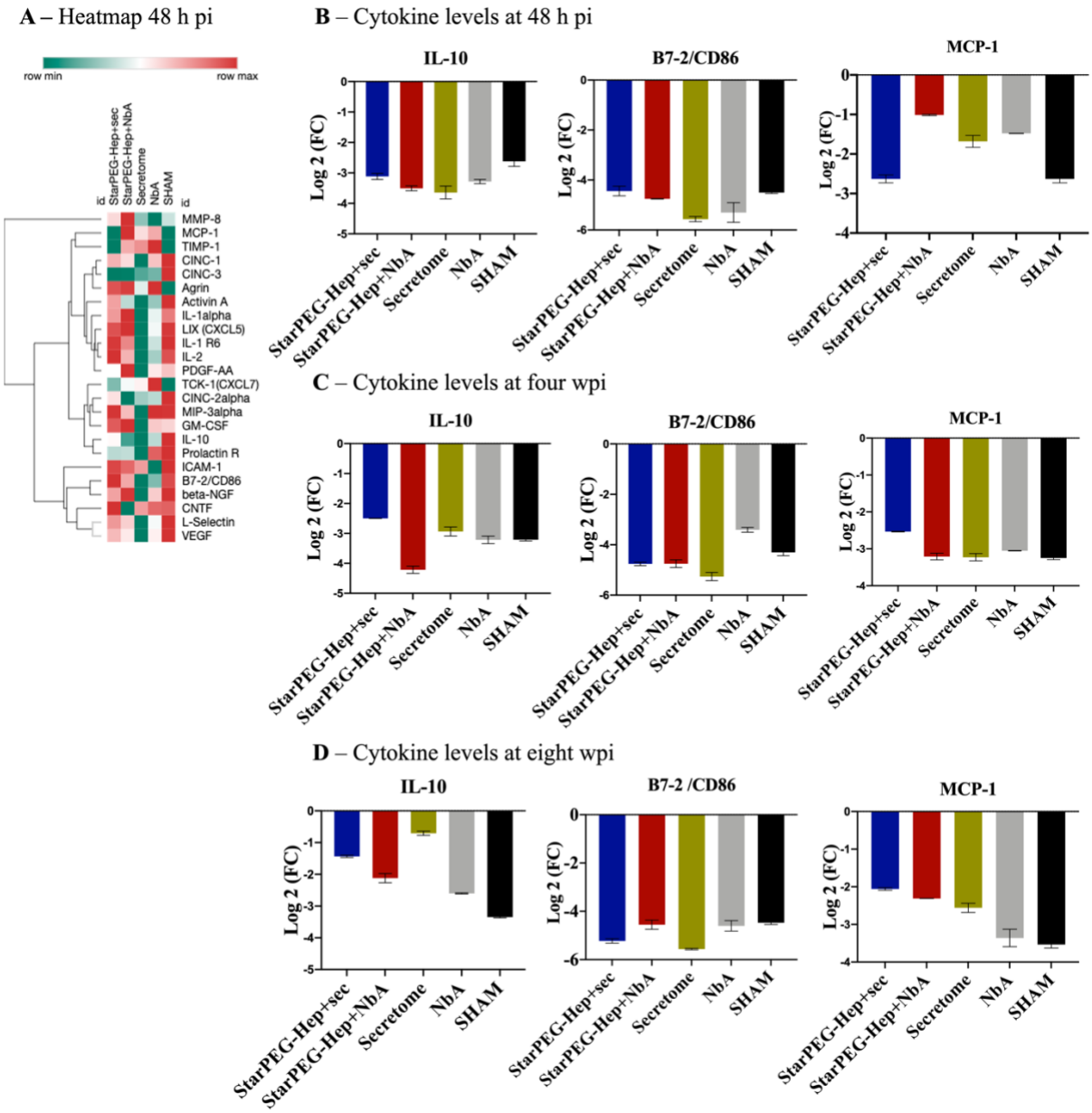

Figure III. 7 Molecular analysis of collected sera following SCI using Rat Cytokine Array C2 from RayBiotech. **A,** Representative heat map at 48 h pi of the panel for the different groups was generated using the BROAD Institute's R implementation of Morpheus with Euclidean distance hierarchical clustering. **B,** Relative expression of selected pro-inflammatory and anti-inflammatory cytokines at 48 h pi, **C**, 4 wpi and **D**, 8 wpi. Data are shown as mean Log2 (fold change - FC) relative to the normalization of each cytokine to the positive controls of each membrane. Error bars represented mean ± SEM.

After four weeks (Figure III. 7C and Supplementary Figure III.S1), animals treated with starPEG-Hep+sec continue to have a higher expression of IL-10 when compared with animals treated with starPEG-Hep+NbA, secretome or NbA, Figure III.7C. Interestingly, at this time point, a decrease in expression of CD86 is observed compared with NbA treated animals. On the other hand, values of MCP-1 remained similar to values obtained at 48h, with a decrease in groups treated with starPEG-Hep+NbA, secretome or NbA.

Right before sacrifice (eight weeks, Figure III. 7D and Supplementary Figure III.S1), sera analysis revealed an increase in IL-10 levels in animals treated with starPEG-Hep+sec and secretome compared to other groups, Figure III. 7D. CD86, a marker of M1 phenotype [55], demonstrated a slight decrease from four weeks post-injury and compared with animals treated with hydrogel and NbA at this time point. It is also worth noting that animals treated with starPEG-Hep+sec have higher levels of VEGF expression than all other groups at all time points.

4. Discussion

Cell-based therapy, particularly transplantation of ASCs has upraised therapeutical approaches to tackle devastating conditions caused by SCI. Furthermore, several studies pointed that their beneficial effects are mediated by their secretome, rather than its presence at injury site [9,17]. Along these lines, stem cell secretome has been raised as a cell free-based therapy in the field of regenerative medicine [56,57]. However, administration methodology is an obstacle to foster their application. Local injection is characterized by the rapid clearance at SCI, while multiple systemic administrations promote their fast diffusion in the body, meaning higher dosage to have effect. Biomaterials, particularly hydrogels, flourished as suitable platforms, not only by their singular characteristics but also their potential in controlling drug delivery at injury site [32–34]. In accordance, in this work we aimed to develop a combinatorial therapy in which hASCs secretome is loaded in starPEG-Hep hydrogels to promote a controlled and prolonged release at SCI injury site. With this strategy, secretome effect can be locally potentiated and regeneration favored.

From data presented in Chapter II, we have shown that starPEG-Hep hydrogels were effective in promoting controlled and prolonged release of hASCs secretome, which was capable of inducing neural differentiation and axonal growth. However, validation of this therapeutic approach in an *in vivo* injury mode was still lacking. Likewise, a complete transection at T8 level was performed in a rat model. These results in a very severe lesion, when compared with hemisection or contusion models [58]. Animals were immediately treated and motor recovery evaluated for eight weeks.

Animals treated with starPEG-Hep+sec presented significant improved motor recovery at two-, six- and eight-weeks post injury in BBB test. Interestingly, comparing the group treated with starPEG-Hep+sec with free secretome, a difference in approximately two points in BBB scale was reported clearly showing a beneficial effect of the hydrogel-based release. Despite these motor improvements, no differences were observed on the swimming velocity in MST. Lesioned animals had no ability to move hindlimbs, but they swim using forelimbs (videos not shown). This may explain the similarities among groups. On the other hand, this behavioral test evaluates gross motor function where animals have no sensory input from water similar to the stimulus, they experienced with direct contact with BBB table. Sensorial inputs are critical to demand locomotion through activation of central pattern generators (CPGs). These circuitries receive inputs from afferent neurons such as muscles or joints and shape locomotor outputs [59,60]. Additionally, proprioceptive feedback and mechanoreceptive circuits are closely interconnected and may contribute for motor recovery. They are known to be important as an alternative for transmission of afferent information after lesion [61,62]. However, this is not the most likely pathway governing motor recovery as evidenced by low sensorial recovery on Von Frey test.

Histological analysis has shown a reduced area occupied by ameboid microglia, a phenotype associated with higher inflammation, in animals treated with starPEG-Hep+sec compared with local secretome or NbA. Previous studies have shown that the starPEG-Hep hydrogels can reduce inflammation by scavenging inflammatory mediators [63,64]. In line with those findings, a slight attenuation of Iba-1 expression was observed in animals treated with starPEG-Hep+NbA, which point to the anti-inflammatory characteristics of the pure hydrogels with only the starPEG-Hep+sec effectively attenuating inflammation in the SCI model.

In addition, no major differences were found in GFAP or NF quantification positive area. The integrity of BBB was also evaluated by SMI-71 staining, but no statistical differences were observed regarding vessel area or length. Altogether, these data indicate that motor recovery seems to be favored by a reduced inflammatory response to treatment in local tissue. Furthermore, it has been previously demonstrated that hASCs secretome promoted a reduced inflammatory response *in vivo*, either by treatment with secretome systemically in mice model [24], or the local cell transplantation [9,10]. Moreover, ASCs secretome can induce M2 polarization, through mammalian target of rapamycin complex 1 (mTORC1) and mTORC2 pathway [65]. Other authors also hypothesized that hASCs transplantation in a contusion injury mice model could reduce neuroinflammation by reducing microglia/macrophages at lesion site, as well as inhibiting Jagged1/Notch pathway [66]. This pathway has been implicated in modulating the immune response after lesion in central nervous system (CNS) by impacting cell fate decisions and

endogenous neurogenesis [67]. On the other hand, interferon gamma (IFN-γ), present in secretome and released by hydrogels, may determine microglia's anti or pro-inflammatory state. Indeed a lower concentration can induce a neuroprotective function [68,69].

Moving to sera analysis, animals treated with starPEG-Hep+sec show an increase in IL-10, an anti-inflammatory cytokine, in all time points after lesion (48h, four and eight wpi). The release of IL-4 or IFN-γ by secretome-loaded hydrogels has been previously shown to induce IL-10 production by microglia/macrophages, leading to increased circulation levels [70,71]. Thus administration of IL-10 has been shown to decrease the levels of pro-inflammatory cytokines and contributed to motor recovery after lesion [72,73]. At the same time, as MCP-1 has been shown to play a critical role in mediating neuron-macrophage interactions that contribute to axonal growth and M2 phenotype polarization, the moderate levels of MCP-1 observed over time may down regulate the inflammatory response and endure the regenerative process [74].

On the other hand, CD86, an M1 marker, is decreased at four and eight weeks after lesion, while MCP-1 was low expressed in the acute phase (48h).

Together, the reported data demonstrate for the first time that a biohybrid hydrogel-based sustained hASCs secretome release comprising pro-regenerative cytokines (IL-4, IL-2) and growth factors (BDNF, GDNF). Significant motor recovery in a complete SCI rat model further confirmed the robustness of the delivery system, accompanied by a reduced ameboid microglia area, as well as increased levels of the anti-inflammatory cytokine IL-10 in animal sera.

5. Conclusions

A starPEG-Hep hydrogel was successfully tuned for sustained hASCs secretome release over weeks as well as for mechanical tissue stabilization to promote neural regeneration [75,76]. The system was demonstrated to be effective in an SCI animal model in reducing inflammation management, reducing ameboid microglia area, as well as increasing anti-inflammatory cytokine IL-10 in animal serum, and initiating pro-regenerative processes. In perspective, the approach may offer unprecedented clinical treatment modalities for SCI.

Acknowledgments

This work was supported by Prémios Santa Casa Neurociências–Prize Melo e Castro for Spinal Cord Injury Research (MC-04/17; MC-18-2021) and the Portuguese Foundation for Science and Technology (Ph.D. Fellowship to D.S (PD/BDE/135567/2018 and COVID/BDE/152051/2022); T. S. P. (PD/BDE/143150/2019); J.R.C (SFRH/BD/145860/2019); J.A (2021.08337.BD); S.B.-A ((PD/BDE/135568/2018). This work was funded by national funds and FEDER, through the Foundation for Science and Technology (FCT), under the scope of the projects UIDB/50026/2020; UIDP/50026/2020; POCI-01-0145-FEDER-029206; POCI-01-0145-FEDER-031392; PTDC/ MED-NEU/31417/2017; NORTE-01-0145-FEDER-029968; POCI-01-0145-FEDER-029751; POCI-01-0145-FEDER-032619. This work has been funded by ICVS Scientific Microscopy Platform, a member of the national infrastructure PPBI - Portuguese Platform of Bioimaging (PPBI-POCI-01-0145-FEDER-022122. This work has also been developed under the scope of the project NORTE-01-0145- FEDER-000013 and NORTE-01-0145-FEDER-000023, supported by the Northern Portugal Regional Operational Programme (NORTE 2020), under the Portugal 2020 Partnership Agreement, through the European Regional Development Fund (FEDER). Work supported by the Portuguese Foundation for Science and Technology (FCT): projects UID/FIS/04650/2020, PTDC/EMD-EMD/28159/2017, and PTDC/BTM-MAT/28237/2017.

Dr. Jeff Gimble and LaCell, Inc. kindly provided the adipose tissue-derived stem cells used in this study. Nelly Rein for her technical advice and support in working with the hydrogel material.

Author contributions

D.S designed and performed most of the experiments, collected and analyzed the data, and drafted the manuscript. T.S.P, J.C.R, R.L, J.A, S.B-A, C.R.M, JD helped *in vitro* and animal experiments. P.A, L.S helped in designing experiments. U. F. and C.W provided hydrogel materials. A.J.S conceived and financially support the study, participated in its design and coordination. L.S, U. F., C.W., A.J. S. critically read the manuscript. Supervision: R.A.S, U. F., C.W., A.J.S. All authors read and approved the final manuscript.

Conflict of Interest

The authors declare that they have no known competing financial interests or personal relationships that could have appeared to influence the work reported in this paper.

Data availability

The data that supports this study is available from the authors upon reasonable request.

References

[1] L. Anderberg, H. Aldskogius, A. Holtz, Spinal cord injury - Scientific challenges for the unknown future, Ups. J. Med. Sci. 112 (2007) 259–288. https://doi.org/10.3109/2000-1967-200.

[2] N. Level, Facts and Figures at a Glance, J. Spinal Cord Med. 30 (2018) 304–305. https://doi.org/10.1080/10790268.2007.11753944.

[3] S. Huh, H.Y. Ko, Recovery target priorities of people with spinal cord injuries in Korea compared with other countries: a survey, Spinal Cord. 58 (2020) 998–1003. https://doi.org/10.1038/s41393-020-0457-z.

[4] K.D. Anderson, Targeting recovery: Priorities of the spinal cord-injured population, J. Neurotrauma. 21 (2004) 1371–1383. https://doi.org/10.1089/neu.2004.21.1371.

[5] M.D. Norenberg, J. Smith, A. Marcillo, The Pathology of Human Spinal Cord Injury: Defining the Problems, J. Neurotrauma. 21 (2004) 429–440. https://doi.org/10.1089/089771504323004575.

[6] J.W. Rowland, G.W.J. Hawryluk, B. Kwon, M.G. Fehlings, Current status of acute spinal cord injury pathophysiology and emerging therapies: Promise on the horizon, Neurosurg. Focus. 25 (2008) 1–3. https://doi.org/10.3171/FOC.2008.25.11.E2.

[7] A. Anjum, M.D. Yazid, M.F. Daud, J. Idris, A.M. Hwei Ng, A.S. Naicker, O.H. Rashidah Ismail, R.K.A. Kumar, Y. Lokanathan, Spinal cord injury: Pathophysiology, multimolecular interactions, and underlying recovery mechanisms, Int. J. Mol. Sci. 21 (2020) 1–35. https://doi.org/10.3390/ijms21207533.

[8] A.P. Tran, P.M. Warren, J. Silver, The biology of regeneration failure and success after spinal cord injury, Physiol. Rev. 98 (2018) 881–917. https://doi.org/10.1152/physrev.00017.2017.

[9] E.D. Gomes, S.S. Mendes, R.C. Assunção-Silva, F.G. Teixeira, A.O. Pires, S.I. Anjo, B. Manadas, H. Leite-Almeida, J.M. Gimble, N. Sousa, A.C. Lepore, N.A. Silva, A.J. Salgado, Co-Transplantation of Adipose Tissue-Derived Stromal Cells and Olfactory Ensheathing Cells for Spinal Cord Injury Repair, Stem Cells. 36 (2018) 696–708. https://doi.org/10.1002/stem.2785.

[10] Z. Zhou, X. Tian, X. Tian, B. Mo, H. Xu, L. Zhang, L. Huang, S. Yao, Z. Huang, Y. Wang, H. Xie, L. Xu, L. Xu, H. Zhang, H. Zhang, Adipose mesenchymal stem cell transplantation alleviates spinal cord injury-induced neuroinflammation partly by suppressing the Jagged1/Notch pathway, Stem Cell Res. Ther. 11 (2020) 1–17. https://doi.org/10.1186/s13287-020-01724-5.

[11] M. Bydon, A.B. Dietz, S. Goncalves, F.M. Moinuddin, M.A. Alvi, A. Goyal, Y. Yolcu, C.L. Hunt, K.L. Garlanger, A.S. Del Fabro, R.K. Reeves, A. Terzic, A.J. Windebank, W. Qu, CELLTOP Clinical Trial: First Report From a Phase 1 Trial of Autologous Adipose Tissue–Derived Mesenchymal Stem Cells in the Treatment of Paralysis Due to Traumatic Spinal Cord Injury, Mayo Clin. Proc. 95 (2020) 406–414. https://doi.org/10.1016/j.mayocp.2019.10.008.

[12] J. Vaquero, M. Zurita, M.A. Rico, C. Bonilla, C. Aguayo, J. Montilla, S. Bustamante, J. Carballido, E. Marin, F. Martinez, A. Parajon, C. Fernandez, L. De Reina, An approach to personalized cell therapy in chronic complete paraplegia: The Puerta de Hierro phase I/II clinical trial, Cytotherapy. 18 (2016) 1025–1036. https://doi.org/10.1016/j.jcyt.2016.05.003.

[13] A. J. Braga Osorio Gomes Salgado, R. L. Goncalves Reis, N. Jorge Carvalho Sousa, J. M. Gimble, A. J. Salgado, R. L. Reis, N. Sousa, Adipose Tissue Derived Stem Cells Secretome: Soluble Factors and Their Roles in Regenerative Medicine, Curr. Stem Cell Res. Ther. 5 (2010) 103–110. https://doi.org/10.2174/157488810791268564.

[14] S. Lu, C. Lu, Q. Han, J. Li, Z. Du, L. Liao, R.C. Zhao, Adipose-derived mesenchymal stem cells protect PC12 cells from glutamate excitotoxicity-induced apoptosis by upregulation of XIAP through PI3-K/Akt activation, Toxicology. 279 (2011) 189–195. https://doi.org/10.1016/j.tox.2010.10.011.

[15] S.K. Kang, E.S. Jun, Y.C. Bae, J.S. Jung, Interactions between human adipose stromal cells and

mouse neural stem cells in vitro, Dev. Brain Res. 145 (2003) 141–149. https://doi.org/10.1016/S0165-3806(03)00224-4.
[16] E.D. Gomes, S.S. Mendes, H. Leite-Almeida, J.M. Gimble, R.Y. Tam, M.S. Shoichet, N. Sousa, N.A. Silva, A.J. Salgado, Combination of a peptide-modified gellan gum hydrogel with cell therapy in a lumbar spinal cord injury animal model, Biomaterials. 105 (2016) 38–51. https://doi.org/10.1016/j.biomaterials.2016.07.019.
[17] E.D. Gomes, B. Ghosh, R. Lima, M. Goulão, T. Moreira-Gomes, J. Martins-Macedo, M.W. Urban, M.C. Wright, J.M. Gimble, N. Sousa, N.A. Silva, A.C. Lepore, A.J. Salgado, Combination of a Gellan Gum-Based Hydrogel With Cell Therapy for the Treatment of Cervical Spinal Cord Injury, Front. Bioeng. Biotechnol. 8 (2020) 1–14. https://doi.org/10.3389/fbioe.2020.00984.
[18] F. Cofano, M. Boido, M. Monticelli, F. Zenga, A. Ducati, A. Vercelli, D. Garbossa, Mesenchymal stem cells for spinal cord injury: Current options limitations, and future of cell therapy, Int. J. Mol. Sci. 20 (2019) 2698. https://doi.org/10.3390/ijms20112698.
[19] M.I. Guillén, J. Platas, M.D. Pérez del Caz, V. Mirabet, M.J. Alcaraz, Paracrine anti-inflammatory effects of adipose tissue-derived mesenchymal stem cells in human monocytes, Front. Physiol. 9 (2018) 1–10. https://doi.org/10.3389/fphys.2018.00661.
[20] C.A. Ribeiro, J.S. Fraga, M. Grãos, N.M. Neves, R.L. Reis, J.M. Gimble, N. Sousa, A.J. Salgado, The secretome of stem cells isolated from the adipose tissue and Wharton jelly acts differently on central nervous system derived cell populations, Stem Cell Res. Ther. 3 (2012) 18. https://doi.org/10.1186/scrt109.
[21] S.C. Serra, J.C. Costa, R.C. Assunção-Silva, F.G. Teixeira, N.A. Silva, S.I. Anjo, B. Manadas, J.M. Gimble, L.A. Behie, A.J. Salgado, Influence of passage number on the impact of the secretome of adipose tissue stem cells on neural survival, neurodifferentiation and axonal growth, Biochimie. 155 (2018) 119–128. https://doi.org/10.1016/j.biochi.2018.09.012.
[22] R.C. Assunção-Silva, B. Mendes-Pinheiro, P. Patrício, L.A. Behie, F.G. Teixeira, L. Pinto, A.J. Salgado, Exploiting the impact of the secretome of MSCs isolated from different tissue sources on neuronal differentiation and axonal growth, Biochimie. 155 (2018) 83–91. https://doi.org/10.1016/j.biochi.2018.07.026.
[23] L.A. Rocha, E.D. Gomes, J.L. Afonso, S. Granja, F. Baltazar, N.A. Silva, M.S. Shoichet, R.A. Sousa, D.A. Learmonth, A.J. Salgado, In vitro Evaluation of ASCs and HUVECs Co-cultures in 3D Biodegradable Hydrogels on Neurite Outgrowth and Vascular Organization, Front. Cell Dev. Biol. 8 (2020) 1–14. https://doi.org/10.3389/fcell.2020.00489.
[24] A.G. Pinho, J.R. Cibrão, R. Lima, E.D. Gomes, S.C. Serra, J. Lentilhas-Graça, C. Ribeiro, S. Lanceros-Mendez, S.F.G. Teixeira, S. Monteiro, N.A. Silva, A.J. Salgado, Immunomodulatory and regenerative effects of the full and fractioned adipose tissue derived stem cells secretome in spinal cord injury, Exp. Neurol. 351 (2022) 113989. https://doi.org/10.1016/j.expneurol.2022.113989.
[25] C.A. Bowers, B. Kundu, G.W.J. Hawryluk, Methylprednisolone for acute spinal cord injury: An increasingly philosophical debate, Neural Regen. Res. 11 (2016) 882–885. https://doi.org/10.4103/1673-5374.184450.
[26] K.A. Follett, R.L. Boortz-Marx, J.M. Drake, S. DuPen, S.J. Schneider, M.S. Turner, R.J. Coffey, Prevention and management of intrathecal drug delivery and spinal cord stimulation system infections, Anesthesiology. 100 (2004) 1582–1594. https://doi.org/10.1097/00000542-200406000-00034.
[27] J.R.W. Kestle, H.J. Hoffman, D. Soloniuk, R.P. Humphreys, J.M. Drake, E.B. Hendrick, A concerted effort to prevent shunt infection, Child's Nerv. Syst. 9 (1993) 163–165. https://doi.org/10.1007/BF00272269.
[28] Z. Gong, D. Lei, C. Wang, C. Yu, K. Xia, J. Shu, L. Ying, J. Du, J. Wang, X. Huang, L. Ni, C. Wang,

J. Lin, F. Li, Z. You, C. Liang, Bioactive Elastic Scaffolds Loaded with Neural Stem Cells Promote Rapid Spinal Cord Regeneration, ACS Biomater. Sci. Eng. 6 (2020) 6331–6343. https://doi.org/10.1021/acsbiomaterials.0c01057.

[29] J. Pan, J. Deng, Y. Luo, L. Yu, W. Zhang, X. Han, Z. You, Y. Liu, Thermosensitive Hydrogel Delivery of Human Periodontal Stem Cells Overexpressing Platelet-Derived Growth Factor-BB Enhances Alveolar Bone Defect Repair, Stem Cells Dev. 28 (2019) 1620–1631. https://doi.org/10.1089/scd.2019.0184.

[30] L. Zeng, J. He, Y. Cao, J. Wang, Z. Qiao, X. Jiang, L. Hou, J. Zhang, Tissue-adhesive and highly mechanical double-network hydrogel for cryopreservation and sustained release of anti-cancer drugs, Smart Mater. Med. 2 (2021) 229–236. https://doi.org/10.1016/j.smaim.2021.07.005.

[31] R. Shultz, Y. Zhong, Hydrogel-based local drug delivery strategies for spinal cord repair, Neural Regen. Res. 16 (2021) 247–253. https://doi.org/10.4103/1673-5374.290882.

[32] J. Piantino, J.A. Burdick, D. Goldberg, R. Langer, L.I. Benowitz, An injectable, biodegradable hydrogel for trophic factor delivery enhances axonal rewiring and improves performance after spinal cord injury, Exp. Neurol. 201 (2006) 359–367. https://doi.org/10.1016/j.expneurol.2006.04.020.

[33] B. Ghosh, J. Nong, Z. Wang, M.W. Urban, N.M. Heinsinger, V.A. Trovillion, M.C. Wright, A.C. Lepore, Y. Zhong, A hydrogel engineered to deliver minocycline locally to the injured cervical spinal cord protects respiratory neural circuitry and preserves diaphragm function, Neurobiol. Dis. 127 (2019) 591–604. https://doi.org/10.1016/j.nbd.2019.04.014.

[34] H.L. Xu, F.R. Tian, J. Xiao, P.P. Chen, J. Xu, Z.L. Fan, J.J. Yang, C.T. Lu, Y.Z. Zhao, Sustained-release of FGF-2 from a hybrid hydrogel of heparin-poloxamer and decellular matrix promotes the neuroprotective effects of proteins after spinal injury, Int. J. Nanomedicine. 13 (2018) 681–694. https://doi.org/10.2147/IJN.S152246.

[35] D. Silva, R.A. Sousa, A.J. Salgado, Hydrogels as delivery systems for spinal cord injury regeneration, Mater. Today Bio. 9 (2021) 100093. https://doi.org/10.1016/j.mtbio.2021.100093.

[36] V. Estrada, N. Brazda, C. Schmitz, S. Heller, H. Blazyca, R. Martini, H.W. Müller, Long-lasting significant functional improvement in chronic severe spinal cord injury following scar resection and polyethylene glycol implantation, Neurobiol. Dis. 67 (2014) 165–179. https://doi.org/10.1016/j.nbd.2014.03.018.

[37] L.T.A. Hong, Y.M. Kim, H.H. Park, D.H. Hwang, Y. Cui, E.M. Lee, S. Yahn, J.K. Lee, S.C. Song, B.G. Kim, An injectable hydrogel enhances tissue repair after spinal cord injury by promoting extracellular matrix remodeling, Nat. Commun. 8 (2017) 1–14. https://doi.org/10.1038/s41467-017-00583-8.

[38] J.A. Burdick, K.S. Anseth, Photoencapsulation of osteoblasts in injectable RGD-modified PEG hydrogels for bone tissue engineering, Biomaterials. 23 (2002) 4315–4323. https://doi.org/10.1016/S0142-9612(02)00176-X.

[39] C.C. Lin, K.S. Anseth, PEG hydrogels for the controlled release of biomolecules in regenerative medicine, Pharm. Res. 26 (2009) 631–643. https://doi.org/10.1007/s11095-008-9801-2.

[40] K.J. Lampe, D.S. Kern, M.J. Mahoney, K.B. Bjugstad, The administration of BDNF and GDNF to the brain via PLGA microparticles patterned within a degradable PEG-based hydrogel: Protein distribution and the glial response, J. Biomed. Mater. Res. - Part A. 96 A (2011) 595–607. https://doi.org/10.1002/jbm.a.33011.

[41] U. Freudenberg, A. Hermann, P.B. Welzel, K. Stirl, S.C. Schwarz, M. Grimmer, A. Zieris, W. Panyanuwat, S. Zschoche, D. Meinhold, A. Storch, C. Werner, A star-PEG-heparin hydrogel platform to aid cell replacement therapies for neurodegenerative diseases, Biomaterials. 30 (2009) 5049–5060. https://doi.org/10.1016/j.biomaterials.2009.06.002.

[42] A. Zieris, K. Chwalek, S. Prokoph, K.R. Levental, P.B. Welzel, U. Freudenberg, C. Werner, Dual independent delivery of pro-angiogenic growth factors from starPEG-heparin hydrogels, J. Control. Release. 156 (2011) 28–36. https://doi.org/10.1016/j.jconrel.2011.06.042.

[43] U. Freudenberg, J.U. Sommer, K.R. Levental, P.B. Welzel, A. Zieris, K. Chwalek, K. Schneider, S. Prokoph, M. Prewitz, R. Dockhorn, C. Werner, Using mean field theory to guide biofunctional materials design, Adv. Funct. Mater. 22 (2012) 1391–1398. https://doi.org/10.1002/adfm.201101868.

[44] I. Capila, R.J. Linhardt, Heparin-protein interactions, Angew. Chemie - Int. Ed. 41 (2002) 390–412. https://doi.org/10.1021/j150493a017.

[45] A. Zieris, S. Prokoph, K.R. Levental, P.B. Welzel, M. Grimmer, U. Freudenberg, C. Werner, FGF-2 and VEGF functionalization of starPEG-heparin hydrogels to modulate biomolecular and physical cues of angiogenesis, Biomaterials. 31 (2010) 7985–7994. https://doi.org/10.1016/j.biomaterials.2010.07.021.

[46] L. Schirmer, P. Atallah, C. Werner, U. Freudenberg, StarPEG-Heparin Hydrogels to Protect and Sustainably Deliver IL-4, Adv. Healthc. Mater. 5 (2016) 3157–3164. https://doi.org/10.1002/adhm.201600797.

[47] M. V. Tsurkan, K. Chwalek, S. Prokoph, A. Zieris, K.R. Levental, U. Freudenberg, C. Werner, Defined polymer-peptide conjugates to form cell-instructive starpeg-heparin matrices in situ, Adv. Mater. 25 (2013) 2606–2610. https://doi.org/10.1002/adma.201300691.

[48] S.G. Dubois, E.Z. Floyd, S. Zvonic, G. Kilroy, X. Wu, S. Carling, Y.D.C. Halvorsen, E. Ravussin, J.M. Gimble, Isolation of human adipose-derived stem cells from biopsies and liposuction specimens, Methods Mol. Biol. 449 (2008) 69–79. https://doi.org/10.1007/978-1-60327-169-1_5.

[49] D.M. Basso, M.S. Beattie, J.C. Bresnahan, A Sensitive and Reliable Locomotor Rating Scale for Open Field Testing in Rats, J. Neurotrauma. 12 (1995) 1–21. https://doi.org/10.1089/neu.1995.12.1.

[50] S.R. Chaplan, F.W. Bach, J.W. Pogrel, J.M. Chung, T.L. Yaksh, Quantitative assessment of tactile allodynia in the rat paw, J. Neurosci. Methods. 53 (1994) 55–63. https://doi.org/10.1016/0165-0270(94)90144-9.

[51] M.R. Guimarães, A.R. Soares, A.M. Cunha, M. Esteves, S. Borges, R. Magalhães, P.S. Moreira, A.J. Rodrigues, N. Sousa, A. Almeida, H. Leite-Almeida, Evidence for lack of direct causality between pain and affective disturbances in a rat peripheral neuropathy model, Genes, Brain Behav. 18 (2019) 1–11. https://doi.org/10.1111/gbb.12542.

[52] E. Zudaire, L. Gambardella, C. Kurcz, S. Vermeren, A computational tool for quantitative analysis of vascular networks, PLoS One. 6 (2011) 1–12. https://doi.org/10.1371/journal.pone.0027385.

[53] LUND ADAM, L. MARK, Laerd Statistics, (n.d.). https://statistics.laerd.com/spss-tutorials/one-way-anova-repeated-measures-using-spss-statistics.php (accessed January 6, 2022).

[54] M. Chudickova, I. Vackova, L.M. Urdzikova, P. Jancova, K. Kekulova, M. Rehorova, K. Turnovcova, P. Jendelova, S. Kubinova, The effect of wharton jelly-derived mesenchymal stromal cells and their conditioned media in the treatment of a rat spinal cord injury, Int. J. Mol. Sci. 20 (2019) 4516. https://doi.org/10.3390/ijms20184516.

[55] X.Q. Su, X.Y. Wang, F.T. Gong, M. Feng, J.J. Bai, R.R. Zhang, X.Q. Dang, Oral treatment with glycyrrhizin inhibits NLRP3 inflammasome activation and promotes microglial M2 polarization after traumatic spinal cord injury, Brain Res. Bull. 158 (2020) 1–8. https://doi.org/10.1016/j.brainresbull.2020.02.009.

[56] L.F. Martins, R.O. Costa, J.R. Pedro, P. Aguiar, S.C. Serra, F.G. Teixeira, N. Sousa, A.J. Salgado, R.D. Almeida, Mesenchymal stem cells secretome-induced axonal outgrowth is mediated by BDNF, Sci. Rep. 7 (2017) 4153. https://doi.org/10.1038/s41598-017-03592-1.

[57] F.G. Teixeira, M.M. Carvalho, A. Neves-Carvalho, K.M. Panchalingam, L.A. Behie, L. Pinto, N. Sousa, A.J. Salgado, Secretome of Mesenchymal Progenitors from the Umbilical Cord Acts as Modulator of Neural/Glial Proliferation and Differentiation, Stem Cell Rev. Reports. 11 (2015) 288–297. https://doi.org/10.1007/s12015-014-9576-2.

[58] T. Cheriyan, D.J. Ryan, J.H. Weinreb, J. Cheriyan, J.C. Paul, V. Lafage, T. Kirsch, T.J. Errico, Spinal cord injury models: A review, Spinal Cord. 52 (2014) 588–595. https://doi.org/10.1038/sc.2014.91.

[59] S. Rossignol, Plasticity of connections underlying locomotor recovery after central and/or peripheral lesions in the adult mammals, Philos. Trans. R. Soc. B Biol. Sci. 361 (2006) 1647–1671. https://doi.org/10.1098/rstb.2006.1889.

[60] S. Rossignol, A. Frigon, Recovery of locomotion after spinal cord injury: Some facts and mechanisms, Annu. Rev. Neurosci. 34 (2011) 413–440. https://doi.org/10.1146/annurev-neuro-061010-113746.

[61] Y. Moreno-López, E.R. Hollis, Sensory Circuit Remodeling and Movement Recovery After Spinal Cord Injury, Front. Neurosci. 15 (2021) 1–5. https://doi.org/10.3389/fnins.2021.787690.

[62] A. Takeoka, S. Arber, Functional Local Proprioceptive Feedback Circuits Initiate and Maintain Locomotor Recovery after Spinal Cord Injury, Cell Rep. 27 (2019) 71-85.e3. https://doi.org/10.1016/j.celrep.2019.03.010.

[63] N. Lohmann, L. Schirmer, P. Atallah, E. Wandel, R.A. Ferrer, C. Werner, J.C. Simon, S. Franz, U. Freudenberg, Glycosaminoglycan-based hydrogels capture inflammatory chemokines and rescue defective wound healing in mice, Sci. Transl. Med. 9 (2017) 9044. https://doi.org/10.1126/scitranslmed.aai9044.

[64] L. Schirmer, P. Atallah, U. Freudenberg, C. Werner, Chemokine-Capturing Wound Contact Layer Rescues Dermal Healing, Adv. Sci. 8 (2021) 1–12. https://doi.org/10.1002/advs.202100293.

[65] L. Souza-Moreira, V.C. Soares, S. da S.G. Dias, P.T. Bozza, Adipose-derived Mesenchymal Stromal Cells Modulate Lipid Metabolism and Lipid Droplet Biogenesis via AKT/mTOR –PPARγ Signalling in Macrophages, Sci. Rep. 9 (2019) 1–11. https://doi.org/10.1038/s41598-019-56835-8.

[66] W. Liu, R. Li, J. Yin, S. Guo, Y. Chen, H. Fan, G. Li, Z. Li, X. Li, X. Zhang, X. He, C. Duan, Mesenchymal stem cells alleviate the early brain injury of subarachnoid hemorrhage partly by suppression of Notch1-dependent neuroinflammation: Involvement of Botch, J. Neuroinflammation. 16 (2019) 1–20. https://doi.org/10.1186/s12974-019-1396-5.

[67] X.Z. Hao, L.K. Yin, J.Q. Tian, C.C. Li, X.Y. Feng, Z.W. Yao, M. Jiang, Y.M. Yang, Inhibition of Notch1 signaling at the subacute stage of stroke promotes endogenous neurogenesis and motor recovery after stroke, Front. Cell. Neurosci. 12 (2018) 1–15. https://doi.org/10.3389/fncel.2018.00245.

[68] I. Shaked, D. Tchoresh, R. Gersner, G. Meiri, S. Mordechai, X. Xiao, R.P. Hart, M. Schwartz, Protective autoimmunity: Interferon-γ enables microglia to remove glutamate without evoking inflammatory mediators, J. Neurochem. 92 (2005) 997–1009. https://doi.org/10.1111/j.1471-4159.2004.02954.x.

[69] O. Butovsky, Y. Ziv, A. Schwartz, G. Landa, A.E. Talpalar, S. Pluchino, G. Martino, M. Schwartz, Microglia activated by IL-4 or IFN-γ differentially induce neurogenesis and oligodendrogenesis from adult stem/progenitor cells, Mol. Cell. Neurosci. 31 (2006) 149–160. https://doi.org/10.1016/j.mcn.2005.10.006.

[70] R. Lima, S. Monteiro, J.P. Lopes, P. Barradas, N.L. Vasconcelos, E.D. Gomes, R.C. Assunção-Silva, F.G. Teixeira, M. Morais, N. Sousa, A.J. Salgado, N.A. Silva, Systemic interleukin-4 administration after spinal cord injury modulates inflammation and promotes neuroprotection, Pharmaceuticals. 10 (2017) 1–16. https://doi.org/10.3390/ph10040083.

[71] H. Ishii, S. Tanabe, M. Ueno, T. Kubo, H. Kayama, S. Serada, M. Fujimoto, K. Takeda, T. Naka, T. Yamashita, Ifn-γ-dependent secretion of IL-10 from Th1 cells and microglia/macrophages

contributes to functional recovery after spinal cord injury, Cell Death Dis. 4 (2013) 1–9. https://doi.org/10.1038/cddis.2013.234.

[72] Z. Zhou, X. Peng, R. Insolera, D.J. Fink, M. Mata, IL-10 promotes neuronal survival following spinal cord injury, Exp Neurol. 220 (2009) 183–190. https://doi.org/10.1016/j.expneurol.2009.08.018.IL-10.

[73] D.J. Hellenbrand, K.A. Reichl, B.J. Travis, M.E. Filipp, A.S. Khalil, D.J. Pulito, A. V. Gavigan, E.R. Maginot, M.T. Arnold, A.G. Adler, W.L. Murphy, A.S. Hanna, Sustained interleukin-10 delivery reduces inflammation and improves motor function after spinal cord injury, J. Neuroinflammation. 16 (2019) 1–19. https://doi.org/10.1186/s12974-019-1479-3.

[74] M.J. Kwon, H.Y. Shin, Y. Cui, H. Kim, A.H. Le Thi, J.Y. Choi, E.Y. Kim, D.H. Hwang, B.G. Kim, CCL2 mediates neuron-macrophage interactions to drive proregenerative macrophage activation following preconditioning injury, J. Neurosci. 35 (2015) 15934–15947. https://doi.org/10.1523/JNEUROSCI.1924-15.2015.

[75] N.A. Silva, A.J. Salgado, R.A. Sousa, J.T. Oliveira, A.J. Pedro, H. Leite-Almeida, R. Cerqueira, A. Almeida, F. Mastronardi, J.F. Mano, N.M. Neves, N. Sousa, R.L. Reis, Development and characterization of a novel hybrid tissue engineering-based scaffold for spinal cord injury repair, Tissue Eng. - Part A. 16 (2010) 45–54. https://doi.org/10.1089/ten.tea.2008.0559.

[76] K.H. Sitoci-Ficici, M. Matyash, O. Uckermann, R. Galli, E. Leipnitz, R. Later, C. Ikonomidou, M. Gelinsky, G. Schackert, M. Kirsch, Non-functionalized soft alginate hydrogel promotes locomotor recovery after spinal cord injury in a rat hemimyelonectomy model, Acta Neurochir. (Wien). 160 (2018) 449–457. https://doi.org/10.1007/s00701-017-3389-4.

Supplementary Information

Supplementary Table III. S1 Pairwise comparisons between groups using Tukey's correction for motor improvements evaluation using BBB test for 8 weeks post-injury.

BBB			
3 Days pi			
Comparison between groups	Mean Difference	SEM	*p*-Value
starPEG-Hep+sec vs starPEG-Hep+NbA	0	0	1
starPEG-Hep+secr vs Secretome	0	0	1
starPEG-Hep+sec vs NbA	0	0	1
starPEG-Hep+sec vs SHAM	-21	0	< 0.0001
starPEG-Hep+NbA vs secretome	0	0	1
starPEG-Hep+NbA vs NbA	0	0	1
starPEG-Hep+NbA vs SHAM	-21	0	< 0.0001
Secretome vs NbA	0	0	1
Secretome vs SHAM	-21	0	< 0.0001
NbA vs SHAM	-21	0	< 0.0001
1 WPI			
starPEG-Hep+sec vs starPEG-Hep+NbA	0.36	0.29	0.24
starPEG-Hep+sec vs Secretome	0.21	0.25	0.4
starPEG-Hep+sec vs NbA	0.36	0.26	0.18
starPEG-Hep+sec vs SHAM	-20.64	0.25	< 0.0001
starPEG-Hep+NbA vs secretome	-0.14	0.29	0.63
starPEG-Hep+NbA vs NbA	3.55E-15	0.30	1
starPEG-Hep+NbA vs SHAM	-21	0.29	0.63
Secretome vs NbA	0.14	0.26	0.58
Secretome vs SHAM	-20.86	0.25	< 0.0001
NbA vs SHAM	-21	0.26	< 0.0001
2 WPI			
starPEG-Hep+sec vs starPEG-Hep+NbA	1.13	0.67	0.10
starPEG-Hep+sec vs Secretome	1.29	0.57	0.03
starPEG-Hep+sec vs NbA	0.67	0.59	0.27
starPEG-Hep+sec vs SHAM	-19	0.57	< 0.0001
starPEG-Hep+NbA vs secretome	0.16	0.67	0.10
starPEG-Hep+NbA vs NbA	-0.46	0.69	0.51
starPEG-Hep+NbA vs SHAM	-20.13	0.69	< 0.0001
Secretome vs NbA	-0.62	0.59	0.30
Secretome vs SHAM	-20.29	0.57	< 0.0001
NbA vs SHAM	-19.67	0.59	< 0.0001
4 WPI			
starPEG-Hep+sec vs starPEG-Hep+NbA	0.88	0.90	0.34
starPEG-Hep+sec vs Secretome	1.36	0.79	0.09
starPEG-Hep+sec vs NbA	1.17	0.82	0.16
starPEG-Hep+sec vs SHAM	-18.5	0.79	< 0.0001

starPEG-Hep+NbA vs secretome	0.48	0.90	0.60
starPEG-Hep+NbA vs NbA	0.29	0.93	0.76
starPEG-Hep+NbA vs SHAM	-19.38	0.90	< 0.0001
Secretome vs NbA	-0.19	0.80	0.81
Secretome vs SHAM	-19.86	0.79	< 0.0001
NbA vs SHAM	-19.67	0.80	< 0.0001
6 WPI			
starPEG-Hep+sec vs starPEG-Hep+NbA	1.38	0.82	0.10
starPEG-Hep+sec vs Secretome	2.21	0.70	0.004
starPEG-Hep+sec vs NbA	1	0.73	0.18
starPEG-Hep+sec vs SHAM	-17.5	0.70	< 0.0001
starPEG-Hep+NbA vs secretome	0.84	0.82	0.31
starPEG-Hep+NbA vs NbA	-0.38	0.84	0.66
starPEG-Hep+NbA vs SHAM	-18.88	0.82	< 0.0001
Secretome vs NbA	-1.21	0.73	0.10
Secretome vs SHAM	-19.71	0.70	< 0.0001
NbA vs SHAM	-18.5	0.73	< 0.0001
8 WPI			
starPEG-Hep+sec vs starPEG-Hep+NbA	2.07	0.77	0.012
starPEG-Hep+sec vs Secretome	2.21	0.65	0.002
starPEG-Hep+sec vs NbA	1.82	0.68	0.013
starPEG-Hep+sec vs SHAM	-16.93	0.66	< 0.0001
starPEG-Hep+NbA vs secretome	0.14	0.77	0.85
starPEG-Hep+NbA vs NbA	-0.25	0.79	0.75
starPEG-Hep+NbA vs SHAM	-19	0.77	< 0.0001
Secretome vs NbA	-0.39	0.68	0.57
Secretome vs SHAM	-19.14	0.65	< 0.0001
NbA vs SHAM	-18.75	0.68	< 0.0001

Supplementary Table III. S2 Pairwise comparisons between groups using Tukey's correction for motor improvements evaluation using MST test at eight weeks post-injury.

MST			
Comparison between groups	Mean Difference	SEM	*p*-Value
starPEG-Hep+sec vs starPEG-Hep+Nba	4.35	2.36	0.38
starPEG-Hep+sec vs Secretome	0.81	2.21	1
starPEG-Hep+sec vs NbA	1.44	2.11	0.96
starPEG-Hep+sec vs SHAM	-16.03	2.03	<0.0001
starPEG-Hep+NbA vs secretome	-3.54	2.45	0.61
starPEG-Hep+NbA vs NbA	-2.91	2.36	0.73
starPEG-Hep+NbA vs SHAM	-20.38	2.29	<0.0001
Secretome vs NbA	0.63	2.21	1
Secretome vs SHAM	-16.84	2.14	<0.0001
NbA vs SHAM	-17.47	2.03	<0.0001

Supplementary Table III. S3 Pairwise comparisons between groups using Tukey's correction for motor sensorial function using Von Frey test at tow and six weeks post-injury, in left and right hindlimbs.

Von Frey			
2 WPI (left)			
Comparison between groups	Mean Difference	SEM	*p*-Value
starPEG-Hep+sec vs starPEG-Hep+NbA	-1.02	2.07	0.63
starPEG-Hep+sec vs Secretome	-0.341	1.76	0.85
starPEG-Hep+sec vs NbA	0.45	1.83	0.81
starPEG-Hep+sec vs SHAM	-6.91	1.76	0.001
starPEG-Hep+NbA vs secretome	0.68	2.07	0.75
starPEG-Hep+NbA vs NbA	1.47	2.13	0.50
starPEG-Hep+NbA vs SHAM	-5.89	2.07	0.008
Secretome vs NbA	0.80	1.83	0.67
Secretome vs SHAM	-6.57	1.76	0.001
NbA vs SHAM	-7.37	1.83	<0.0001
6 WPI (left)			
starPEG-Hep+sec vs starPEG-Hep+NbA	2.41	1.83	0.20
starPEG-Hep+sec vs Secretome	1.49	1.56	0.35
starPEG-Hep+sec vs NbA	1.79	1.63	0.28
starPEG-Hep+sec vs SHAM	-6.45	1.56	<0.0001
starPEG-Hep+NbA vs secretome	-0.92	1.83	0.62
starPEG-Hep+NbA vs NbA	-0.63	1.89	0.74
starPEG-Hep+NbA vs SHAM	-8.86	1.83	0.86
Secretome vs NbA	0.30	1.63	0.86
Secretome vs SHAM	-7.93	1.56	<0.0001
NbA vs SHAM	-8.23	1.63	<0.0001
2 WPI (Right)			
starPEG-Hep+sec vs starPEG-Hep+NbA	1.51	1.89	0.43
starPEG-Hep+sec vs Secretome	1.01	1.61	0.54
starPEG-Hep+sec vs NbA	0.79	1.68	0.64
starPEG-Hep+sec vs SHAM	-4.87	1.61	0.006
starPEG-Hep+NbA vs Secretome	-0.51	1.89	0.79
starPEG-Hep+NbA vs NbA	-0.73	1.95	0.71
starPEG-Hep+NbA vs SHAM	-6.38	1.89	0.002
Secretome vs NbA	-0.22	1.68	0.90
Secretome vs SHAM	-5.87	1.61	0.001
NbA vs SHAM	-5.65	1.68	0.002
6 WPI (Right)			
starPEG-Hep+sec vs starPEG-Hep+NbA	-0.12	2.47	0.96
starPEG-Hep+sec vs Secretome	0.14	2.11	0.95
starPEG-Hep+sec vs NbA	1.45	2.20	0.51

starPEG-Hep+sec vs SHAM	-8.49	2.11	<0.0001
starPEG-Hep+NbA vs Secretome	0.26	2.47	0.92
starPEG-Hep+NbA vs NbA	1.57	2.55	0.54
starPEG-Hep+NbA vs SHAM	-8.38	2.47	0.002
Secretome vs NbA	1.31	2.20	0.56
Secretome vs SHAM	-8.64	2.11	<0.0001
NbA vs SHAM	-9.95	2.20	<0.0001

Supplementary Table III. S4 Multiple comparisons between groups using Tukey's correction for the percentage of Iba1 ameboid area in spinal cord longitudinal sections.

Iba1 ameboid area			
Comparison between groups	Mean Difference	SEM	*p*-Value
starPEG-Hep+sec vs starPEG-Hep+NbA	-5.55	3.39	0.49
starPEG-Hep+sec vs Secretome	-9.71	2.89	0.019
starPEG-Hep+sec vs NbA	-10.40	3.01	0.015
starPEG-Hep+sec vs SHAM	38.49	2.89	<0.0001
starPEG-Hep+NbA vs Secretome	-4.16	3.39	0.74
starPEG-Hep+NbA vs NbA	-4.86	3.49	0.64
starPEG-Hep+NbA vs SHAM	44.04	3.39	<0.0001
Secretome vs NbA	-0.70	3.01	0.99
Secretome vs SHAM	48.20	2.89	<0.0001
NbA vs SHAM	48.89	3.01	<0.0001

Supplementary Table III. S5 Pairwise comparisons between groups using Tukey's correction for positive area of GFAP and NF.

GFAP			
Rostral			
Comparison between groups	Mean Difference	SEM	*p*-Value
starPEG-Hep+secr vs starPEG-Hep+NbA	-1.19	2.49	0.99
starPEG-Hep+sec vs Secretome	-0.35	2.12	1
starPEG-Hep+sec vs NbA	-1.36	2.21	0.97
starPEG-Hep+sec vs SHAM	4.37	2.12	0.27
starPEG-Hep+NbA vs secretome	0.83	2.49	0.99
starPEG-Hep+NbA vs NbA	-0.18	2.56	1
starPEG-Hep+NbA vs SHAM	5.55	2.49	0.2
Secretome vs NbA	-1.00	2.21	0.99
Secretome vs SHAM	4.72	2.12	0.20
NbA vs SHAM	5.73	2.21	0.10
Epicenter			
starPEG-Hep+sec vs starPEG-Hep+NbA	0.03	1.79	1
starPEG-Hep+secvs Secretome	-1.60	1.53	0.83
starPEG-Hep+sec vs NbA	-1.2	1.59	0.94

starPEG-Hep+sec vs SHAM	-3.75	1.53	0.13
starPEG-Hep+NbA vs secretome	-1.62	1.79	0.25
starPEG-Hep+NbA vs NbA	-1.23	1.85	0.96
starPEG-Hep+NbA vs SHAM	-3.77	1.79	0.25
Secretome vs NbA	0.39	1.59	0,99
Secretome vs SHAM	-2.15	1.53	0.63
NbA vs SHAM	-2.54	1.59	0.51
Caudal			
starPEG-Hep+secr vs starPEG-Hep+Nba	0.83	2.27	0.99
starPEG-Hep+sec vs Secretome	-2.20	1.94	0.79
starPEG-Hep+sec vs NbA	-0.41	2.02	1
starPEG-Hep+sec vs SHAM	2.96	1.94	0.56
starPEG-Hep+NbA vs secretome	-3.02	2.27	0.99
starPEG-Hep+NbA vs NbA	-1.24	2.34	0.98
starPEG-Hep+NbA vs SHAM	2.14	2.27	0.88
Secretome vs NbA	1.79	2.02	0.89
Secretome vs SHAM	5.16	1.94	0.08
NbA vs SHAM	3.37	2.02	0.46
NF			
Rostral			
starPEG-Hep+sec vs starPEG-Hep+Nba	-2.14	1.55	0.64
starPEG-Hep+sec vs Secretome	-0.88	1.32	0.96
starPEG-Hep+sec vs NbA	-2.49	1.38	0.39
starPEG-Hep+sec vs SHAM	-0.80	1.32	0.97
starPEG-Hep+NbA vs secretome	1.26	1.55	0.92
starPEG-Hep+NbA vs NbA	-0.34	1.60	0.99
starPEG-Hep+NbA vs SHAM	1.35	1.55	0.91
Secretome vs NbA	-1.61	1.38	0.77
Secretome vs SHAM	0.085	1.32	1
NbA vs SHAM	1.69	1.38	0.74
Epicenter			
starPEG-Hep+sec vs starPEG-Hep+NbA	1.50	1.48	0.85
starPEG-Hep+sec vs Secretome	0.68	1.26	0.98
starPEG-Hep+sec vs NbA	0.64	1.31	0.99
starPEG-Hep+sec vs SHAM	0.46	1.26	0.99
starPEG-Hep+NbA vs secretome	-0.82	1.48	0.98
starPEG-Hep+NbA vs NbA	-0.86	1.53	0.97
starPEG-Hep+NbA vs SHAM	-1.04	1.48	0.95
Secretome vs NbA	-0.04	1.31	1
Secretome vs SHAM	-0.22	1.26	1
NbA vs SHAM	-0.18	1.26	1
Caudal			
starPEG-Hep+sec vs starPEG-Hep+NbA	-1.63	1.30	0.72
starPEG-Hep+sec vs Secretome	-1.22	1.11	0.80
starPEG-Hep+sec vs NbA	-1.81	1.15	0.53
starPEG-Hep+sec vs SHAM	-0.04	1.11	1

starPEG-Hep+NbA vs secretome	0.40	1.30	0.99
starPEG-Hep+NbA vs NbA	-0.18	1.34	1
starPEG-Hep+NbA vs SHAM	1.59	1.30	0.74
Secretome vs NbA	-0.58	1.15	0.99
Secretome vs SHAM	1.18	1.11	0.82
NbA vs SHAM	1.77	1.15	0.55

Supplementary Table III. S6 Pairwise comparisons between groups using Tukey's correction for SMI-71 quantification. Parameters such as Vessel Area, Vessel Length and Average Vessel Length in Angio Tool software.

SMI			
Vessel Area			
Comparison between groups	Mean Difference	SEM	*p*-Value
starPEG-Hep+sec vs StarPEG-Hep+NbA	0.02	0.02	0.83
starPEG-Hep+sec vs Secretome	0.00	0.02	1
starPEG-Hep+sec vs NbA	0.01	0.02	0.96
starPEG-Hep+sec vs SHAM	-0.02	0.02	0.83
starPEG-Hep+NbA vs Secretome	-0.02	0.02	0.85
starPEG-Hep+NbA vs NbA	-0.01	0.02	0.99
starPEG-Hep+NbA vs SHAM	-0.04	0.02	0.31
Secretome vs NbA	0.01	0.02	0,97
Secretome vs SHAM	-0.02	0.02	0.79
NbA vs SHAM	-0.03	0.02	0.46
Vessel Length			
starPEG-Hep+sec vs starPEG-Hep+NbA	1.03	1.01	0.84
starPEG-Hep+sec vs Secretome	0.47	0.86	0.98
starPEG-Hep+sec vs NbA	0.32	0.89	1
starPEG-Hep+sec vs SHAM	-0.81	0.86	0.88
starPEG-Hep+NbA vs Secretome	-0.56	1.01	0.98
starPEG-Hep+NbA vs NbA	-0.71	1.04	0.96
starPEG-Hep+NbA vs SHAM	-1.84	1.01	0.38
Secretome vs NbA	-0.15	0.89	1
Secretome vs SHAM	-1.28	0.86	0.58
NbA vs SHAM	-1.13	0.89	0.71
Average vessel length			
starPEG-Hep+sec vs starPEG-Hep+NbA	-0.01	0.01	0.74
starPEG-Hep+sec vs Secretome	0.00	0.01	0.99
starPEG-Hep+sec vs NbA	-0.00	0.01	0.94
starPEG-Hep+sec vs SHAM	0.01	0.01	0.88
starPEG-Hep+NbA vs Secretome	0.01	0.01	0.53
starPEG-Hep+NbA vs NbA	0.00	0.01	0.98
starPEG-Hep+NbA vs SHAM	0.01	0.01	0.29

Secretome vs NbA	-0.00	0.01	0.78
Secretome vs SHAM	0.00	0.01	0.98
NbA vs SHAM	0.01	0.01	0.48

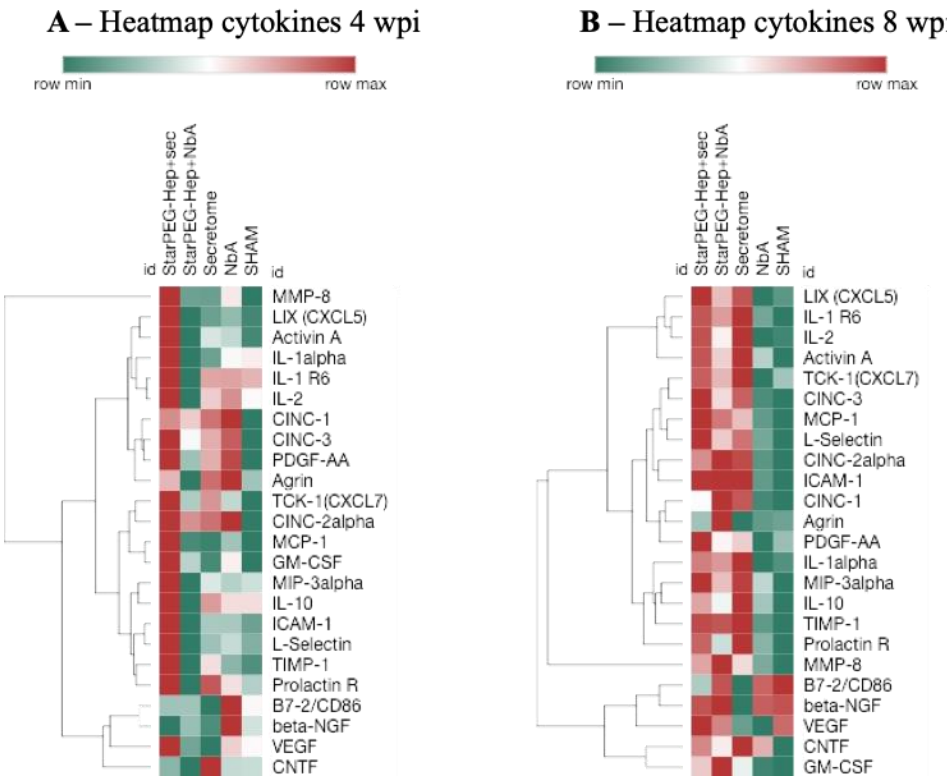

Supplementary Figure III. S1 Molecular analysis of collected sera following SCI using Rat Cytokine Array C2 from RayBiotech. Representative heat map of the panel for the different groups was generated using the BROAD Institute's R implementation of Morpheus with Euclidean distance hierarchical clustering at four wpi (A) and eight wpi (B).

CHAPTER IV

Conclusions and Future Perspectives

General Discussion

Central Nervous System reveals as a fascinating structure that encompasses all functions in the body. Injuries in each region totally disturb the overall normal function. Particularly, spinal cord injury (SCI) is responsible for total or partial loss of both motor and sensorial functions below the level of injury. Both have a huge impact on patient's life quality at physical and psychological burdens. For scientists, SCI remains a challenge either by its pathophysiological complexity or unknown processes that are responsible for degeneration or regeneration. A cascade of events goes from acute to chronic phase within seconds to months. After a mechanical insult, a myriad of events comprehends I) vascular disruption; II) inflammation; III) release of inflammatory cytokines; IV) excitotoxicity; V) apoptosis and VI) axonal degeneration [1]. Ultimately, the establishment of the chronic phase is characterized by the glial scar formation, which is composed of lesion core and border. In the lesion core, stromal-derived fibroblasts and inflammatory immune cells fill all space, while the lesion border is formed by reactive astrocytes. The scar acts as a barrier for axonal growth or tissue regeneration and at the same time circumvents the injury locally, preventing its spread [2,3].

In the last years, we have witnessed a growth of multivariate fields in developing therapies to tackle SCI regeneration. Drugs such as methylprednisolone (MPSS) were vastly used in an attempt to reduce inflammation and promote recovery [4,5]. Although upon the report of severe side effects, such as liver toxicity or hemorrhages, it was highly unadvised it use [6,7]. Other approaches in clinical trials try to promote regeneration by administering growth factors [8,9] or even anti-bodies [10], promising approaches to improve neurological outcomes. However, side effects or administration routes are still a concern in their translation to the clinic. Other interesting approaches rely on the use of cell-based therapy. The purpose is the repopulation of spinal cord tissue with new cells, that will migrate to injured tissue and replace dead neuronal cells. In clinical trials, they were able to promote improvements in sensory function [11] or bladder control [12] after transplantation. Our group has shown that adipose tissue-derived stem cells (ASCs) were able to promote recovery after transplantation at injury site [13–15]. However, their effects are mainly attributed to intense paracrine effects, their secretome. Secreted molecules have been shown to play an important role in regenerative processes, such as axonal growth, suporte cell survival, and differentiation [16–18] and ultimately lead to motor recovery after systemic administration [19].

Considering all mentioned facts, in this work, we envisioned designing a more effective way to deliver hASCs secretome at SCI injury site. The advantages include a more target and specific therapy, reduce the dosage needed, protecting molecules from enzymatic degradation, and minimizing the risk of off-

target effects. For that, hydrogels have been revealed as a suitable platform to use. They are similar to the extracelular matrix (ECM), have high water content and *per se* improve motor function in SCI animal models as in the case of use poly(ethilene glycol) (PEG) hydrogels [20]. Freudenberg et al developed a biohybrid hydrogel made of star-shaped PEG hydrogel starPEG) and the glycosaminoglycan (GAG) Heparin (Hep) [21]. The rationale is based on affinity-based systems where, anionic charge arising from the high density of sulfate moieties on heparin results in a high affinity for a broad range of growth factors, cytokines, and chemokines mainly due to electrostatic interactions [22]. Remarkably, controlling their release in a time-dependent manner. Importantly is the fact that these matrices can be injected in a liquid state and by Michael type reaction form *in situ* polymerization hydrogels [23].

In chapter II, we performed the mechanical characterization of starPEG-Hep hydrogels showing modulation of stiffness, mesh size, and swelling degree. Those are important features not only for *in vivo* implantation but also for their use as delivery systems. Upon hASCS secretome loading in starPEG-Hep hydrogels, a controlled and prolonged release was achieved for over 10 days. At that time point approximately 70% of cumulative release, was demonstrated in fluorescence experiments. A similar profile to other release systems of growth factors and cytokines [24,25]. Moreover, Gal-1 was found to be released in a continuous and extended way in the multiplex assay. The sensitivity of the multiplex assay was revealed to be very low, most probably by the low concentration of analytes in released samples, which did not allow the identification of more molecules. To pursue this, membrane-based protein arrays were used and released samples were collected at only two and ten days. The results revealed a release profile in which cytokines or factors involved in angiogenesis processes were mainly released after two days. The burst release in the first days, shown in fluorescence assays, was mainly due to the high release of these molecules. On the other side, extended release is supported by neuroregulatory growth factors that had a higher cumulative release from two to ten days. In studies in which these molecules are independently loaded in these hydrogels, continuous release profile was reported [26–28]. Despite the known role of heparin in affinity-based systems, is interesting to highlight this release profile. The results suggest that molecules have a different interaction with heparin as well as dissociation rate which impacts their release [29]. Another alternative is that the high amount of diverse proteins was impacting individual interactions with heparin. It would be interesting to perform electrophoretic techniques such as surface plasmon resonance [30], or *in silico* calculations [31] to decode affinity and kinetics of heparin-protein interactions.

Additionally, starPEG-Hep loading secretome could promote significant higher neuronal differentiation of immature (DCX) and mature (MAP2) neurons, when compared with hydrogel loading vehicle. Also, higher

neurite outgrowth was observed in organotypic spinal cord slices. In addition, we hypothesized that these processes were mediated by molecules identified in membrane-based protein arrays, such as BDNF, GDNF, ß-NGF, previously shown to modulate those processes [32,33]. Subsequently, these results corroborate the fact that starPEG-Hep hydrogels are continuously releasing secretome, once the percentage of differentiated cells was similar to the levels of free secretome, which was in higher contact with cells during the experiment. In the case of neurite outgrowth, starPEG-Hep+sec promoted a significantly higher percentage of neurofilament area, in contrast to free secretome that was removed after 48h.

The last question of this work (Chapter III) was to evaluate the capacity of the developed release system in promoting motor recovery in T8 transection SCI rat model. This results in a very severe lesion, when compared with hemisection or contusion models [34]. This happens due to complete interruption of neuronal transmission when cutting the spinal cord, resulting in total paralysis of the hindlimbs. Besides this, the total transection model does not reproduce the most frequent lesions in human [35]. However, in tissue engineering field, particularly with biomaterials, the advantage of this model is related with the depot created upon lesion that is easily filled by the hydrogel (combined or not with a loading agent) [34,36].

Motor recovery indicated that starPEG-Hep+sec led to a more robust motor recovery, traducing in significance BBB score at two, and six and eight weeks in comparison treated groups. Interestingly, lower motor recovery was observed in animals treated with local secretome, evidencing that local treatment has a low potential to promote regeneration, probably due to fast clearance from injury site. These results are in accordance with neurite outgrowth in spinal cord slices cultures (Chapter II) where the free secretome condition had a lower neurite extension. Gross motor function or sensorial function were evaluated, but no significant recovery was observed. Histological analysis revealed a significant reduction of ameboid microglia, associated with a more active state, in animals treated with starPEG-Hep+sec in comparison to free secretome or vehicle. Importantly, animals treated with only starPEG-Hep+NbA, did not show further inflammation at injury site, which has disclosed the safety of the hydrogel. Other markers for astrocytes (GFAP), axonal regeneration (NF), or blood brain barrier integrity (SMI-71) did not present significant results. Regarding the SMI-71 results, it would be interesting to evaluate the vascular integrity in early time points, once BSCB integrity is gradually restored until 14 days post-injury [37]. Coupling with an assessment of BBB permeability with occludin, would clarify the revascularization process after lesion [38]. Restoration of vasculature in SCI is crucial to restore nutrient diffusion and cellular maintenance [39]. Altogether, these results reinforce the fact that hASCs secretome was mainly impacting as

immunomodulatory agent locally. Systemic characterization of inflammatory levels was also performed during three distinct phases of the condition (acute, intermediate and chronic). From acute to chronic stage, starPEG-Hep+sec treated group promoted increased levels of IL-10, an anti-inflammatory cytokine. At the same time, CD86 and MCP-1, have different expressions. CD86, a M1 marker, is highly expressed at 48h and decrease in intermediate and chronic phase, compared with animals treated with vehicle. In case of MCP-1, a decreased expression in acute phase is counteracted with increased expression in chronic phase. All inflammatory processes could be mediated by pro- and anti-inflammatory cytokines highly released in membrane-based protein arrays (Chapter II). This includes IL-4 and IFN-γ demonstrated to be able of inducing IL-10 increase systemically [40,41] or VEGF that promote motor recovery by reducing autophagy [42]. This could also point out that inflammatory stimulus could in some extent contribute to regenerative favoring [43,44]. Remarkably, even though the treatment was applied locally, it also has the capacity to modulate the systemic inflammatory response.

Despite some improvements that could be done in order to refine the use of starPEG-Hep+sec as delivery systems, in this work we demonstrated for the first time that a biohybrid hydrogel was able to sustainably release hASCs secretome. Several factors released were found to play a critical role in modulating essential processes to foster regenerative processes, demonstrated by increase neuronal differentiation and neurite outgrowth in *in vitro* assays. SCI lesioned animals were capable of a significant motor improvement when treated with starPEG-Hep+sec compared to other treated groups. We have shown that modulating the inflammatory response after lesion is primarily responsible for this recovery. Altogether, this data highly supports the use of starPEG-Hep+sec to trigger and modulate pro-regenerative processes, which may offer an effective clinical approach to tackle SCI.

Thesis Graphical Abstract

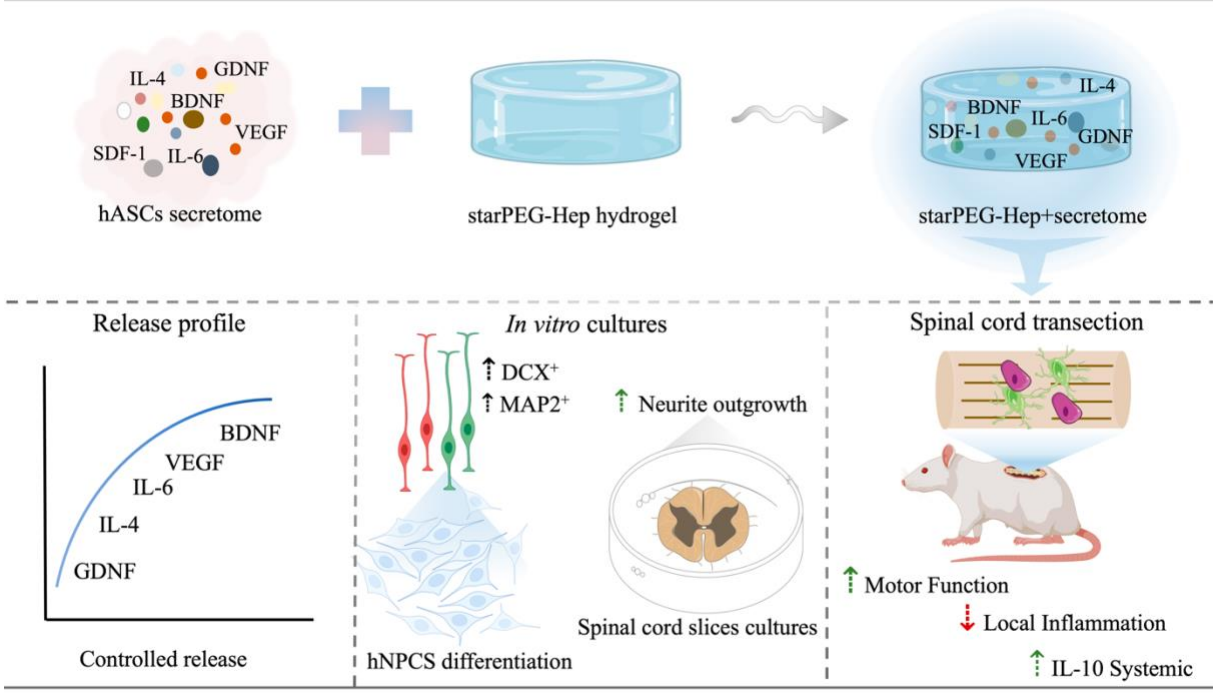

Previous studies have highlighted the robust beneficial effects of ASCs secretome in modulating crucial processes in SCI regenerative medicine. Herein, using a hydrogel as a release system, we showed the controlled and prolonged release of ASCs secretome that is positively associated with regenerative events *in vitro* and *in vivo* models.

Future Perspectives and Concluding Remarks

Independently of the interesting results achieved in this work, there are important questions that should be considered and addressed to improve the therapeutic approach herein presented. Herein we have shown that starPEG-Hep loading secretome hydrogels where capable of promoting motor recovery mainly by reducing the pro-inflammatory response local and systemically. It would be interesting to explore this role in *in vitro* cultures, either by evaluating the microglia response in primary cultures with neurons, astrocytes and microglia interactions [45]. The next step would be the translation for a contusion SCI animal model, if possible, in cervical regions (most frequent human injuries). To emphasize, the hydrogel used is suitable for injection and *in situ* polymerization, which confers an advantage for its use. However, for contusion injuries, it would be interesting if, upon injection, it could form a thin layer, like a sealant, in a manner to cover all lesioned area and release secretome at the same time. Looking at mechanical characteristics it would not promote further compression due to low swelling degree. At the same time, considering slightly increasing the secretome volume could also benefit the regenerative process. Lately, the translation for other animal models such as dogs, pigs, or primates should be considered for clinical translation. It is important to highlight that starPEG-Hep have been extensively used in the context of wound healing in animal models with proven safety, but more than that, PEG is an FDA approved material and already used in food, cosmetics, pharmaceuticals, and medical devices, which is an advantage for the bench to bedside translation [46–48].

Despite of what is already known about hASCs secretome and their advantages when compared with cell transplantation, it is important to pursue the knowledge of their components and their role in regenerative processes. Moreover, genetic MSCs modification is a possible strategy to enhance beneficial effects of growth factors, cytokines chemokines or even vesicles present in secretome [49]. In this way, processes such as axonal regeneration, vascularization or even cell survival could be privileged. Also, the scalable production of secretome to clinical translation using bioreactors in GMP conditions is an ongoing work that will favor this therapy.

Overall, herein we present for the first time a hydrogel capable of efficiently loading and release hASCs secretome for an extended period of time. In the field, this is a very important step in the development of drug delivery systems locally. Thus, many important issues raised during clinical trials could be surpassed.

During decades SCI field has witnessed major breakthroughs and only recently we could testify for the first time clinical gains, with help of electrostimulation [50]. This is a turning point in the field and a hope for people in the same condition. However, lost functions were not recovered permanently. The near

future will challenge us in developing interconnected knowledge in diverse subjects not only biology, chemistry, pharmacology but also physicians, doctors, engineers, informatics in a way to develop a robust therapy in which all single potentials are linked. Pharmacology, cell free-based therapies, and biomaterials could target the regeneration of biological processes in the acute phase, while electrostimulation or even artificial intelligence (IA) could bypass the spinal cord injury and stimulate neural circuitries to induce movement in more intermediate and chronic phases. All of those processes should be strongly connected with rehabilitative processes in a way to recover the deleterious effects experienced after SCI lesions.

References

[1] N.A. Silva, N. Sousa, R.L. Reis, A.J. Salgado, From basics to clinical: A comprehensive review on spinal cord injury, Prog. Neurobiol. 114 (2014) 25–57. https://doi.org/10.1016/j.pneurobio.2013.11.002.

[2] J. Silver, J.H. Miller, Regeneration beyond the glial scar, Nat. Rev. Neurosci. 5 (2004) 146–156. https://doi.org/10.1038/nrn1326.

[3] E.J. Bradbury, E.R. Burnside, Moving beyond the glial scar for spinal cord repair, Nat. Commun. 10 (2019) 1–15. https://doi.org/10.1038/s41467-019-11707-7.

[4] M.B. Bracken, M.J. Shepard, W.F. Collins, T.R. Holford, W. Young, D.S. Baskin, H.M. Eisenberg, E. Flamm, L. Leo-Summers, J. Maroon, L.F. Marshall, P.L. Perot, J. Piepmeier, V.K.H. Sonntag, F.C. Wagner, J.E. Wilberger, H.R. Winn, A Randomized, Controlled Trial of Methylprednisolone or Naloxone in the Treatment of Acute Spinal-Cord Injury, N. Engl. J. Med. 322 (1990) 1405–1411.

[5] Z. Liu, Y. Yang, L. He, M. Pang, C. Luo, B. Liu, L. Rong, High-dose methylprednisolone for acute traumatic spinal cord injury: A meta-analysis, Neurology. 93 (2019) e841–e850. https://doi.org/10.1212/WNL.0000000000007998.

[6] B.C. Walters, M.N. Hadley, R.J. Hurlbert, B. Aarabi, S.S. Dhall, D.E. Gelb, M.R. Harrigan, C.J. Rozelle, T.C. Ryken, N. Theodore, Guidelines for the management of acute cervical spine and spinal cord injuries: 2013 update, Neurosurgery. 60 (2013) 82–91. https://doi.org/10.1227/01.neu.0000430319.32247.7f.

[7] M.B. Bracken, M.J. Shepard, T.R. Holford, L. Leo-Summers, E.F. Aldrich, M. Fazl, M. Fehlings, D.L. Herr, P.W. Hitchon, L.F. Marshall, R.P. Nockels, V. Pascale, P.L. Perot, J. Piepmeier, V.K.H. Sonntag, F. Wagner, J.E. Wilberger, H.R. Winn, W. Young, Administration of methylprednisolone for 24 or 48 hours or tirilazad mesylate for 48 hours in the treatment of acute spinal cord injury: Results of the Third National Acute Spinal Cord Injury randomized controlled trial, J. Am. Med. Assoc. 277 (1997) 1597–1604. https://doi.org/10.1097/00132586-199808000-00011.

[8] N. Derakhshanrad, H. Saberi, M.S. Yekaninejad, M.T. Joghataei, A. Sheikhrezaei, Granulocyte-colony stimulating factor administration for neurological improvement in patients with postrehabilitation chronic incomplete traumatic spinal cord injuries: A double-blind randomized controlled clinical trial, J. Neurosurg. Spine. 29 (2018) 97–107. https://doi.org/10.3171/2017.11.SPINE17769.

[9] K. Kitamura, N. Nagoshi, O. Tsuji, M. Matsumoto, H. Okano, M. Nakamura, Application of hepatocyte growth factor for acute spinal cord injury: The road from basic studies to human treatment, Int. J. Mol. Sci. 20 (2019). https://doi.org/10.3390/ijms20051054.

[10] K. Kucher, D. Johns, D. Maier, R. Abel, A. Badke, H. Baron, R. Thietje, S. Casha, R. Meindl, B. Gomez-Mancilla, C. Pfister, R. Rupp, N. Weidner, A. Mir, M.E. Schwab, A. Curt, First-in-man intrathecal application of neurite growth-promoting anti-nogo- a antibodies in acute spinal cord injury, Neurorehabil. Neural Repair. 32 (2018) 578–589. https://doi.org/10.1177/1545968318776371.

[11] M. Bydon, A.B. Dietz, S. Goncalves, F.M. Moinuddin, M.A. Alvi, A. Goyal, Y. Yolcu, C.L. Hunt, K.L. Garlanger, A.S. Del Fabro, R.K. Reeves, A. Terzic, A.J. Windebank, W. Qu, CELLTOP Clinical Trial: First Report From a Phase 1 Trial of Autologous Adipose Tissue–Derived Mesenchymal Stem Cells in the Treatment of Paralysis Due to Traumatic Spinal Cord Injury, Mayo Clin. Proc. 95 (2020)

406–414. https://doi.org/10.1016/j.mayocp.2019.10.008.

[12] J. Vaquero, M. Zurita, M.A. Rico, C. Bonilla, C. Aguayo, J. Montilla, S. Bustamante, J. Carballido, E. Marin, F. Martinez, A. Parajon, C. Fernandez, L. De Reina, An approach to personalized cell therapy in chronic complete paraplegia: The Puerta de Hierro phase I/II clinical trial, Cytotherapy. 18 (2016) 1025–1036. https://doi.org/10.1016/j.jcyt.2016.05.003.

[13] E.D. Gomes, S.S. Mendes, H. Leite-Almeida, J.M. Gimble, R.Y. Tam, M.S. Shoichet, N. Sousa, N.A. Silva, A.J. Salgado, Combination of a peptide-modified gellan gum hydrogel with cell therapy in a lumbar spinal cord injury animal model, Biomaterials. 105 (2016) 38–51. https://doi.org/10.1016/j.biomaterials.2016.07.019.

[14] E.D. Gomes, S.S. Mendes, R.C. Assunção-Silva, F.G. Teixeira, A.O. Pires, S.I. Anjo, B. Manadas, H. Leite-Almeida, J.M. Gimble, N. Sousa, A.C. Lepore, N.A. Silva, A.J. Salgado, Co-Transplantation of Adipose Tissue-Derived Stromal Cells and Olfactory Ensheathing Cells for Spinal Cord Injury Repair, Stem Cells. 36 (2018) 696–708. https://doi.org/10.1002/stem.2785.

[15] E.D. Gomes, B. Ghosh, R. Lima, M. Goulão, T. Moreira-Gomes, J. Martins-Macedo, M.W. Urban, M.C. Wright, J.M. Gimble, N. Sousa, N.A. Silva, A.C. Lepore, A.J. Salgado, Combination of a Gellan Gum-Based Hydrogel With Cell Therapy for the Treatment of Cervical Spinal Cord Injury, Front. Bioeng. Biotechnol. 8 (2020) 1–14. https://doi.org/10.3389/fbioe.2020.00984.

[16] C.A. Ribeiro, A.J. Salgado, J.S. Fraga, N.A. Silva, R.L. Reis, N. Sousa, The secretome of bone marrow mesenchymal stem cells-conditioned media varies with time and drives a distinct effect on mature neurons and glial cells (primary cultures), J. Tissue Eng. Regen. Med. 5 (2011) 668–672. https://doi.org/10.1002/term.365.

[17] R.C. Assunção-Silva, B. Mendes-Pinheiro, P. Patrício, L.A. Behie, F.G. Teixeira, L. Pinto, A.J. Salgado, Exploiting the impact of the secretome of MSCs isolated from different tissue sources on neuronal differentiation and axonal growth, Biochimie. 155 (2018) 83–91. https://doi.org/10.1016/j.biochi.2018.07.026.

[18] S.C. Serra, J.C. Costa, R.C. Assunção-Silva, F.G. Teixeira, N.A. Silva, S.I. Anjo, B. Manadas, J.M. Gimble, L.A. Behie, A.J. Salgado, Influence of passage number on the impact of the secretome of adipose tissue stem cells on neural survival, neurodifferentiation and axonal growth, Biochimie. 155 (2018) 119–128. https://doi.org/10.1016/j.biochi.2018.09.012.

[19] A.G. Pinho, J.R. Cibrão, R. Lima, E.D. Gomes, S.C. Serra, J. Lentilhas-Graça, C. Ribeiro, S. Lanceros-Mendez, S.F.G. Teixeira, S. Monteiro, N.A. Silva, A.J. Salgado, Immunomodulatory and regenerative effects of the full and fractioned adipose tissue derived stem cells secretome in spinal cord injury, Exp. Neurol. 351 (2022) 113989. https://doi.org/10.1016/j.expneurol.2022.113989.

[20] S. Ren, Z.H. Liu, Q. Wu, K. Fu, J. Wu, L.T. Hou, M. Li, X. Zhao, Q. Miao, Y.L. Zhao, S.Y. Wang, Y. Xue, Z. Xue, Y.S. Guo, S. Canavero, X.P. Ren, Polyethylene glycol-induced motor recovery after total spinal transection in rats, CNS Neurosci. Ther. 23 (2017) 680–685. https://doi.org/10.1111/cns.12713.

[21] U. Freudenberg, A. Hermann, P.B. Welzel, K. Stirl, S.C. Schwarz, M. Grimmer, A. Zieris, W. Panyanuwat, S. Zschoche, D. Meinhold, A. Storch, C. Werner, A star-PEG-heparin hydrogel platform to aid cell replacement therapies for neurodegenerative diseases, Biomaterials. 30 (2009) 5049–5060. https://doi.org/10.1016/j.biomaterials.2009.06.002.

[22] I. Capila, R.J. Linhardt, Heparin-protein interactions, Angew. Chemie - Int. Ed. 41 (2002) 390–412. https://doi.org/10.1021/j150493a017.

[23] M. V. Tsurkan, K. Chwalek, S. Prokoph, A. Zieris, K.R. Levental, U. Freudenberg, C. Werner, Defined polymer-peptide conjugates to form cell-instructive starpeg-heparin matrices in situ, Adv. Mater. 25 (2013) 2606–2610. https://doi.org/10.1002/adma.201300691.

[24] H.L. Xu, F.R. Tian, J. Xiao, P.P. Chen, J. Xu, Z.L. Fan, J.J. Yang, C.T. Lu, Y.Z. Zhao, Sustained-release of FGF-2 from a hybrid hydrogel of heparin-poloxamer and decellular matrix promotes the neuroprotective effects of proteins after spinal injury, Int. J. Nanomedicine. 13 (2018) 681–694. https://doi.org/10.2147/IJN.S152246.

[25] H.L. Xu, F.R. Tian, C.T. Lu, J. Xu, Z.L. Fan, J.J. Yang, P.P. Chen, Y.D. Huang, J. Xiao, Y.Z. Zhao, Thermo-sensitive hydrogels combined with decellularised matrix deliver bFGF for the functional recovery of rats after a spinal cord injury, Sci. Rep. 6 (2016) 1–15. https://doi.org/10.1038/srep38332.

[26] U. Freudenberg, A. Zieris, K. Chwalek, M. V. Tsurkan, M.F. Maitz, P. Atallah, K.R. Levental, S.A. Eming, C. Werner, Heparin desulfation modulates VEGF release and angiogenesis in diabetic wounds, J. Control. Release. 220 (2015) 79–88. https://doi.org/10.1016/j.jconrel.2015.10.028.

[27] L. Schirmer, P. Atallah, C. Werner, U. Freudenberg, StarPEG-Heparin Hydrogels to Protect and Sustainably Deliver IL-4, Adv. Healthc. Mater. 5 (2016) 3157–3164. https://doi.org/10.1002/adhm.201600797.

[28] S. Prokoph, E. Chavakis, K.R. Levental, A. Zieris, U. Freudenberg, S. Dimmeler, C. Werner, Sustained delivery of SDF-1α from heparin-based hydrogels to attract circulating pro-angiogenic cells, Biomaterials. 33 (2012) 4792–4800. https://doi.org/10.1016/j.biomaterials.2012.03.039.

[29] F. Peysselon, S. Ricard-Blum, Heparin-protein interactions: From affinity and kinetics to biological roles. Application to an interaction network regulating angiogenesis, Matrix Biol. 35 (2014) 73–81. https://doi.org/10.1016/j.matbio.2013.11.001.

[30] A.K. Powell, E.A. Yates, D.G. Fernig, J.E. Turnbull, Interactions of heparin/heparan sulfate with proteins: Appraisal of structural factors and experimental approaches, Glycobiology. 14 (2004). https://doi.org/10.1093/glycob/cwh051.

[31] Y. Huang, Z. Liu, Kinetic Advantage of Intrinsically Disordered Proteins in Coupled Folding-Binding Process: A Critical Assessment of the "Fly-Casting" Mechanism, J. Mol. Biol. 393 (2009) 1143–1159. https://doi.org/10.1016/j.jmb.2009.09.010.

[32] S.Q. Chen, Q. Cai, Y.Y. Shen, X.Y. Cai, H.Y. Lei, Combined use of NGF/BDNF/bFGF promotes proliferation and differentiation of neural stem cells in vitro, Int. J. Dev. Neurosci. 38 (2014) 74–78. https://doi.org/10.1016/j.ijdevneu.2014.08.002.

[33] L. Crigler, R.C. Robey, A. Asawachaicharn, D. Gaupp, D.G. Phinney, Human mesenchymal stem cell subpopulations express a variety of neuro-regulatory molecules and promote neuronal cell survival and neuritogenesis, Exp. Neurol. 198 (2006) 54–64. https://doi.org/10.1016/j.expneurol.2005.10.029.

[34] T. Cheriyan, D.J. Ryan, J.H. Weinreb, J. Cheriyan, J.C. Paul, V. Lafage, T. Kirsch, T.J. Errico, Spinal cord injury models: A review, Spinal Cord. 52 (2014) 588–595.

https://doi.org/10.1038/sc.2014.91.

[35] A. Alizadeh, S.M. Dyck, S. Karimi-Abdolrezaee, Traumatic Spinal Cord Injury: An Overview of Pathophysiology, Models and Acute Injury Mechanisms, Front. Neurol. 10 (2019) 1–25. https://doi.org/10.3389/fneur.2019.00282.

[36] D. Lukovic, V. Moreno-Manzano, E. Lopez-Mocholi, F.J. Rodriguez-Jiménez, P. Jendelova, E. Sykova, M. Oria, M. Stojkovic, S. Erceg, Complete rat spinal cord transection as a faithful model of spinal cord injury for translational cell transplantation, Sci. Rep. 5 (2015) 1–7. https://doi.org/10.1038/srep09640.

[37] L.J. Noble, J.R. Wrathall, Distribution and time course of protein extravasation in the rat spinal cord after contusive injury, Brain Res. 482 (1989) 57–66. https://doi.org/10.1016/0006-8993(89)90542-8.

[38] G. Mccaffrey, C.L. Willis, W.D. Staatz, N. Nametz, C.A. Quigley, S. Hom, J.J. Lochhead, T.P. Davis, Occludin oligomeric assemblies at tight junctions of the blood– brain barrier are altered by hypoxia and reoxygenation stress, J Neurochem. 110 (2009) 58–71. https://doi.org/10.1111/j.1471-4159.2009.06113.x.Occludin.

[39] P. Himmels, I. Paredes, H. Adler, A. Karakatsani, R. Luck, H.H. Marti, O. Ermakova, E. Rempel, E.T. Stoeckli, C. Ruiz De Almodóvar, Motor neurons control blood vessel patterning in the developing spinal cord, Nat. Commun. 8 (2017). https://doi.org/10.1038/ncomms14583.

[40] R. Lima, S. Monteiro, J.P. Lopes, P. Barradas, N.L. Vasconcelos, E.D. Gomes, R.C. Assunção-Silva, F.G. Teixeira, M. Morais, N. Sousa, A.J. Salgado, N.A. Silva, Systemic interleukin-4 administration after spinal cord injury modulates inflammation and promotes neuroprotection, Pharmaceuticals. 10 (2017) 1–16. https://doi.org/10.3390/ph10040083.

[41] H. Ishii, S. Tanabe, M. Ueno, T. Kubo, H. Kayama, S. Serada, M. Fujimoto, K. Takeda, T. Naka, T. Yamashita, Ifn-γ-dependent secretion of IL-10 from Th1 cells and microglia/macrophages contributes to functional recovery after spinal cord injury, Cell Death Dis. 4 (2013) 1–9. https://doi.org/10.1038/cddis.2013.234.

[42] H. Wang, Y. Wang, D. Li, Z. Liu, Z. Zhao, D. Han, Y. Yuan, J. Bi, X. Mei, VEGF inhibits the inflammation in spinal cord injury through activation of autophagy, Biochem. Biophys. Res. Commun. 464 (2015) 453–458. https://doi.org/10.1016/j.bbrc.2015.06.146.

[43] A. Torres-Espín, J. Forero, K.K. Fenrich, A.M. Lucas-Osma, A. Krajacic, E. Schmidt, R. Vavrek, P. Raposo, D.J. Bennett, P.G. Popovich, K. Fouad, Eliciting inflammation enables successful rehabilitative training in chronic spinal cord injury, Brain. 141 (2018) 1946–1962. https://doi.org/10.1093/brain/awy128.

[44] E. Schmidt, P. Raposo, R. Vavrek, K. Fouad, Inducing inflammation following subacute spinal cord injury in female rats: A double-edged sword to promote motor recovery, Brain. Behav. Immun. 93 (2021) 55–65. https://doi.org/10.1016/j.bbi.2020.12.013.

[45] N. Goshi, R.K. Morgan, P.J. Lein, E. Seker, A primary neural cell culture model to study neuron, astrocyte, and microglia interactions in neuroinflammation, J. Neuroinflammation. 17 (2020) 1–16. https://doi.org/10.1186/s12974-020-01819-z.

[46] G. Pasut, A. Panisello, E. Folch-Puy, A. Lopez, C. Castro-Benítez, M. Calvo, T. Carbonell, A. García-Gil, R. Adam, J. Roselló-Catafau, Polyethylene glycols: An effective strategy for limiting liver ischemia reperfusion injury, World J. Gastroenterol. 22 (2016) 6501–6508.

https://doi.org/10.3748/wjg.v22.i28.6501.

[47] Y. Neuzillet, S. Giraud, L. Lagorce, M. Eugene, P. Debre, F. Richard, B. Barrou, Effects of the Molecular Weight of Peg Molecules (8, 20 and 35 KDA) on Cell Function and Allograft Survival Prolongation in Pancreatic Islets Transplantation, Transplant. Proc. 38 (2006) 2354–2355. https://doi.org/10.1016/j.transproceed.2006.06.117.

[48] Y.J. Lim, S.J. Hong, What is the best strategy for successful bowel preparation under special conditions?, World J. Gastroenterol. 20 (2014) 2741–2745. https://doi.org/10.3748/wjg.v20.i11.2741.

[49] P.K.F. Damasceno, T.A. de Santana, G.C. Santos, I.D. Orge, D.N. Silva, J.F. Albuquerque, G. Golinelli, G. Grisendi, M. Pinelli, R. Ribeiro dos Santos, M. Dominici, M.B.P. Soares, Genetic Engineering as a Strategy to Improve the Therapeutic Efficacy of Mesenchymal Stem/Stromal Cells in Regenerative Medicine, Front. Cell Dev. Biol. 8 (2020) 1–24. https://doi.org/10.3389/fcell.2020.00737.

[50] A. Rowald, S. Komi, R. Demesmaeker, et.al, Activity-dependent spinal cord neuromodulation rapidly restores trunk and leg motor functions after complete paralysis, Nat. Med. (2022).